Hydraulic Model Study
of
Bed Level Changes of Alluvial River

by

MD. ATAUR RAHMAN

(Roll No: 9616043 P)

MASTER OF SCIENCE IN WATER RESOURCES ENGINEERING

Department of Water Resources Engineering

BANGLADESH UNIVERSITY OF ENGINEERING AND TECHNOLOGY

(BUET), DHAKA-1000

2002

CERTIFICATE OF APPROVAL

The thesis titled **"Hydraulic Model Study of Bed Level Changes of Alluvial River"** submitted by Md. Ataur Rahman, Roll No: 9616043 (P) , Session 1995-96-97 has been accepted as satisfactory in partial fulfillment of the requirement for the degree of Master of Science in Water Resources Engineering on August 2002.

BOARD OF EXAMINERS

1. Dr. Md. Abdul Matin — Chairman
Professor & Head
Dept. of WRE, BUET

2. M. K. Alam
Dr. Md. Khorshed Alam — Member
Professor
Dept. of WRE, BUET

3. Dr. Muhammed Ali Bhuiyan — Member
Professor
Dept. of WRE, BUET

4. Anisul Haque
Dr. Muhammad Anisul Haque — Member (External)
Associate Professor
IWFM, BUET

AUGUST 2002

DECLARATION

It is hereby declared that this thesis or any part of it has not been submitted elsewhere for the award of any degree or diploma.

Md. Ataur Rahman
(Candidate)

TABLE OF CONTENTS

LIST OF TABLES

LIST OF FIGURES

6.3	Bed surface profiles (Run 3)	101

LIST OF PLATES

LIST OF NOTATIONS

Notation	Meaning
A	Area of flow
Q	Water discharge
x	Spatial variable
t	Time variable
q_l	Lateral inflow per unit length of channel
β	Momentum flux correction factor
g	Acceleration due to gravity
h	Depth of flow
S_0	Channel bed slope
S_f	Friction / energy slope
V_x	x-component of the inflow velocity vector
Qs	Sediment discharge
λ	Porosity
P	Wetted perimeter
Z_b	Bed elevation
C_t	Mean sediment concentration
q_{sl}	Lateral sediment inflow per unit length of channel
C_n	Courant number
C^+	Positive characteristics
C^-	Negative characteristics
q	water discharge per unit width
q_s	Unit sediment discharge
n	Manning roughness coefficient
i	The node in spatial grid
k	The node in time grid
Δx	The distance step

Δt	The time step
u	Flow velocity
ρ_s	Density of sediment
ρ	Density of water
d_{50}	Average particle size
C	Chezy's roughness coefficient
K	Aggradation coefficient
K_0	Theoretical value of aggradation coefficient

ACKNOWLEDGEMENT

I would like to express my sincere gratitude and thanks to my supervisor Dr. Md. Abdul Matin, Professor and Head, Department of Water Resources Engineering, BUET for his constant guidance and supervision during the period of this research. I am really grateful to my supervisor for his encouragement throughout the experimental investigation and during the preparation of this thesis.

My sincere thanks are also to the Members of the Examination Committee, Dr. Md. Khorshed Alam, Professor of Water Resources Engineering Department, Dr. Muhammed Ali Bhuiyan, Professor of Water Resources Engineering Department and Dr. Muhammad Anisul Haque, Associate Professor of Institute of Water and Flood Management, BUET for their special interest on this study. Their valuable comments, constructive criticism and suggestions on this work are duly acknowledged.

I also wish to thank Mr. Nazimuddin and Mr. Mostofa for their kind and constant assistance in performing the laboratory tests.

Md. Ataur Rahman
August 2002

ABSTRACT

The Saint-Venant equations describing unsteady flow in open channels and the continuity equation for the conservation of sediment mass are numerically solved to determine the aggradation-degradation of channel bottom due to an imbalance between water flow and sediment discharge. For this purpose the MacCormack explicit finite difference scheme is used. The scheme is second order accurate, handles shocks and discontinuities in the solution without any special treatment, and allows simultaneous solution of the water and sediment equations, thereby obviating the need for iterations. The sediment transport relationship in any form may be included in the computations. The mathematical model presented here is applied to predict the bed level changes of alluvial channel due to sediment over loading.

To verify this model, the laboratory experiment is carried out at the Hydraulics and River Engineering Laboratory of Department of Water Resources Engineering, Bangladesh University of Engineering and Technology, Dhaka. The sediment transport equation $q_s = au^b$ is calibrated through experimental runs and the value of the coefficient 'a' and 'b' is determined, which are used in the mathematical model. Fifteen experimental runs were carried out for different water discharge (q), different bed slope (S_0) and different sediment over loading ratio. For each run, four transient bed profiles are plotted at one-hour interval of flow. The computed results are compared with the experimental data. The agreement between the computed and experimental results is satisfactory.

CHAPTER ONE

INTRODUCTION

1.1 General

The term "alluvial" is usually applied to streams in which the moving sediment and the sediment in the underlying bed is of the same character. An alluvial channel has a mobile bed, composed of non-cohesive granular materials. Such materials are unconsolidated silts, sands and gravels. The channel banks are usually composed of clay, silt or sand. Many natural water courses and the majority of the man made canals are example of alluvial channels.

When a stream of water flows over a sand bed transporting a constant rate of bed load for a sufficiently long time, it attains a steady uniform condition of flow in due time. The bed remains stable and is free of aggradation and degradation. If now the rate of sediment supply is suddenly increased locally at a given section without altering any other flow parameter, the initial state of equilibrium is disturbed and the stream starts steepening its slope by depositing quantities of sediment over the channel bed. The bed is in a state of aggradation. In due time, the stream may attain another condition of equilibrium.

The water and sediment discharges in natural alluvial streams, which have evolved over geologic times, are in equilibrium and produce no objectionable scour or deposition. Because such alluvial rivers or natural streams have reached a state of dynamic equilibrium when the governing factors such as water and sediment discharges, channel geometry, slope, water and sediment properties have remained unchanged for a long enough period of time. However, if this delicate balance is disturbed by changing any of these properties through natural or man-made factors, e.g., the construction of weirs, barrages, dams, sudden cha1lge in sediment supply rate due to heavy erosion or landslide in the river basin, narrowing of river for navigation, river dredging, bend cutting, lowering of the channel bottom, migration of knick points, etc.) a process of achieving another state of equilibrium begins. The process is inevitably accompanied by aggradation and/or degradation along the river bed.

Most of the river courses in Bangladesh are of alluvial nature. In fact, Bangladesh is one of the biggest Deltas in the world, which is composed of sediments carried by the three major river systems, namely, the Ganges, the Brahmaputra-Jamuna and the Meghna. The huge catchment area of these river systems supplies enormous amount of sediment to the rivers. Proper quantification of aggradation and/or degradation and changes in channel form of such alluvial rivers still has been a subject of considerable research. A systematic study on the aggradation- degradation phenomenon of these alluvial rivers of Bangladesh is, therefore, of utmost importance from the viewpoint of improved planning and design of various water development projects.

1.2 Need of Mathematical model

Problems related to alluvial rivers can be studied in the following four ways:

- Field investigation
- Laboratory study
- Physical scale mode
- Mathematical model

Field methods are directly associated with the analysis and computation based on field measurements. It is not always possible to have field measurements of all parameters for a sustainable period of time. Laboratory studies are based on experimental runs and data collection and their analysis that demonstrate a particular phenomenon. Laboratory set up and environment can seldom reach field condition because it is difficult to take all the degrees of freedom (DOF's) as variables at a time. Newton (1951), Lane and Borland (1954), Brush and Wolman (1960), Suryanarayana (1969), Soni et al. (1980), Begin et al. (1981) etc. conducted laboratory tests to study bed level changes in alluvial channels.

In the context of many uncertainties involved in the complex process of flow pattern, physical scale models have become very indispensable tools for the solution of alluvial stream problems in the last few decades. When properly built and run, scale models provide the answer to the engineer's eternal question qualitatively as well as quantitatively. Unfortunately, they can only model the immediate neighborhood of the structures being studied and when large scale and long term consequences of man's intervention are concerned (e.g., hundreds of kilometers of river course, tens of years of morphological variations), a study made by an expert consultant possibly using a mathematical model is the only solution. These models can play very important role in providing qualitative as well as quantitative results on which design decisions may be done. Nowadays water resource projects are becoming larger in volume and economic considerations are more pronounced, and so physical scale models have practical limitation to the scope of their application. Hence, mathematical models can serve very effectively in the planning and design of river-control engineering.

Various researchers have developed analytical solutions after suitable simplifications of the set of basic governing equations. Jain (1981), Jaramillo and Jain (1984) presented analytical solutions for bed aggradation of alluvial channels. Soni et al. (1980), Begin et al. (1981), Gill (1983 a,b) used linear diffusion models while Zhang and Kahawita (1987) and Gill (1987) presented non linear solution for aggradation-degradation phenomenon. However, a closed- form solution of the partial differential equations describing the unsteady flows in open channels coupled with sediment continuity equation is not available, except in few specially simplified cases. Therefore, numerical methods have been used effectively to solve the system of equations. Finite element methods are not so good to solve the non-linear hyperbolic governing equations due to their complexity in the formulation of the phenomena. Finite difference methods both implicit and explicit schemes are used thereof. Explicit numerical methods have not been used extensively because of its stability restriction on the time step. Even though several second-order accurate explicit methods have been reported which are more accurate than first-order methods and are easier to apply than many implicit schemes (Fennema and Chaudhry, 1986). In this view point MacCormack explicit finite difference scheme has been chosen to study aggradation-degradation phenomenon in alluvial channels.

1.3 Objectives of the Study

The main objectives of this study are as follows:

- To study the physics of phenomena of changes in bed level of an alluvial river with various sediment concentration.
- To determine the values of 'a' and 'b' in sediment transport law $q_s = a(u)^b$
- To develop a numerical model for studying the bed level changes in alluvial river and to verify the model with the experimental data.
- To estimate the sediment transport rate

1.4 Organization of Contents

The first chapter of the study gives a brief introduction of the aggradation- degradation phenomenon in an alluvial river reach. It emphasizes the need of mathematical tools for analyzing the phenomenon. It also includes the organization and main objectives of the study.

The second chapter gives a short account of previous studies and literature available for the study. Some of the important numerical schemes (both finite difference and finite element) are illustrated thereof.

The third chapter deals with the MacCormack scheme in details. It shows the gradual development of the mathematical model using the governing hydrodynamic and sediment continuity equation.

The detail experimental set up is discussed in chapter four. Chapter five deals with the experimental procedure. The sixth chapter incorporates the results of the model application. The study comes to an end in chapter seven by drawing conclusions, limitations and recommendations for further study.

CHAPTER TWO

REVIEW OF LITERATURE

2.1 General

A brief view of various earlier studies is presented in this chapter. The principal methods of studies include experimental studies, simplified analytical solutions and numerical techniques. In addition, the description of relevant equations and the solution methods used in this study are briefly illustrated.

2.2 Experimental studies

A number of experimental studies had been conducted to study the effect of the long term and short-term bed level changes in alluvial channels with different flow conditions. Newton (1951) conducted a series of degradation experiments due to sediment diminution using uniform sediment and concluded that the bed elevation and the bed slope decreased asymptotically with time. Lane and Borland (1954) obtained laboratory data to study the river bed scour during floods. Brush and Wolman (1960) measured the time variation of bed levels in a laboratory channel due to migration of the knick points or the points of abrupt change in the longitudinal profile. Begin et al. (1981) experimentally studied degradation of alluvial channels in response to lowering of the base level.

Some of the most important degradation studies in rivers were presented by Lane (1955), Stanley (1951), and Livesey (1963). These studies attempted to find the rate of degradation, which was obtained by taking periodic water surface readings below the dam. Simmons (1965) gave various methods of estimating the magnitude of degradation from stable channel concepts, experimental observations, and the concept of critical traction force. Harrison (1950) concluded from his experiments that the bed degrades as a unit, and the final profile is parallel to the initial profile if nonmoving particles are evenly distributed along the bed.

Bhamidipaty and Shen (1971) studied degradation of the bed profile below a dam due to release of relatively sediment free water from a reservoir and aggradation in a canal (by withdrawing water from the river) due to the difference in sediment transport capabilities between the canal and river. Their study was made in a laboratory flume with rigid banks and mainly relatively uniform size sediment. They developed an equation of the bed profile of a degrading channel, which depicts that the bed elevation decreases exponentially with time. They also concluded that during aggradation incoming sediment deposits at the upstream reach with a resulting bed slope increase and depth decrease.

Soni et al. (1980) conducted an experiment that covered a wide range of flow and sediment loading conditions. They have also developed an analytical mathematical model for aggradation in an infinitely long channel where the results from the analytical study have been suitably modified on the basis of carefully controlled laboratory experiments. They observed that after a long time, the aggradation in downstream of the section of increased sediment supply is closed once the hydraulic conditions became compatible with the increased sediment load.

Yen et al. (1988a) performed a series of overloading experiments with uniform coarse sediment and found that both the aggradation wave speed and the mean sediment transport velocity increase with the initial equilibrium bed slope and with decreasing loading ratio. As to the study of aggradation and degradation of non-uniform sediment, Little and Mayer (1972) performed a series of degradation experiments. They focused on the variation in sediment gradation of the bed surface during the armoring process. Ribberink (1983) experimentally studied the vertical sorting phenomenon of sediment having an idealized gradation under equilibrium conditions and proposed a transport layer concept. Wilcock and Southard (1989) investigated the interaction between the transport, bed surface texture, and bed configuration by making careful measurements and observations in the startup and equilibrium states in a recirculating laboratory flume.

The fundamental behavior of the whole process of bed aggradation due to overloading and then followed by degradation due to under-loading have been studied by Yen et al. (1992). Series of experiments were conducted by Yen et al. (1998) to study the reversibility of an alternating aggradation-degradation process. The results show that the recovery rate decreases as standard deviation of sediment gradation increases. They derived an equation for aggradation-degradation wave resulting from the change in sediment loading which characterizes the response of the channel reach at a pace depending on the response time. Experimental results show that the channel bed roughness increases in all cases of sediment under-loading preceded by overloading and most of the medium-size fraction grains are transported downstream in the aggradation period. They concluded that the response time for the aggradation process is greater than that for degradation process and the aggradation- degradation cycle in the alluvial channel composed of non-uniform bed material is irreversible due to the effects of hydraulic sorting and armoring.

2.3 Analytical Studies

The fundamental notions and hypothesis used in the mathematical modeling of rivers are formulized in the equations of unsteady open channel flow. Three conservation of laws mass, momentum and energy - are used to describe the equations. These equations are simple models of extremely complex phenomenon. Two governing equations may be used to analyze a typical flow situation. The continuity and momentum equations, referred to as de Saint Venant equations, are usually used because the momentum equation is applicable to both discontinuous and continuous flow situations. The different forms of the de Saint Venant equations are:

Continuity equation: $$\frac{\partial A}{\partial t} + \frac{\partial A}{\partial x} = q_l \qquad (2.1)$$

Where, A = area of flow

Q = water discharge

x = spatial variable

t = time variable

q_l = lateral inflow per unit length of channel

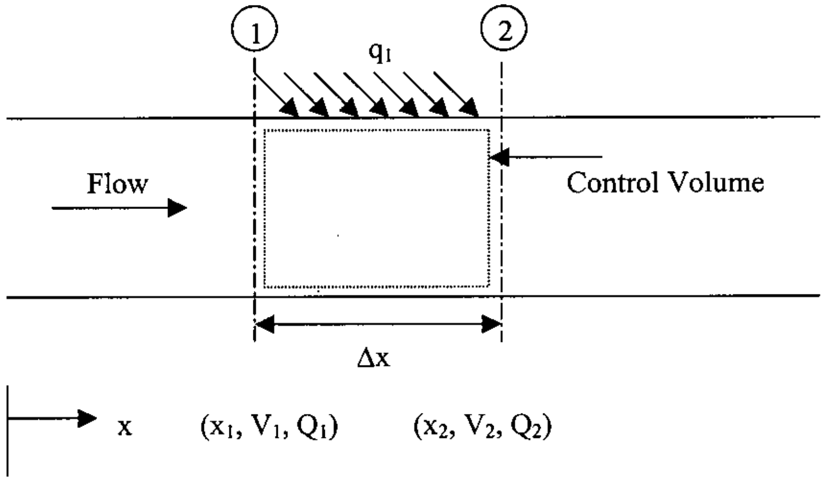

Fig. 2.1 Definition sketch for continuity equation

Momentum equation: $$\frac{\partial Q}{\partial t}+\frac{\partial}{\partial x}\left(\frac{\beta}{A}Q^2\right)+gA\left(\frac{\partial h}{\partial x}-S_0\right)+gAS_f=q_1V_x \qquad (2.2)$$

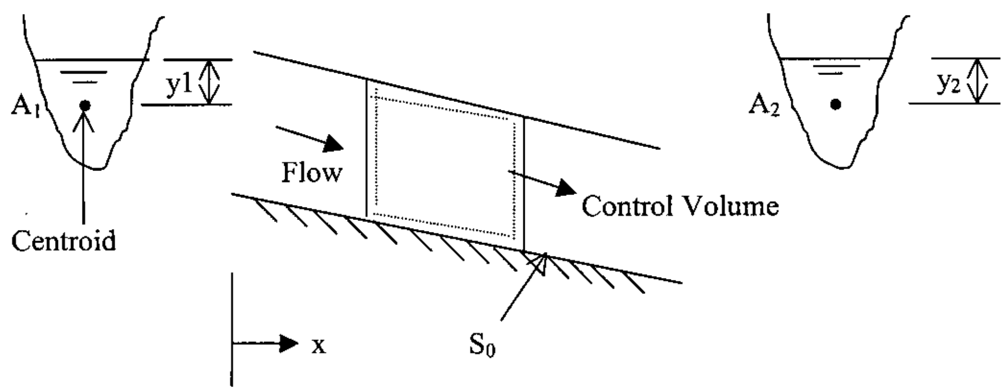

Fig. 2.2 Definition sketch for momentum equation

Where, β = momentum flux correction factor

g = acceleration due to gravity

h = depth of flow

S_o = cham1el bed slope

S_f = friction/energy slope

V_x = x-component (longitudinal direction) of the inflow velocity vector

When aggradation and degradation are concerned, a third equation is necessary for the computation of bed elevation. In fact the sediment transport and water flow are interrelated in such a way that they can never be completely disassociated. There are many formulations expressing the interrelation of the two phenomena in unsteady situations; one of the acceptable mathematical descriptions is presented by the following equation:

Sediment continuity equation: $$\frac{\partial Q_s}{\partial x} + (1-\lambda)\frac{\partial}{\partial t}(PZ_b) + \frac{\partial}{\partial t}(AC_t) = q_{sl} \qquad (2.3)$$

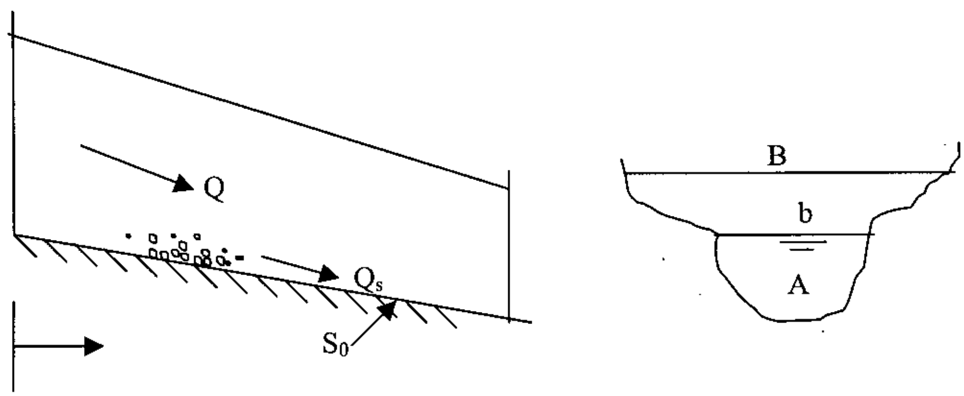

(a) (b)

Fig. 2.3 Definition sketch for one-dimensional flow in a movable bed river: (a) longitudinal profile (b) cross-section

Where, Q_s = sediment discharge

λ = porosity

P = wetted perimeter

Z_b = bed elevation

C_t = mean sediment concentration

q_{sl} = lateral sediment inflow per unit length of channel

The fundamental assumptions made in the derivation of these equations are:

1. The flow is assumed to be one-dimensional, i.e., the channel is fairly straight such that the centrifugal effect due to channel curvature is negligible, the velocity is uniform over the cross-section, and the free surface is taken to b horizontal line across the section.

2. The pressure distribution is hydrostatic along a vertical, i.e., the streamlines do not have sharp curvatures, and the accelerations are negligible.

3. The head losses in unsteady flow may be simulated by using the steady state resistance laws, such as the Manning's or Chezy's equation, i.e., effects of boundary friction and turbulence during unsteady flow are the same as that during steady flow.

4. The channel bed slope is small, so that the flow depths measured normal to the channel bottom and measured vertically are approximately the same.

5. The density of the sediment-laden water is assumed to be homogeneous.

The governing equations are of first order, nonlinear partial differential equations of the hyperbolic type. It is extremely difficult and almost impossible at present to develop analytical solutions altogether of the system. Useful insight into the complex problem can however be gained by studying an idealized and simple situation that is amenable to analytical solution. Alternatively, for a given stretch of a river and a set of flow conditions, a mathematical model can be constructed. While such a mathematical model is usually valid and useful for the given reach and the specified flow conditions only, it is often possible to deduce far-reaching conclusions of a general nature from an analytical solution.

Soni et al. (1980) developed a linear diffusion model to predict the transient bed profile due to sediment overloading. Drastic simplifications made in arriving at the equation of the bed profile could not predict the transient bed profiles satisfactorily.

The writers, however, empirically modified the aggradation coefficient suitably in the equation to obtain satisfactory prediction of bed profiles retaining the essential form of the solution. Jain (1981) pointed out an error in the boundary condition of their analytical model. He presented the analytical solution of the aggradation problem for a more appropriate boundary condition. The analytical results were in agreement with the experimental data.

Gill (1983 a, b) prepared linear diffusion model for aggrading and degrading channel. With a suitable value of diffusion coefficient, the diffusion model quite adequately predicts bed level changes due to aggradation and degradation. He obtained two types of solutions, namely, Fourier series solution and Error function solution and concluded that the Fourier series solution is best suited for computations at large values of time and the Error function solution at small values of time.

A nonlinear parabolic model for non-equilibrium processes in alluvial river was presented by Jaramillo and Jain (1984) in an attempt to circumvent some of the limitations of the classical linear parabolic model. They used the method of weighted residuals for the solution to the nonlinear parabolic sediment transport (diffusion) equation which is in concert with sediment continuity equation and compared the model for the case of aggradation due to sediment augmentation data collected by Soni et al. (1980) and for degradation due to sediment diminution observation by Newton (1951).

Zhang and Kallawita (1987) and Gill (1987) also developed nonlinear solution for aggradation and degradation in alluvial channels and showed better accuracy with the experimental data then the linear solutions. Gill (1987) used the method of perturbation in which the "pseudo-diffusion" coefficient was a function of the local sediment transport but was regarded a constant in the earlier linear solutions.

Ribberink and Sande (1984, 1985) discussed the aggradation problem using a hyperbolic partial differential equation. The proposed hyperbolic model is presumably better than the parabolic (diffusion) model in that some of the acceleration terms that are neglected in the parabolic model are preserved in it. They could not obtain the general solution of the partial differential equation that they used. They presented exact solution for some specified values of distance x and approximate solutions for small and large values of time. A general solution of the proposed hyperbolic equation was developed by Gill (1988) and yielded the solutions previously given by Ribberink and Sande (1984, 1985) as special cases. Qualitatively, the general solutions were capable of predicting the physical conditions more accurately than any other presently available solutions.

2.4 Numerical Simulations

There are several numerical methods available for the solution of unsteady open channel problems with movable bed. The methods can be classified in to the following three categories.

1. Method of characteristics
2. Finite element method
3. Finite difference method

Alam (1998) developed a hydrodynamic model to compute aggradation and degradation using MacCormack second order accurate finite difference scheme. He also applied this model to Jamuna River to verify the capability of handling real field situation. In the present study, this model is used to study the bed level changes of an alluvial channel set up in the laboratory. The computed results are compared with the experimental data to verify the validity of the model.

2.4.1 Method of Characteristics

Monge developed a graphical procedure in 1789 for the integration of partial differential equations. He called this procedure the method of characteristics. It was used by Massau (1889) and Craya (1946) for analyzing surges in open channels and it was utilized to investigate the propagation of flood waves (Isaacson et al., 1954) and other unsteady flow problems (Chaudhry, 1993). The characteristic method has two important fields of application (Cunge et al. 1980):

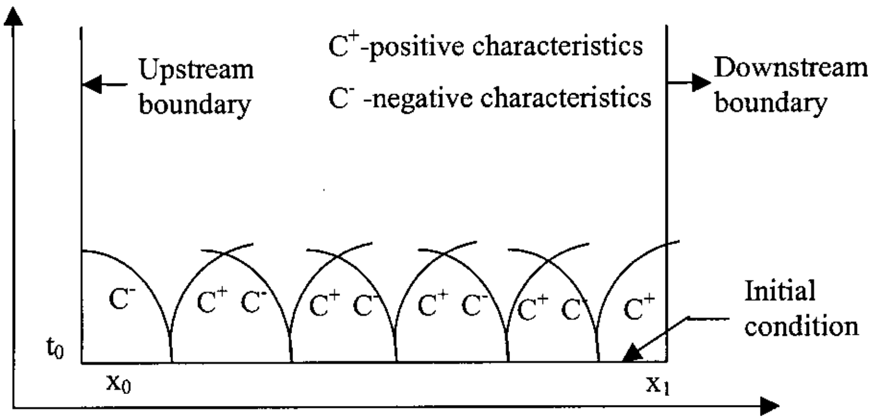

Fig 2.4 Computational domain for a one-dimensional system

- as a standard for other methods, since it is possible to prove that its solutions may be brought as close to the solution of the basic equations as one desires;
- as a means of representing the boundary conditions in methods which cannot compute all flow variables at exterior or interior boundary points of the model.

In applying the method of characteristics, one must transform the basic partial differential equations into equivalent ordinary differential equations. The transformed equations, known as the compatibility equations, are valid only along the characteristics, namely, the positive characteristic, C^+ and the negative characteristic, C^-. After the proper inclusion of initial and boundary conditions one can reach at the solution by two different formulations. One of the formulations is the method of specified intervals, where interpolations become necessary either in time or in space, since all characteristics do not pass through the grid points. The other one is characteristic grid method where one integrates along the characteristics and does not use specified intervals for time and distance. This procedure gives satisfactory results for continuous flows.

Although the method of characteristics has become a standard method for the analysis of transients in closed conduits, its application to open channel flow has become almost negligible. However, the concept of characteristics curves is helpful in understanding the propagation of waves and the development of boundary conditions for explicit finite difference methods.

The original method of characteristics on a variable computational grid is not widely used for industrial modeling because of its complexity and the need to interpolate both the original topographic data and the final results. Characteristics on specified intervals are employed somewhat more frequently, but this method is complex and more costly than finite difference methods without offering any improvement in accuracy. The principal advantage of characteristic methods would seem to be their capability of dealing easily with supercritical flow, which is however rarely encountered in river modeling problems. A notable exception is the study of dam break waves for which the variable grid characteristics method is often used (Chervet and Dalleves, 1970; after Cunge et al., 1980).

2.4.2 Finite Difference Method

The finite difference method (FDM) has been used very extensively in the solution of de Saint Venant equation. The method appears, at first sight, as exceedingly simple. Integration of the partial differential equations is performed merely by changing the differentials into their divided differences. Thus, the differential equations, i.e., the laws describing the evolution of the continuum, are replaced by algebraic finite difference relationships. These relationships aid to obtain an arithmetic analog equation that can be solved numerically on the computer.

The different ways in which derivatives and integrals are expressed by discrete functions are called finite difference schemes. These schemes can be classified into explicit schemes or implicit schemes. The implicit schemes permit numerical solutions over large time steps but require the solution of large sets of simultaneous algebraic equations at each time step. On the contrary, explicit schemes are easy to understand and formulate but require small time steps in order to maintain stability.

2.4.2.1 Finite Difference Approximations

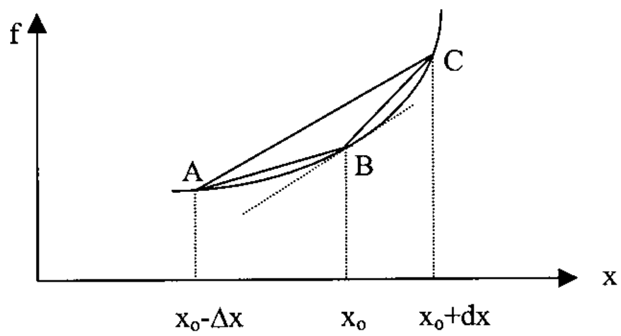

Fig 2.5 Graphical representation of finite difference approximations

Forward finite difference $$\left.\frac{df}{dx}\right|_{x=x0} = \frac{f(x_0+\Delta x)-f(x_o)}{\Delta x} \qquad (2.4)$$

Backward finite difference $$\left.\frac{df}{dx}\right|_{x=x_0} = \frac{f(x_0)-f(x_o-\Delta x)}{\Delta x} \qquad (2.5)$$

Central finite difference $$\left.\frac{df}{dx}\right|_{x=x_0} = \frac{f(x_0+\Delta x-f(x_o-\Delta x)}{2\Delta x} \qquad (2.6)$$

Both backward and forward finite difference approximations are first-order accurate. Central finite difference approximation is referred to as second-order accurate. It is clear from the Fig. 2.5 that the central difference approximation is more accurate than the forward or backward finite difference approximations.

Now let us consider finite difference approximations for a partial derivative. Let us consider a function f (x,t). We may divide the x-t plane into a grid as shown in Fig. 2.6. To refer to different variables at these grid points, we will use the number of the spatial grid as a subscript and that of the time grid as a superscript. For example, the flow depth y at the ith spatial grid point and kth time grid point is denoted by y_i^k. The known time level is denoted by superscript k and the unknown time level by k+ I. If the computations progress from one step to the next, then the procedure is referred to as a marching procedure. Most of the phenomena described by hyperbolic partial differential equations are solved by using marching procedure. The conditions specified at time t = 0 are referred to as the initial conditions. The conditions specified at the channel ends are called end, or boundary conditions.

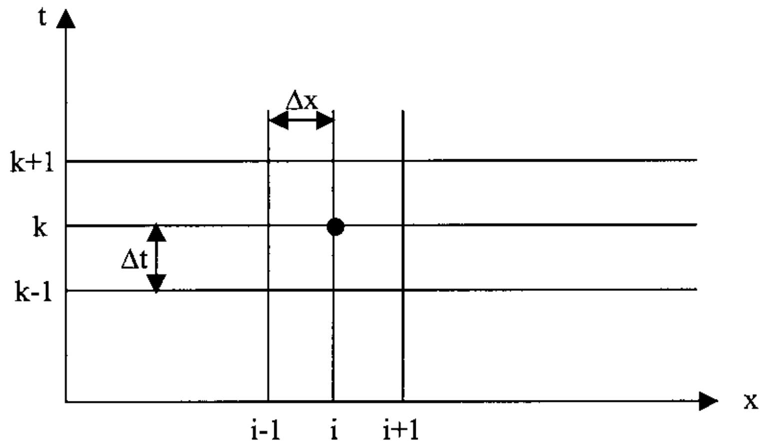

Fig. 2.6 Finite difference computational grid

There are several possibilities for approximating the partial derivatives. The spatial partial derivatives replaced in terms of the variables at the known time level are referred to as the explicit finite differences, whereas those in terms of the variables at the unknown time level are called implicit finite differences. Some typical finite difference approximations for the spatial partial derivative, $\frac{\partial f}{\partial x}$, at the grid point (i,k) are as follows:

Explicit finite differences

Backward: $$\frac{\partial f}{\partial x} = \frac{f_i^k - f_{i-1}^{k+1}}{\Delta x} \tag{2.7}$$

Forward: $$\frac{\partial f}{\partial x} = \frac{f_{i+1}^k - f_i^{k+1}}{\Delta x} \tag{2.8}$$

Central: $$\frac{\partial f}{\partial x} = \frac{f_{i+1}^k - f_{i-1}^{k+1}}{2\Delta x} \tag{2.9}$$

Implicit finite differences

Backward: $$\frac{\partial f}{\partial x} = \frac{f_i^{k+1} - f_{i-1}^{k+1}}{\Delta x} \tag{2.10}$$

Forward: $$\frac{\partial f}{\partial x} = \frac{f_{i+1}^{k+1} - f_i^{k+1}}{\Delta x} \tag{2.11}$$

Central: $$\frac{\partial f}{\partial x} = \frac{f_{i+1}^{k+1} - f_{i-1}^{k+1}}{2\Delta x} \tag{2.12}$$

Many other finite difference approximations are possible if the values at three or more grid points, instead of just two grid points, are used.

2.4.2.2 Some Explicit Schemes

There are several explicit finite difference schemes proposed for the solution of hyperbolic partial differential equations. These schemes do not lead to a system of algebraic equations, since each point can be computed separately. Some typical explicit schemes employed in hydraulic engineering are discussed below:

i. Leap-frog Scheme

The leap-frog method is the earliest scheme used for numerical solution of one-dimensional wave equation. In this method finite difference approximations are:

$$\frac{\partial f}{\partial t} = \frac{f_i^{k+1} - f_i^{k-1}}{2\Delta t} \tag{2.13}$$

$$\frac{\partial f}{\partial x} = \frac{f_{i+1}^{k} - f_{i-1}^{k}}{2\Delta x} \tag{2.14}$$

The scheme approximates the derivative with an accuracy of second order in Δx as well as in Δt. Matsutomi (1983) used this scheme to compute dam-break flow profiles over a dry bed. He employed shock fitting to track the bore and used Ritter's solution for the first few time steps.

ii. Lax Scheme

Lax developed this method in 1954. This scheme is one of the simplest to program and yields satisfactory results for typical hydraulic engineering applications. The partial derivatives and other variables are approximated in this scheme as follows:

$$\frac{\partial f}{\partial x} = \frac{f_{i+1}^{k} - f_{i-1}^{k}}{2\Delta x} \tag{2.15}$$

$$\frac{\partial f}{\partial t} = \frac{f_{i}^{k+1} - f_{i}^{*}}{\Delta t} \tag{2.16}$$

$$f^{*} = \frac{1}{2}(f_{i-1}^{k} + f_{i+1}^{k}) \tag{2.17}$$

$$R^{*} = \frac{1}{2}(R_{i-1}^{k} + R_{i+1}^{k}) \tag{2.18}$$

$$S_f^{*} = \frac{1}{2}(S_{i-1}^{k} + S_{i+1}^{k}) \tag{2.19}$$

For the stability of the scheme, it must satisfy Courant number, C_n condition.

$$Cn = \frac{\text{actual wave velosity}}{\text{numericalwavevelosity}} = \frac{|V| \pm c}{\Delta x/\Delta t} \tag{2.20}$$

For stability, $Cn \leq 1$

iii. MacCormack Scheme

An interesting and simpler variation of the lax-wendroff scheme was introduced by MacCormack and has been widely used in computational fluid dynamics.

The detail discussion of the scheme has been presented in Chapter 3.

iv. Lambda Scheme

The governing equations are transformed into λ-form and then they are discretized according to the sign of the characteristic directions, thereby enforcing the correct signal direction. This allows analysis of flows having sub- and super-critical flows. This scheme was proposed by Moretti in 1979. The spatial finite differences are written in terms of values at three grid points and the scheme comprises the predictor and corrector parts.

Predictor Part

$$f_x^+ = \frac{2f_i^k - 3f_{i-1}^k + f_{i-2}^k}{\Delta x} \tag{2.21}$$

$$f_x^- = \frac{f_{i+1}^k - f_i^k}{\Delta x} \tag{2.22}$$

$$\frac{\partial f}{\partial t} = \frac{f_i^* - f_k^i}{\Delta t} \tag{2.23}$$

Corrector Part

$$f_x^+ = \frac{f_i^* - f_{i-1}^*}{\Delta x} \tag{2.24}$$

$$f_x^- = \frac{-2f_i^* + 3f_{i+1}^* - f_{i+2}^*}{\Delta x} \tag{2.25}$$

$$\frac{\partial f}{\partial t} = \frac{f_i^{**} - f_k^i}{\Delta t} \tag{2.26}$$

Values at k+ 1 time step are determined from

$$f_i^{k+1} = \frac{1}{2}(f_i^* + f_i^{**}) \tag{2.27}$$

For the scheme to be stable, Courant number, C_n must be less than or equal to 1 at all grid points during each time step.

Fennema and Chaudhry (1986) used this scheme to the analysis of unsteady free surface flows having shocks or bores.

v. Gabutti Scheme

The Lambda scheme has the disadvantage that it does not follow the characteristics exactly for a linear problem (Anderson et al., 1984). Gabutti extended the scheme in order to rectify this problem (Gabutti, 1983). The Gabutti scheme is identical to the Lambda scheme in its development of the equations in the λ form; however, it differs in its approximation for the partial derivatives by finite differences. In the Gabutti scheme, a two-part predictor step and a single corrector step are used with the derivatives approximated as follows:

Predictor step, part 1

$$\bar{\bar{f}}_x^{+} = \frac{f_i^k - f_{i-1}^k}{\Delta x} \tag{2.28}$$

$$\bar{\bar{f}}_x^{-} = \frac{f_{i+1}^k - f_i^k}{\Delta x} \tag{2.29}$$

Predictor step, part 2

$$\bar{f}_x^{+} = \frac{2f_i^k - 3f_{i-1}^k + f_{i-2}^k}{\Delta x} \tag{2.30}$$

$$\bar{f}_x^{-} = \frac{-2f_i^k + 3f_{i+1}^k - f_{i+2}^k}{\Delta x} \tag{2.31}$$

Corrector step

$$\hat{f}_x^{+} = \frac{\bar{f}_i - \bar{f}_{i-1}}{\Delta x} \tag{2.32}$$

$$\hat{f}_x^- = \frac{\dot{f}_{i+1} - \bar{f}_i}{\Delta x} \tag{2.33}$$

The value of f at the new time k+ 1 becomes

$$f_i^{k+1} = \frac{1}{2}\left(f_i^k + \bar{f}_i + \hat{f}_i - \bar{\bar{f}}_i \right) \tag{2.34}$$

For the scheme to be stable, Cn must be less than or equal to 1 at all grid points during each time step. However, if the unsteady flow equations are solved until the solution converges to a steady state, then the stability criterion may be relaxed to $C_n \leq 2$. This scheme was used by Ferulema and Chaudhry (1986, 1987).

2.4.2.3 Some Implicit Schemes

In implicit finite difference schemes, the spatial partial derivatives and/or the coefficients are replaced in terms of the values at the unknown time level. The unknown variables, therefore, appear implicitly in the algebraic equations, and the methods are called implicit methods. The algebraic equations for the entire system have to be solved simultaneously in these methods. Some of the implicit schemes are discussed below:

i) Preissmann Scheme

The Preissmann scheme has been extensively used since the early 1960s. It has the advantages that a variable spatial grid may be used; steep wave fronts may be properly simulated by varying the weighting coefficient; and the scheme yields an exact solution of the linearized form of the governing equations for a particular value of Δx and Δt. The partial derivatives and other coefficients are approximated as follows:

$$\frac{\partial f}{\partial t}=\frac{(f_i^{k+1}+f_{i+1}^{k+1})-(f_i^k+f_{i+1}^k)}{2\Delta t} \tag{2.35}$$

$$\frac{\partial f}{\partial x}=\frac{\alpha(f_{i+1}^{k+1}-f_i^{k+1})}{\Delta x}+\frac{(1-\alpha)(f_{i+1}^k-f_i^k)}{\Delta x} \tag{2.36}$$

$$f=\frac{1}{2}\alpha(f_{i+1}^{k+1}+f_i^{k+1})+\frac{1}{2}(1-\alpha)(f_{i+1}^k+f_i^k) \tag{2.37}$$

in which α is a weighting coefficient; in the partial derivative f refers to both V and y, and f as a coefficient stands for S_f and V. By selecting a suitable value for α, the scheme may be made totally explicit (α=0) or implicit (α= 1). The scheme is unconditionally stable if $0.55 < \alpha \leq 1$. An unconditional stability means that there is no restriction on the size of Δx and Δt for stability. However, for accuracy C_n, should be close to l. Fennema and Chaudhry (1986), Park and lain (1986), Lyn (1987) etc. used this scheme to solve unsteady open channel flow equation.

ii. Vasiliev Scheme

The Vasiliev scheme was developed by a team of researchers at the Institute of Hydrodynamics, Novosibirsk, Russia (Vasiliev et al., 1965). The scheme is a fully implicit one in which both dependent variables are computed at all grid points. It uses the following approximation of time and space derivatives:

$$\frac{\partial f}{\partial t}=\frac{f_i^{k+1}-f_i^k}{\Delta t} \tag{2.38}$$

$$\frac{\partial f}{\partial x}=\frac{f_{i+1}^{k+1}-f_{i-1}^{k+1}}{\Delta x} \tag{2.39}$$

iii. Gunaratnam-Perkins Scheme

This scheme was developed by Gunaratnam and Perkins in 1970. The finite difference approximation of the flow equations are written in a linearized homogeneous characteristics form in this scheme. The derivatives are replaced by:

$$\frac{\partial f}{\partial t} = \frac{1}{6}\frac{f_{i-1}^{k+1} - f_{i-1}^{k}}{\Delta t} + \frac{2}{3}\frac{f_{i}^{k+1} - f_{i-1}^{k}}{\Delta t} + \frac{1}{6}\frac{f_{i+1}^{k+1} - f_{i+1}^{k}}{\Delta t} \quad (2.40)$$

$$\frac{\partial f}{\partial x} = \frac{f_{i+1}^{k+1} - f_{i-1}^{k+1}}{2\Delta x} \quad (2.41)$$

iv. Abbott-Ionescu Scheme

This scheme was first proposed by Abbott and lonescu (1967) at the International Institute for Hydraulic and Environmental Engineering in Delft, the Netherlands. In this scheme two dependent variables (e.g., discharge Q and depth h) are computed at different grid points as shown in Fig. 2.7.

Consider the following system of homogeneous flow equations:

$$g\frac{\partial u}{\partial t} - u\frac{\partial u}{\partial t} - (u^2 - gh)\frac{\partial u}{\partial x} = 0 \quad (2.42)$$

$$h\frac{\partial u}{\partial t} - u\frac{\partial h}{\partial t} - (u^2 - gh)\frac{\partial h}{\partial x} = 0 \quad (2.43)$$

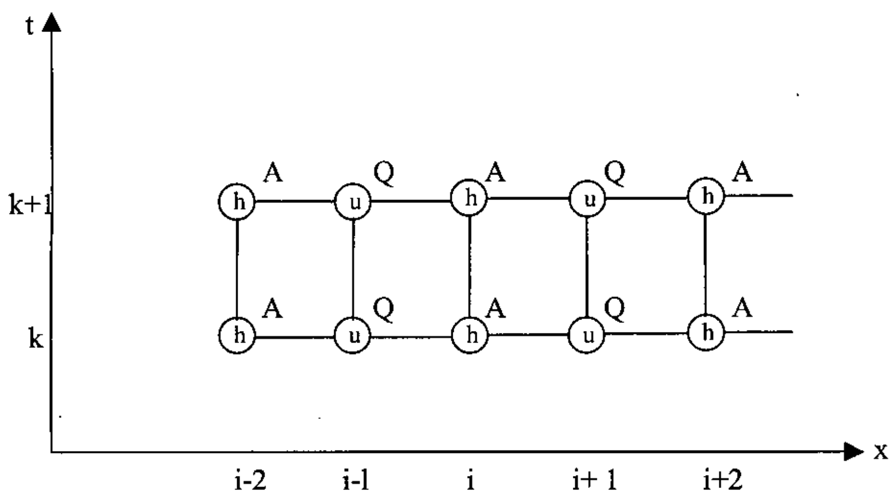

Fig. 2.7 Computational grid for the Abbott-lonescu scheme

Eq. (2.42) is replaced by following derivative approximations:

$$\frac{\partial h}{\partial t} = \frac{h_i^{k+1} - h_i^k}{\Delta t} \tag{2.44}$$

$$\frac{\partial u}{\partial t} = \frac{1}{2}\left(\frac{u_{i+1}^{k+1} - u_{i+1}^{k}}{\Delta t} + \frac{u_{i-1}^{k+1} - u_{i-1}^{k}}{\Delta t}\right) \tag{2.45}$$

$$\frac{\partial u}{\partial x} = \frac{1}{2}\left(\frac{u_{i+1}^{k+1} - u_{i-1}^{k+1}}{2\Delta x} + \frac{u_{i+1}^{k} - u_{i-1}^{k}}{2\Delta x}\right) \tag{2.46}$$

and in Eq. (2.43)

$$\frac{\partial u}{\partial t} = \frac{u_i^{k+1} - u_i^k}{\Delta t} \tag{2.47}$$

$$\frac{\partial h}{\partial t} = \frac{1}{2}\left(\frac{h_{i+2}^{k+1} - h_{i+2}^{k}}{\Delta t} + \frac{h_{i}^{k+1} - h_{i}^{k}}{\Delta t}\right) \tag{2.48}$$

$$\frac{\partial h}{\partial x} = \frac{1}{2}\left(\frac{h_{i+2}^{k+1} - u_{i}^{k+1}}{2\Delta x} + \frac{h_{i+2}^{k} - u_{i}^{k}}{2\Delta x}\right) \tag{2.49}$$

v. Delft Hydraulics Laboratory Scheme

This scheme was described by Vreugdenhil (1973). It is based on the concept of nodes, or computational cells at the center of which water stages are computed, and which are linked to other cells on the left and on the right through discharge laws. The space derivatives are weighted between k and k+ 1 time level using a weighting coefficient θ:

$$\frac{\partial f}{\partial x} = \theta \frac{f_{i+1}^{k+1} - f_{i-1}^{k+1}}{2\Delta x} + (1-\theta)\frac{f_{i+1}^{k} - f_{i-1}^{k}}{2\Delta x} \tag{2.50}$$

where, $0.5 \leq \theta \leq 1.0$

The Delft scheme is identical to the Abbott-Ionescu scheme, differences appearing at the level of definition of the equation coefficients, coefficient θ, convective momentum term, and solution algorithm.

2.4.2.4 Related Previous Studies

Tinney (1955) presented a method of predicting the bed profile of a degrading channel by combining a sediment transport continuity equation and sediment transport equation. He also predicted the final depth of flow and final slope at the end of degradation for uniform sediments by solving simultaneously the flow and the critical tractive force equations. It was also assumed that the bed was plane at the end of degradation. His results were in close agreement with Newton's (1951) experimental results.

Lu and Shen (1986) analyzed three different numerical models for degradation studies. The models are: uncoupled solution with kinematic wave assumption, uncoupled solution based on the quasi-steady assumption, and known discharge implicit model. They compared and modified the models with Suryanarayana's (1969) laboratory experiment data.

Lyn (1987) used perturbation techniques to identify multiple time scales in the governing equations, and suggested that complete coupling between the full unsteady water flow equations and the sediment continuity equation is desirable in cases where the conditions change rapidly at the boundaries. He proposed use of the Preissmann linearized implicit scheme for a simultaneous solution of the governing equations.

Ponce et al. (1979) developed a mathematical model to simulate bed transient formation and propagation in alluvial channels. The model was of the known-discharge type, i.e., within one time step, the water discharge was considered steady. This technique allowed for the Four-Point implicit finite difference scheme to use larger time steps. Using a power relation between bed material discharge and mean flow velocity circumvented instability due to ill posing of the sediment transport function. They analyzed stability and convergence, and established criteria to ensure a successful model operation.

An unsteady, uncoupled model for determining river bed profiles with imposed sediment load was developed by Park and Jain (1986) using Preissmann implicit scheme. The iteration scheme was necessary in the model whenever the spatial gradient of change in bed level became very large. They compared the model with analytical and laboratory data prepared by Soni et al. (1980). The agreement between the numerical results and available experimental data was satisfactory. The results of the numerical analysis were presented in the form of algebraic relations that could be easily applied by practicing engineers to predict the river- bed aggradation due to an increased sediment load larger than the sediment transport capacity of the river.

Dawdy and Vanoni (1986) described the characteristics of several presently available numerical simulation models along with their similarities and differences. They pointed out the general problems in present models which include the choice of sediment transport function, assessment of resistance to flow and how it varies with changes in flow and cross section, modeling of bed armoring and its effect on sediment transport, the allocation of net scour a11d fill in a stream cross section, and the handling of upstream and downstream boundary conditions.

Momentum and continuity equations for water and sediment flows in a wide prismatic channel were solved numerically using a verified model for the armoring process by Jain and Park (1989). The changes in bed level a11d mean sediment size, and the length of degradation, determined from the numerical experiments, were correlated by multiple regression analysis to the independent dimensionless variables. The details of the numerical simulation model, which was verified by using the classical experimental data of Little and Mayer (1972), were given by Park and Jain (1987). They concluded that the depth of degradation depends on Froude number, the geometric standard deviation, and the normalized median size of the bed material. The proposed relationship for bed degradation was verified with the field data of Missouri river near Yankton, South Dakota following the closure of the Gavins Point Dam.

Bhallamudi and Chaudhry (1991) developed a mathematical tool by using MacCormack finite difference scheme and applied to predict (I) Bed level changes due to sediment overloading; (2) development of longitudinal profile due to base-level lowering; (3) and bed-level changes associated with the migration of knick points. The computed results were compared with the available experimental data obtained on laboratory flumes. The agreement between the computed and experimental result was satisfactory.

2.4.3 Finite Element Method

The finite element method (FEM) is an alternative technique for solving the same partial differential equations by means of piecewise approximations. It is a newer technique, has not been as extensively used as the finite difference method, and does not offer any significant advantage for one-dimensional problems.

The main advantage of the finite element method is its ability to handle irregular boundaries and grid refinement. The finite difference solutions have grids with square corners, straight edges, and mostly uniform grid spacing. The finite element method adapts easily to problems where these boundary characteristics are unsuitable. The computational grids for the finite difference method are usually defined by parallel lines and cannot easily be used to simulate natural boundaries. Smaller grid spacings are frequently required with either method for areas where variables change rapidly (e.g., near edges and corners). These grid refinements are easily handled by the finite element method but require additional effort when using the finite difference method.

The basic steps required to analyze a physical phenomenon by finite element method are as follows:

i. The domain is subdivided into many small-interconnected sub-domains or finite elements; the process is called discretization.

ii. A matrix known as element matrix is formed to relate the nodal variables of each element.

iii. The element matrices are assembled to form a set of algebraic equations that describe the entire domain. The coefficient matrix of the final set of equations is called global matrix. The formulation is done in such a manner that certain compatibility conditions are met at each node.

iv. Boundary conditions are properly incorporated.

v. The resulting set of simultaneous algebraic equations is solved then to obtain the solution at every nodal point.

The essential step in solving a differential equation is to convert it into an integral equation. For this purpose, the following three finite element approaches are available: direct, variational, and weighted residual methods. Each results in an identical integral equation for linear partial differential equations.

2.4.3.1 Variational Approach

In this method, the problem of finding a solution of the governing differential equation is replaced by an equivalent variational problem that consists of finding a known function that extremizes a certain integral quantity, subject to the prescribed boundary conditions. Such an integral is called a functional. A general expression for this functional, U over a one-dimensional domain R is given by

$$U = \int_R F\left(x, u, \frac{\partial u}{\partial x}, \frac{\partial^2 u}{\partial x^2}, ... \right) dx \qquad (2.51)$$

Within each sub-domain, the unknown function u is approximated by a trial function $\hat{u}$,

$$\hat{u} = \sum_{j=1}^{N^e} \phi j_j(x) u_j \tag{2.52}$$

where, $\phi_j\{x\}$ are linearly independent functions, known as basis functions.

The total functional, U

$$U = \sum_{e=1}^{m} U^e \tag{2.53}$$

where,
$$U^e = \int_{R^e} F\left(x, \hat{u}, \frac{d\hat{u}}{dx}, \frac{d^2\hat{u}}{dx^2}, \ldots\ldots\ldots\ldots \right) dx \tag{2.54}$$

Applying nodal compatibility,

$$U = U(u_1, u_2, u_3, \ldots\ldots\ldots\ldots, u_n) \tag{2.55}$$

After assembly of all elements, the global matrix equation takes the form

$$[C]\{u\} = \{F\} \tag{2.56}$$

where,
$$[C] = \sum_{e=1}^{m} [C]^e \tag{2.57}$$

$$\{F\} = \sum_{e=1}^{m} \{F\}^e \tag{2.58}$$

2.4.3.2 Method of Weighted Residuals

The weighted residual methods are general methods that can be applied in cases where direct and variational methods does not work. In this method, the desired function, say u(*) is replaced by a finite series approximation, u(*)

$$u(*) \approx \hat{u}(*) = \sum_{j=1}^{N^e} u_j \phi_j(*) \tag{2.59}$$

where, $\phi_j(*)$ are denoted as basis functions.

The basis functions are chosen to satisfy all boundary conditions. Substitution of

$\hat{u}(*)$ in the partial differential equations of the general form

$$Lu(*) - f = 0 \tag{2.60}$$

results in a residual, R

$$R(*) = L\,\hat{u}(*) - f \tag{2.61}$$

the objective that the residual is minimized by introducing N^e weighting functions, W(*)

$$\int_U \int_V R(*) W_i(*) dV dt = 0 \quad ; \quad i = 1,2,\ldots\ldots\ldots\ldots N^e \tag{2.62}$$

The method of weighted residuals may be classified into the following three approaches: Galerkin, Collocation, and Sub-domain method.

i. Galerkin method

When the weighting function is chosen to be the basis function, the method results in Galerkin method.

$$\int_U \int_V R(*) \phi_i (*) dV dt = 0 \qquad ; \qquad i = 1,2,\ldots\ldots\ldots.N^e \tag{2.63}$$

In this case, R(*) and ϕ_i (*) are orthogonal to each other and the residual is forced to zero.

ii. Sub-domain Method

In the sub-domain method the weighting function is chosen to be unity in the sub-domain V_i and zero elsewhere.

$$\int_V R(*) W_i (*) dV = 0 \qquad ; \qquad i = 1,2,\ldots\ldots\ldots.N^e \tag{2.64}$$

where, $W_i = 1$, (x,y,z) within V_i

$= 0$, (x,y ,z) outside V_i

The integration is less tedious in this method than the Galerkin method because of simplicity of the fofll1 of the Wi(*) function.

iii. Collocation Method

Collocation method is the simplest of the method of weighted residuals to implement. The weighting function, W_i is chosen here to be the Dirac delta, that is,

$$W_i = \delta(x - x_i) \tag{2.65}$$

The Dirac delta function has the following important property

$$\int_U \int_V a(*) \delta(* - x_i, y - y_i, z - z_i, t - t_i) dV dt = a|x_i, y_i, z_i, t_i \tag{2.66}$$

Thus, the orthogonality constraints for the collocation method are

$$\int_U \int_V R(*)\delta_i(*)dVdt = 0 \qquad ; \qquad i = 1,2,\ldots\ldots\ldots N^e \qquad (2.67)$$

The residual vanishes at each collocation points (x_i, y_i, z_i, t_i). Hence, the accuracy of this method depends heavily on the location of the collocation points.

CHAPTER THREE

DEVELOPMENT OF NUMERICAL MODEL

3.1 General

The prediction technique of aggradation and degradation in an alluvial river reach is based on the procedure used to develop a model. The successful application of a model largely depends on the search for the correct path to develop the model for a particular problem. The assumptions used in the model development to simplify a phenomenon are sometimes crucial to the extent of their validity. Considering all these constraints, a model is developed from the basic equations describing the problem.

3.2 Governing Equations

The basic one-dimensional partial differential equations describing unsteady flow in a wide rectangular channel with movable bed are given by:

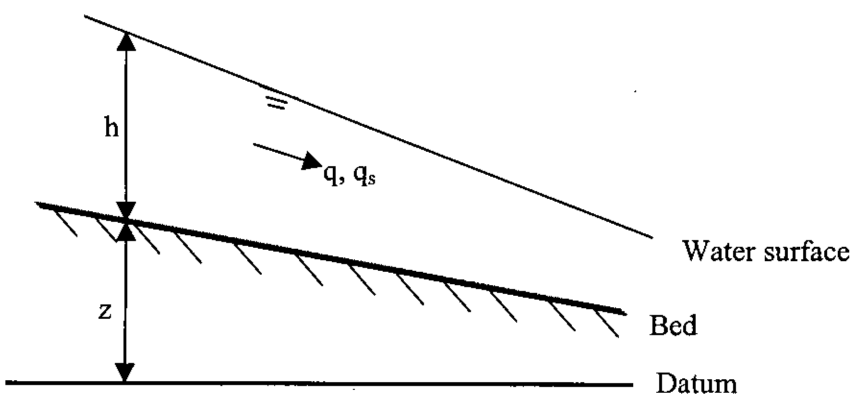

Fig: 3.1 Definition sketch of flow variables

- Continuity equation for water

$$\frac{\partial h}{\partial t} + \frac{\partial q}{\partial x} = 0 \tag{3.1}$$

- Momentum equation for water

$$\frac{\partial q}{\partial t}+\frac{\partial}{\partial x}(\frac{q^2}{h}+\frac{gh^2}{2})+gh\frac{\partial z}{\partial x}+ghS_f=0 \tag{3.2}$$

- Continuity equation for sediment

$$\frac{\partial}{\partial t}\left[(1-\lambda)z+\frac{q_s h}{q}\right]+\frac{\partial q_s}{\partial x}=0 \tag{3.3}$$

Where,

q	=	Water discharge per unit width
h	=	Depth of flow
z	=	Bed elevation
q_s	=	unit sediment discharge
g	=	Acceleration due to gravity
S_f	=	Friction slope
x	=	Longitudinal distance along the channel
t	=	Time
λ	=	Porosity of the bed layer

The friction slope, S_f is determined using the Manning equation (SI unit):

$$S_f=\frac{q^2n^2}{h^{3.333}} \tag{3.4}$$

Where, n = The Manning roughness coefficient.

The sediment discharge is estimated by an empirical power function of the flow velocity, u:

$q_s = au^b$

$$\text{or,}\quad q_s=a\left(\frac{q}{h}\right)^b \tag{3.5}$$

Where, a and b are empirical constants for which the values depend on the sediment properties.

The relationship for the friction slope and sediment discharge, defined by Eq. (3.4) alld Eq. (3.5) are used in the model for the sake of simplicity. More elaborate or different relations can be included in the model.

3.3 Numerical Scheme

It was previously stated that Eq. (3.1) through Eq. (3.3) represent nonlinear hyperbolic partial differential equations and closed form solutions of these equations are not possible except for a few simplified cases. Therefore, they are solved by numerical schemes. In this model, a finite difference scheme developed by MacCormack (1969) is used. The scheme is chosen for its following reasons:

i) The MacCormack scheme is simple, easy to implement and does not require solution of large matrices.

ii) There is no need for iteration.

iii) The scheme has excellent capability of capturing the shocks without isolating them.

iv) Empirical relationship for roughness and sediment discharge can be incorporated in the scheme.

v) The scheme is second order accurate in both space and time. Therefore, longer distance steps can be used to obtain the same accuracy as that obtained using first order schemes.

The MacCormack scheme is a two level predictor-corrector scheme. For one-dimensional flow two alternatives of this scheme are possible. In one alternative, backward finite differences are used to approximate the spatial partial derivatives in the predictor part and forward finite differences are utilized in the corrector part. The values of the variables so determined during the predictor part are used during the corrector part. In the second alternative, forward finite differences are used in the predictor part and backward finite differences are used in the corrector part.

With reference to the finite difference grid shown in Fig. 2.6, the finite difference approximations for the derivatives of a variable 'f' are as follows:

Predictor step:

$$\frac{\partial f}{\partial t} = \frac{f_i^* - f_i^k}{\Delta t} \tag{3.6}$$

$$\frac{\partial f}{\partial x} = \frac{f_{i+1}^k - f_i^k}{\Delta x} \tag{3.7}$$

Where,

i= the node in spatial grid;

k = the node in time grid;

Δx = the distance step;

Δt = the time step.

An asterisk refers to the predicted values of the variable.

Using these approximations in Eq. (3.1) to Eq. (3.5) one obtains the predicted values of the variables h_i*, q_i* and z_i*

$$h_i^* = h_i^k - \frac{\Delta t}{\Delta x}(q_{i+1}^k - q_i^k) \tag{3.8}$$

$$q_i^* = q_i^k - \frac{\Delta t}{\Delta x}\left\{\frac{\left(q_{i+1}^k\right)^2}{h_{i+1}^k} - \frac{(q_i^k)^2}{h_i^k} + \frac{g}{2}\left[\left(h_{i+1}^k\right)^2 - \left(h_i^k\right)^2\right]\right\} - gh_i^k\frac{\Delta t}{\Delta x}(z_{i+1}^k - z_i^k) - gh_i^k\Delta t\frac{\left(q_i^k n\right)^2}{\left(h_i^k\right)^{3.33}} \tag{3.9}$$

$$(q_s)_i^* = a\left(\frac{q_i^*}{h_i^*}\right)^b \tag{3.10}$$

$$z_i^* = z_i^k + \frac{1}{1-\lambda}\left[\left(\frac{q_s h}{q}\right)_i^k - \left(\frac{q_s h}{q}\right)_i^*\right] - \frac{\Delta t}{(1-\lambda)\Delta x}\left[(q_s)_{i+1}^k - (q_s)_i^k\right] \tag{3.11}$$

Corrector step:

$$\frac{\partial f}{\partial t} = \frac{f_i^{**} - f_i^*}{\Delta t} \tag{3.12}$$

$$\frac{\partial f}{\partial x} = \frac{f_i^* - f_{i-1}^*}{\Delta x} \tag{3.13}$$

Where, the two asterisks denote the value of the variables calculated in the corrector step.

After substituting these finite difference approximations in Eq. (3.1) to Eq. (3.5), the corrected values of the variables h_i^{**}, q_i^{**} and z_i^{**} are obtained:

$$h_i^{**} = h_i^{*} - \frac{\Delta t}{\Delta x}(q_i^{*} - q_{i-1}^{*}) \tag{3.14}$$

$$q_i^{**} = q_i^{*} - \frac{\Delta t}{\Delta x}\left\{\frac{(q_i^{*})^2}{h_i^{*}} - \frac{(q_{i-1}^{*})^2}{h_{i-1}^{*}} + \frac{g}{2}\left[(h_i^{*})^2 - (h_{i-1}^{*})^2\right]\right\} - gh_i^{*}\frac{\Delta t}{\Delta x}(z_i^{*} - z_{i-1}^{*}) - gh_i^{*}\Delta t\frac{(q_i^{*}n)^2}{(h_i^{*})^{3.33}} \tag{3.15}$$

$$(q_s)_i^{**} = a\left(\frac{q_i^{**}}{h_i^{**}}\right)^b \tag{3.16}$$

$$z_i^{**} = z_i^{*} + \frac{1}{1-\lambda}\left[\left(\frac{q_s h}{q}\right)_i^{*} - \left(\frac{q_s h}{q}\right)_i^{**}\right] - \frac{\Delta t}{(1-\lambda)\Delta x}\left[(q_s)_i^{*} - (q_s)_{i-1}^{*}\right] \tag{3.17}$$

Finally, the values of the unknown variables at time level k+ 1, i.e., at the end of the time interval Δt, are given by

$$h_i^{k+1} = \frac{1}{2}\left(h_i^{k} + h_i^{**}\right) \tag{3.18}$$

$$q_i^{k+1} = \frac{1}{2}\left(q_i^{k} + q_i^{**}\right) \tag{3.19}$$

$$(q_s)_i^{k+1} = \frac{1}{2}\left[(q_s)_i^{k} + (q_s)_i^{**}\right] \tag{3.20}$$

$$z_i^{k+1} = \frac{1}{2}\left(z_i^{k} + z_i^{**}\right) \tag{3.21}$$

3.4 Boundary Conditions

The preceding equations determine the values of h, q, and z at the new time level k+1 at every interior grid points (i = 2,3 ...N-1). The values at the boundary grid points (i = 1 and N) cannot be determined by using these equations, since there are no grid points outside the flow domain. Hence, they are determined by using boundary conditions. For one-dimensional flows, the specified interval approach of characteristic method gives acceptable results and is employed herein.

By applying the characteristic theory, it can be shown that for subcritical flow conditions, two boundary conditions must be imposed at the upstream boundary, and one boundary condition must be imposed at downstream boundary. The values of the dependent variables that are not specified through boundary conditions can be determined by using the characteristic equations. Their values may also be determined by interpolation from the known values at the interior nodes (Roache, 1972). The inclusion of these boundary conditions into the finite difference scheme is problem specific and has to deal with individually for specific studies.

It has been mentioned earlier that two boundary conditions at upstream boundary and one boundary condition at downstream end are required for the proper functioning of the model. In addition to these, initial conditions are needed at every computational finite difference grid point. Uniform unit discharge (q_o), uniform flow depth (h_0) and bed levels as calculated from initial bed slope (S_o) were provided as initial conditions, i.e.,

$q(x, 0) = q_o$

$h(x,0)=h_o$

$z(x,o)=z_o$ for $x=0$

Constant measured discharge per unit width was imposed as an upstream boundary condition. Another boundary condition came from increment of sediment discharge. However, this was not as straight forward as the former one. It was required to be translated into an equation by which the bed elevation at the upstream end could be calculated. This was achieved by assuming a fictitious node upstream from node 1 and specifying the sediment discharge at that node equal to $q_{so}+\Delta q_s$. Then, applying the backward finite difference on the spatial differential term of the sediment continuity equation, one can get the bed level at node 1 for the unknown time level k+1.

$$\frac{\partial}{\partial t}\left[(1-\lambda)z+\frac{q_s h}{q}\right]+\frac{\partial q_s}{\partial x}=0\;. \tag{3.22}$$

$$\frac{\left[(1-\lambda)z+\dfrac{q_s h}{q}\right]_k^{k+1}-\left[(1-\lambda)z+\dfrac{q_s h}{q}\right]_1^k}{\Delta t}+\frac{[q_s]_1^k-[q_s]_f^k}{\Delta x}=0 \tag{3.23}$$

$$\left[(1-\lambda)z+\frac{q_s h}{q}\right]_k^{k+1}=\left[(1-\lambda)z+\frac{q_s h}{q}\right]_1^k+\frac{\Delta t}{\Delta x}\left[(q_{s0}+\Delta q_s)-(q_s)_1^k\right] \tag{3.24}$$

$$z_1^{k+1}=z_1^k+\frac{1}{(1-\lambda)}\left(\frac{q_s h}{q}\right)_1^k-\frac{1}{(1-\lambda)}\left(\frac{q_s h}{q}\right)_1^{k+1}+\frac{1}{(1-\lambda)}\frac{\Delta t}{\Delta x}\left[(q_{s0}+\Delta q_s)-(q_s)_1^k\right]$$

(3.25)

The flow depth, h at node 1 was determined by extrapolation from the already calculated values at the interior nodes using the MacCormack scheme. The downstream boundary condition was the constant depth, which was specified by

$h(x_n,t) = h_o$ for all $t \geq 0$

This was based on the assumption that the channel was long and the bed transients would not reach the downstream end within the period for which conditions were computed and that the variation in flow depth would be negligible. The discharge and the bed elevation at the downstream end were determined by extrapolation from the values at the interior nodes.

3.5 Stability

Stability of a numerical scheme is very essential as the solution progresses. When an error grows continuously the scheme becomes unstable. The MacCormack scheme must satisfy the Courant-Friedrichs-Lewy (CFL) condition for stability. Since the water waves travel at a much higher velocity than the bed transients, this condition is given by:

$$C_n = \left(\frac{q}{h} + \sqrt{gh}\right)\frac{\Delta t}{\Delta x} \tag{3.26}$$

For stability, $Cn \leq 1$

This criterion must be satisfied at every grid point of each time step for the scheme to be stable.

3.6 Artificial Viscosity

The solution obtained by a finite difference scheme has dissipative errors if the leading term of the truncation error in the scheme has even derivatives, and the solution has dispersive errors if the leading term has odd derivatives. The dispersive errors usually produce oscillations in the computed results in the vicinity of steep wave fronts. These oscillations are purely due to numerical errors (mainly due to large grid spacing Δx and Δt for a particular Courant number) and have nothing to do with the physical phenomenon being simulated. This phenomenon is more pronounced in case of higher order schemes like the MacCormack scheme. To smooth these oscillations, artificial viscosity is introduced. There are several ways to add artificial viscosity to a scheme. Jameson et al. (1981) developed a procedure to dampen the oscillations produced by large gradients while leaving the relatively smooth areas unaffected.

The values of the variables at the end of the time step computed by MacCormack scheme are modified using the following parameter based on the normalized form of the computed water surface gradients:

$$v_i = \frac{\left|h_{i+1} - 2h_i + h_{i-1}\right|}{\left|h_{i+1}\right| - 2\left|h_i\right| + \left|h_{i-1}\right|} \tag{3.27}$$

$$\varepsilon_{i+1/2} = \kappa \max(v_{i+1}, v_i) \tag{3.28}$$

$$\varepsilon_{i-1/2} = \kappa \max(v_i, v_{i-1}) \tag{3.29}$$

Where, κ = a dissipation constant which is used to regulate the amount of artificial viscosity.

At grid points where h_{i+1} and h_{i-1} do not exist, the following expressions are used instead of Eq. (3.27)

$$v_i = \frac{|h_i - h_{i-1}|}{|h_i| + |h_{i-1}|} \tag{3.30}$$

$$v_i = \frac{|h_{i+1} - h_i|}{|h_{i+1}| + |h_i|} \tag{3.31}$$

The corrected values off to be used at the new time step are given by:

$$f_i^{k+1} = f_i^k + \varepsilon_{i+1/2}\left(f_{i+1}^{k+1} - f_i^{k+1}\right) - \varepsilon_{i-1/2}\left(f_i^{k+1} - f_{i-1}^{k+1}\right) \tag{3.32}$$

The value of κ should be chosen such that it is as small as possible, but at the same time smoothens the high frequency oscillations.

For one dimensional momentum equation, the artificial viscosity can act like turbulent momentum transport, which can be an additional advantage of using artificial viscosity.

3.7 Methodological Steps

Before the start of the model application, the topographic data (z_i^k at t = 0) and hydraulic data (h_i^k and q_i^k at t = 0) should be known as initial conditions at all the grid points. The new values of h_i^{k+1}, q_i^{k+1} and z_i^{k+1} after the time interval Δt are calculated as follows:

i. The predicted values of $h_i^*, q_i^*, (q_s)_i^*$ and z_i^* are computed by applying Eq. (3.8) through Eq. (3.11) at the interior nodes (i = 2,........ , N-1).

ii. The corrected values of $h_i^{**}, q_i^{**}, (q_s)_i^{**}$ and z_i^{**}. at the interior nodes (i =2,.......... , N-1) are determined by using Eq. (3.14) to Eq. (3.17).

iii. The new values of h, q, q_s and z at the end of the time step Δt, i.e., $h_i^{k+1}, q_i^{k+1}, (q_s)_i^{k+1}$ and z_i^{k+1} are determined from Eq. (3.18) to Eq. (3.21) at the interior nodes. The values at the boundary (i = 1 and i = N) are determined by utilizing proper boundary conditions.

iv. The values determined from previous steps are modified (if required) to dampen higher order oscillations by adding artificial viscosity.

v. $hk, q_i^k, (q_s)_i^k$ and z_i^k for the next time step are set equal to $h_i^{k+1}, q_i^{k+1}, (q_s)_i^{k+1}$ and z_i^{k+1} respectively.

vi. The time interval Δt for the next time step is determined from Courant-Friedrichs-Lewy stability criterion (Eq. 3.26).

The procedure is repeated until the required time is reached.

3.8 Coupling of the Scheme

The MacCormack scheme is an explicit numerical scheme, and the unknowns in each algebraic equation representing the finite difference form of the governing equations are those resulting from the temporal derivative in these equations. The coupling of flow equations and the sediment continuity equation is achieved in this method because it uses a two-level predictor-corrector approach. In fact, there is no coupling during the predictor part. However, the predicted values of bed elevation are used to determine the corrected values of discharge through the term $\partial z/\partial x$ in Eq. (3.15). Similarly, the predicted values of h and q are used to both determine q_s in Eq. (3.10) and evaluate the spatial derivative term in Eq. (3.13). Thus, for one time step, the ultimate computation of each dependent variable at the end of the time step takes into account the changes in all the other variables. In fact the methodological steps of the scheme are such that coupling is achieved automatically. It does not require any special treatment for that. On the other hand coupling is not achieved if Eq. (3.3) is solved after completed solving Eq. (3.1) and Eq. (3.2), i.e., after corrector step for Eq. (3.14) and Eq. (3.15). The latter approach is similar to the uncoupled implicit method. Park and Jain (1986) pointed out, this approach resulted in numerical instabilities whenever the bed level gradient became too large. They, however, achieved coupling and numerical stability by iterating the solution during each time step.

CHAPTER FOUR

EXPERIMENTAL SET –UP

The experimental model described herein was constructed on the sand bed in the Hydraulics and River Engineering Laboratory of the Water Resources Engineering Department of the Bangladesh University of Engineering and Technology, Dhaka, during the period of August 2001 to March 2002. The detail of the experimental set-up as well as the measuring techniques is described in the following articles. General layout plan of the set-up is shown in Fig. 4.1 and Plate 4.6.

4.1 Experimental Set-Up

The experimental set-up consists of two separate parts, a temporary part and a permanent part. The permanent part is the experimental facility necessary for the storage and regulation of the water circulating through the model and the guidance part. The temporary part contains the actual experimental mobile-bed model in a river. It is possible to change the configuration of this part as and when needed for carrying out further research, using the permanent part of the model without any drastic constructive changes.

4.1.1 The Temporary Part

The model is built in the temporary part of the set-up. It is a mobile-bed model with fixed banks. The layout of the channel comprises of a main branch. A sediment trap is situated at the end of the branch, followed by a tail gate for the control of water levels. A detail drawing of the temporary part is shown in Fig. 4.2.

In the following sections all elements of the temporary part are described in detail.

4.1.1.1 Main Channel

This is a straight channel of length about 12 meters, width 1 meter and height 0.61 meter. Both of the channel banks are vertical and fixed. Water is flowed from the upstream reservoir to the channel through the PVC tubes (D=2.7 cm: L =30 cm) placed over the width of the entrance to get rid of larger eddies present in the water coming from the upstream reservoir. Immediately after the arrangement of such flow stabilizing tubes the sand is distributed over the width of the channel by sand feeder. The distribution of sand over the width of the channel is done by a wooden structure which is shown in Plate 4.1 and Plat 4.2.

4.1.1.2 Sandtrap

A sandtrap is located at the end of the channel to intercept all sediment transported through the channel. It is 1.8 m long, 1 m wide and 1.3 m deep (Plate 4.7). It also prevents the sand to enter into the permanent part of the model. Once the sandtrap is emptied and its content is measured, the average sediment transport rate for the channel is computed for the time interval observed. This is done by dividing the amount of sediment by the time elapsed.

4.1.1.3 Outflow Section

At the downstream end of the model, the water in each branch flows over a tail gate into the permanent part of the model. The discharge is measured before spilling into the downstream reservoir. The tail gates have two functions,

a) They regulate the water level in the branch, and
b) They prevent the sand bed from running dry if a power failure occurs during experimentation or when it becomes necessary to stop the run for some reason

The view of the tail gate is shown in Fig. 4.3 and Plate 4.7.

4.1.2 The Permanent Part

The permanent part is the hardware of the set-up. It acts as a facility to conduct all different types of experiment in the sand bed. The components of the permanent part are given below:

I. Downstream Reservoir

II. Pump

III. Pipe line

IV. Upstream Reservoir

V. The Regulating arid Measuring System

The components of the permanent part are described below in brief

4.1.2.1 Downstream Reservoir

The downstream reservoir (Fig. 4.4) serves as storage reservoir. Its volume is 11.5 m^3. The maximum water level can be at 0.77 m elevation with respect to reservoir bottom. There is a spillway at the end of the downstream reservoir for excess water to spill out. In every one or two weeks the tank had to be cleaned and emptied. The fine particles of the sediment that are deposited at the bottom are removed through a valve placed at the lowest level of overflowing spillway. The cross-section of the spillway is shown in Fig. 4.5.

4.1.2.2 Pump

The circulating pump near the measuring flume draw water from the downstream reservoir. The pump has a maximum delivery of up to 90 l/sec and head of 7 m.

4.1.2.3 Pipe Line

1ne layout of the pipe line is shown in Fig. 4.6. The pipeline has three parts:

(1) Suction pipe line

(2) Delivery pipe line and

(3) Excess discharge pipe line

The rate of water flow is taken care of by the pipe line system. The pump sucks the water from the downstream reservoir into the pipe line. The T -joint on top of the pump divides the water over the excess pipe and the delivery or supply pipe, depending on the regulation of the valves in the respective pipes. As the pump delivers a constant discharge, the required discharge through the model must be regulated by these valves.

(I) Suction pipe line: It draws water from the downstream reservoir to the pump. It is 1.63 m long and the diameter of the pipe is 0.2 m. The suction pipe line is made up by three pipes. The mouth of the suction pipe is placed 0 .2 m above the floor of the downstream reservoir (Fig. 4.7).

(2) Delivery pipe line: The purpose of delivery pipe line is to deliver water from the pump to the upstream reservoir. The length of the delivery pipe is 14.27 m and dia of the pipe is 0.2 m. It has a valve to control water discharge through the model.

(3) Excess discharge pipe line: Its purpose is to discharge the excess water into the downstream reservoir with the help of the valve which controls the excess water discharge amount. It is 9.61 m long and of diameter 0.2 m.

So, the pipe line consists of three parts. The flow in the channel is controlled with the help of two valves, one in the delivery pipe and another in the excess discharge pipe. When more discharge is required in the channel the valve in the delivery pipe line had to be opened and the other valve has to be closed accordingly. In this way flow of water is controlled in the channel. The details of the pipe line are shown in Fig. 4.7 and Fig. 4.8.

4.1.2.4 Upstream Reservoir

The pump draws water from the downstream reservoir and the discharge into this reservoir through the pipe line system. The volume of the upstream reservoir is 4.8 m^3.

The maximum water depth in the upstream reservoir can be 1.25 m. It has two chambers one big and the other is small. Water is dropped into the small chamber of the reservoir from the delivery pipe line. The main purpose of making the small chamber is to dampen the delivery pipe line. The main purpose of making the small chamber is to dampen the turbulence in the water. This small chamber is separated by a wall (with a number of opening in it) from the large chamber of the upstream reservoir (Fig. 4.9). This is done to create a smooth inflow into the big chamber. As undisturbed water is wanted in the channel a number of plastic pipes are placed in such a way that water passes through them before going into the main channel. In this way the disturbance was removed. For maintenance purpose the upstream reservoir can be emptied through a small regulated opening placed at the lower level of the reservoir wall. This also acts as a storage reservoir.

4.1.2.5 The Regulating And Measuring System

The regulating and measuring system (Fig. 4.10) of the model consists of the following:

- The Tail Gates
- The Stilling Basin and Transition Flumes
- The Guiding Vanes and Tubes
- The Approach Channel and The Rehbock Weir
- The Stilling Basins Connected With Rehbock Weirs

4.1.2.5.1 The Tail Gate

At the downstream end of the sand trap of channel the tail gate is placed. The details of the tail gate are shown in Fig. 4.3 and Plate 4.7. It is made of cast iron and encircled with rubber flaps, so that water flows only over the gates. It also has steel plates on both sides for guidance of flow. Ventilation tubes are provided under both tailgates. The ventilating tube has a valve at the middle of the tube so that if water gets inside the tube it can be drained out. The downstream regulation is performed by the tailgate.

4.1.2.5.2 Transition Flumes

Behind the tail gate water falls into the transition flumes. The width of the transition flume is equal to the width of the approach channel, which is 0.50 m.

4.1.2.5.3 The Guiding Vanes And Tubes

To ensure a more smooth flow towards the approach channels guiding vanes are placed between the transition flumes and the approach channels which are at right angle to each other. These vanes guide the water around the corner. In order to prevent creation of extra unwanted turbulence in the approach channels, PVC tubes are used on both the upstream and downstream side of the guiding vanes (Fig. 4.10).

4.1.2.5.4 The Approach Channel And The Rehbock Weir

The water flows over the tail gate downstream of the sand trap into the stilling basin before entering the approach channel. The approach channel is 5.27 m long and 0.50 m wide. The approach channel and Rehbock weir are designed according to ISO standards, thus avoiding an extra cumbersome calibration. These standard can be found in the ISO standard Handbook 16, ISO 1438-1975 (E) and ISO 1438/1-1980 (E). The approach channel should have a minimum length of ten times the width of the channel and must be straight and must have smooth walls, all these conditions are fulfilled here. The dimensions for the Rehbock weir can be found from Appendix A. In order to measure the water height above the Rehbock weir, stilling basin is built and point gage is also installed there (Fig. 4.11).

4.1.2.5.5 The Stilling Basins Connected With Rehbock Weirs

For the measurement of the water height above the Rehbock weir the stilling basin are built along the downstream reservoir. According to ISO 1975, the water level has to be measured at a upstream position 3 to 4 times the maximum level above the crest of the weir. Hence at such location in each channel a small hole is made in the floor of the approach channel through which a pipe line was fixed. This pipe line connects the approach channel with the stilling basin (Fig. 4.11). The water level in the stilling basin is representative for the water level at the Rehbock weir. In the stilling basin the water level is measured with a point gauge.

4.2 The Water Circuit

The water circuit is a closed system in which water is recirculated. From the downstream reservoir water is pumped to the upstream reservoir through the 0.2 m diameter pipeline. Before water enters into main channel it passes through the plastic pipes to remove the turbulence. After that water flows through the measuring flumes back into the downstream reservoir.

4.3 Sediment Circuit

During the experiment the sediment is supplied from the sand feeder into the bed at a suitable rate. After passing through the main channel the sediment falls in the floor of the sand strap. The sediment accumulated in the sand trap is weighed. After weighing the sediment it is left for a certain period to dry and subsequently is transported into the silo of the sediment hopper. This recirculating procedure will be repeated every time.

4.4 Sand Feeder

To feed sediment and to maintain equilibrium state in the main channel a sediment hopper or sand feeder was installed. A sediment feeder is a mechanical device run by electrical power, which feeds sediment into streams of flow of water at measured rates, and is used for model studies of rivers. A detail drawing of the sand feeder is given in Fig. 4.12, Plate 4.3 and Plate 4.4. It is composed of a rectifier, a varia, a DC motor, a gearbox, a gear plate, a hopper and a sand bucket. The hopper just holds a large amount of sand within it. There is a narrow slit at the front base of the hopper through which the sand passes out and gathers at the rim of the gear plate. As the sand gathers and grow in amount they finally falls into the sand bucket at measured rates depending on the rotation speed of the gear plate. The sediment that is feed by the sediment feeder is the same as that of the channel bed material. The calibration curves of the feeders are presented in Fig. 4.13(a) & Fig. 4.13(b). The sediment falls from the sediment feeder into the wooden structure, which distribute the sediment uniformly over the main channel width.

4.5 Sediments

The sediment that is specifically chosen for this experiment was bought from the market. Then it was washed with water so that there is no dirt in it. Several samples were taken from the washed sand for sieve analysis in order to find the grain size distribution. The grain size distribution can be seen from Fig. 4.14.

4.6 The Measuring Techniques

In this section the measurements to be made during experimentation are discussed.

4.6.1 Discharge Measurements

The discharge is measured at the Rehbock weir (Plate 4.11). The weir was made according to the specifications mentioned in ISO (1975). Details of the Rehbock Dimensions are given in Appendix A. The water level at the crest of the weir is measured in stilling basins with point gauges, with an accuracy of 0.05 mm. The zero of the point gauge was set by filling the approach channel with water up to the crest level of the weir. The point gauge was then adjusted and in this way the zero was fixed. The Rehbock weir can measure the discharge properly up to a discharge of 60 l/s, with an accuracy (in the worst case) of 1.8%. This is detailed in Appendix B.

4.6.2 Sediment Transport Measurements

The sediment transport rate is determined with the help of the sand trap located at the end of channel. The sand trap intercepts all sediment transported through the branch. Once a sand trap is emptied and its content measured, the average sediment transport rate is computed for the time-interval observed. This is done by dividing the amount of sediment by the time elapsed. The sand trap can be emptied once the model is put to a standstill. Water is always present in the model. The way of removing sediment from the sand trap is to place stop logs in the slots directly upstream of the sand trap, siphon out the water, and then scoop out the sediment by hand. The method is time-consuming but still this is the method that has been followed here. After the water is siphoned out, the sediment is taken out from the sand trap with the help of buckets. After that the sediment is spread in a thin layer across the floor of the laboratory to let it dry. Drying takes about three days. This weight is translated into a volume. The transport rate is an average for the time interval chosen.

4.6.4 Bed Level Measurements

The bed level was measured with a point gauge in which a special pin is used. A square plate of 2 x 2 cm^2 is fixed to the point of the pin to prevent it from sinking into the sand bed (Fig. 4.15 and Plate 4.12). The gauge is mounted on a frame that is laid across the channel on the branch walls. The bed level is measured at intervals of 0.5 m, in 23 marked cross-sections. The bed level is measured at 5 points at each cross-section. The measuring gauge is placed on a wooden frame which is laid across the width of the channel at one of the cross-sections previously mentioned. The gauge can slide on the frame across the width of the channel in order to make a measurement at the desired point of the cross-section.

CHAPTER FIVE

EXPERIMENTAL PROCEDURE

For conducting the experiment the following procedure was followed.

5.1 Before Starting The Experimental Runs Following Steps Were Done

Step 1:

Sand was bought from market and washed with water so that there is no dirt in it. After that sieve analysis was done in order to find the grain size distribution. The sieve analysis data is given in Table 5.1 and the grain size distribution curve is shown in Fig. 4.14.

Step 2:

All the items such as stilling basins, point gauges, tail gates and other items were checked whether they were working well and whether these were in the right place of the model.

Step 3:

Bed level measurements were done with respect to a specific reference level. First the model is filled with water to a certain arbitrary level (z) above the laboratory floor. In case of no water movement this should provide a perfectly horizontal reference level. This reference level is measured with the equipment, which is used for measuring bed levels during the experiments.

Step 4:

Calibrating the instruments:

(1) Sand feeder- The sand feeders have different speeds. At different speeds the rate of sand outflow was measured and a calibration curve was developed. For each speed three

measurements were carried out to make the calibration curve more accurate. The calibration curves of the two sand feeders were given in Fig. 4.13 (a) and Fig. 4.13 (b).

(2) Discharge of water was measured by Rehbock weir. The calibration chart of the Rehbock weir was made by a standard equation. For detail see appendix A.

5.2 During The Experimental Run Following Steps Were Done:

5.2.1 Calibration of Sediment Transport Equation

The second objective of this study is to determine the values of 'a' and 'b' in sediment transport law $q_s = a(u)^b$. This calibration is done by following steps:

Step 1:

The first step is the fixation of the discharge. Both the excess and the supply pipe line have valves for the regulation of the discharge. A wheel on top of the valve is turned to determine the vertical position of the steel plate. Before starting the pump the valves in the excess and the delivery pipe line should be closed. Sufficient depth of water in the downstream reservoir should be present before starting the pump. After that by adjusting both the valves, the desired flow rate through the model was achieved. When the desired discharged was achieved the key from both the valves were removed so that nobody can turn the keys anymore.

Step 2:

After selecting the discharge the pump should be stopped and the sand feeder should be checked. Even though the sand feeders were calibrated it should be checked before every run to check whether they feed sand according to the calibration charts. From the calibration chart, the speed of the sand feeder was found with respect to the calculated amount of the sand. Then the sand feeder was checked three times, whether at that speed it drops the desired amount of sediment. After that the sand feeder was stopped and water was allowed to drain out from the temporary part of the model. This was done to dry the sand lying on the channel bed.

Step 3:

Before doing an experiment on the model it is very important to prepare the bed. The bed preparation has always been done after fixing the discharge, because in this way, the prepared bed will not be disturbed. The discharge would be fixed such that the flow velocity must be lower than that value at which the inception motion of the bed particles occurs. That means the flow discharge would be such that the prepared bed should not be disturbed. The flow velocity at which inception motion of the bed particles occurs is obtained from Shields diagram. If the bed is prepared before fixing the discharge, the bed may be completely destroyed while adjusting the desired discharge. During the preparation of the bed the sediment should be dry enough otherwise, it is not possible to prepare the desired bed level.

Step 4:

After preparing the bed the tail gate was lifted to its maximum position. This is done because, the next thing is to fill the temporary part of the model with water, so, no water should be allowed to pass over the tail gate.

Step 5:

Once the bed is prepared, the channel is filled with water. This step has to be done very carefully because a slight mistake can damage the prepared bed: By the help of a half horse power pump the sand trap was filled up to the concrete floor of the channels. When the water level reaches the floor level of the branches the sand traps were filled very slowly so that the bed is not disturbed.

Step 6:

When the channels are filled with water all the measuring instruments were checked, whether these were working well with reference to any arbitrary water level. The pitot tube of stilling basin was checked and also the silo of the sand feeder was checked whether it is filled with sand or not.

Step 7:

Now the pump was started and water allowed rising in the temporary part of the model. Care was taken so that the pump and the sand feeders were started more or less at the same time.

Step 8:

The tail gate was opened very slowly to the desired level. The tail gate should be opened at the same time and with care so that there is no sudden disturbance in the bed of the channel.

Step 9:

After setting the tail gate to their desired level readings of the Rehbock weir was taken after about 20 minutes of running the model and the discharge was checked whether the model was running with the desired discharge.

Step 10:

After completing the above steps the model was allowed to run for 4 hours. Then the tail gate was raised to its maximum position very slowly and then the pump was stopped. The tail gate was raised very slowly so that there was no disturbance in the channel beds. The sand feeder was also stopped at the same time.

Step 11:

When the model was stopped, time was given for the water level to settle. Water from the sand trap was siphoned by the help of two plastic pipes. Care was taken so that no sediment was siphoned out. After the water was siphoned out from the sand trap the sediment was collected and weighed. This was the amount of sediment that passed through the channel for that particular run time.

Step 12:

After taking the sediment from the sand traps the sand was allowed to dry for several days and then it was ready for the next run. The weight of sediment is divided by the run time and the average sediment transport rate, q_s is calculated for that particular run.

Sixteen such runs were done with different discharges and of different run time. Finally the values of all q_s and u are plotted in a log-log graph paper. From this graph paper the value of a' and 'b' is calculated (Fig. 5.1). The experimental data are given in Table 5.2.

5.2.2 Measurement of Bed Level Changes

In order to have good experiments proper handling of both the temporary and permanent part of the model is required. During an experimental run following things are done:

The steps 1 through 6 of the previous article are followed exactly. Then following steps are done:

Step 1:

When the channel is filled up with water, it is time to take the initial bed level reading. The bed level reading was taken by point gauge. Five readings were taken at each section. The channel was 11 m long and the readings were taken at 22 sections of 0.5 m interval.

Step 2:

The rate at which the sand feeders would discharge was calculated for a particular flow velocity that should be governed in a particular run. Now the pump was started and water allowed rising in the temporary part of the model. Care was taken so that the pump and the sand feeders were started more or less at the same time. The sediment discharge rates of the sand feeders were set with the predetermined sediment ratio value.

Step 3:

The tail gate was opened very slowly to the desired level. The tail gate should be opened at the same time and with care so that there is no sudden disturbance in the bed of the branches.

Step 4:

After setting the tail gate to their desired level readings of the Rehbock weir was taken after about 20 min. of running the model and the discharge was checked whether the model was running with the desired discharge.

Step 5:

After completing the above steps the model was allowed to run for 1 hour. Then the tail gate was raised to its maximum position very slowly and then the pump was stopped. The tail gate was raised very slowly so that there was no disturbance in the channel beds. The sand feeder was also stopped at the same time.

Step 6:

When the model was stopped, about half an hour time was given for the water level to settle. Then the bed level reading was taken. This was done in the same process as before (step 1) and that gave the final bed level reading.

Step 7:

The steps 2 through 6 are repeated and the run is done for another hour. Then the final bed level reading is taken. This is the cumulative bed level for 2 hours running. In the same procedure, the bed level elevation readings are taken for 3 hours running and 4 hours running.

Fifteen such 4 hours runs were carried out with different bed slope, different flow discharge and different sediment ratio. The channel bed elevation was measured after each run. The input data for fifteen runs are given in Table 5.3. The results of such runs are discussed in next chapter.

CHAPTER SIX

DATA ANALYSIS, RESULTS AND DISCUSSIONS

6.1 Introduction

The mathematical model has been applied to the laboratory investigation in order to demonstrate its capability. The detail of the data analysis and results of the experimental investigation in the laboratory is discussed in this chapter.

6.2 Laboratory Application

In order to obtain information on bed surface profiles under transient conditions, experiments were carried out. The experiments were conducted in the physical model setup of Hydraulics and River Engineering Laboratory of Water Resources Engineering Department, Bangladesh University of Engineering and Technology, Dhaka. This setup is a straight channel of length 11 meters, width 1 meter and height 0.61 meter. Both of the channel banks are vertical and fixed. Water discharge was controlled by a valve and discharge was measured by means of a Rehbock weir. The detail of the Rehbock weir and its accuracy is shown in Appendix-A and Appendix-B respectively. The sieve analysis of the sand forming the bed and injected material was done. The median diameter of the sand was 0.285 mm (Fig. 4.14 and Table 5.1) and the value of the coefficient of uniformity was 2. That means the sand used herein was uniformly graded.

6.2.1 Determination of Sediment Transport Constants

To calibrate the sediment transport law, $q_s = a(u)^b$, 16 experimental runs were conducted with different discharges (q), and of different duration (t). After each run, sediment transported by water flow that deposited in the sand trap was collected. Then it was dried and weighted. This weight value divided by the duration of the run give the value of q_s.

Finally the values of q_s and u for such 16 runs are plotted in a log-log graph paper. From this graph paper the value of a' and 'b' is calculated (Fig. 5.1). The best fit line drawn through these points yielded values of 'a' and 'b' as 0.00205 and 5.25, respectively for the sediment size used in the study. These values of 'a' and 'b' are used in the mathematical model. The very small portion of the sediment suspended in the flow and passed over the tail gate was not measured.

6.2.2 Determination of bed level changes

After the establishment of uniform flow conditions for a given discharge and slope, the sediment supply rate was increased to a predetermined value by continuously feeding excess sediment at the upstream end of the channel at a constant rate. The excess sediment load was progressively deposited in the channel. Fifteen experimental runs were carried out for different discharge (q), different bed slope (S_0) and different sediment over loading ratio. Water discharge variation was within the range of 18 l/s to 20 l/s. Flow discharge was selected with the consideration of maximum feeding capacity of two sand feeders. The slope of the channel bed was varied from 0.00272 to 00454. The rate of sediment addition was varied from $0.5q_{s0}$ to $5q_{s0}$, where q_{s0} is the sediment transport rate for a particular run. Each run was conducted for 4 hours duration. The Manning n was considered as 0.022 and the porosity p of the sediment bed layer was taken as 0.4. The input data for experimental and numerical runs are given in Table 5.3. The bed surface profiles were recorded by using a point gauge with a flat bottom at 23 sections of the 11 m long channel at 0.5 m interval of length. Five readings of bed elevation were taken at every section and average value of these five readings was considered as the bed elevation of that section. There was no such variation of bed form along the channel length. That's why the bed form was not considered.

The mathematical model was used by dividing the channel with a total length of 11m into 22 reaches (Δx = 0.5 m). The computational time step Δt was selected according to the Courant-Friedrichs-Lewy (CFL) condition for stability, for this case it was taken to be Cn = 0.85.

6.3 Laboratory Study Evaluation

6.3.1 Sediment transport equation

Numerous theoretical and semi-empirical approaches have been developed for the calculation of sediment transport rates, for example, Einstein (1950), Yalin (1963), Bagnold (1966), Engelund-Hansen (1967), Ackers & White (1973), Yang (1973), Van Rijn (1984), Hossain (1985) – mainly based on observation on laboratory experimental flumes and small streams. However, few attempts were met to test their applicability in large sand bed rivers, where the river morphology may strongly control the transport rates. A formula that predicts sediment discharges accurately for one river does very poorly for the other river. In the following tables the expressions of exponent 'b' for each total load and bed load formula are given:

Total load formula	Expression for exponent 'b'
Ackers & White (1973)	$b = 1 + \dfrac{m}{1 - \dfrac{Y_{cr}}{Y}}$
Bagnold (1966)	$b = 3 + \dfrac{1}{1 + \dfrac{e_b}{e_s(1-e_b)\tan\phi} \cdot \dfrac{\gamma_s}{c\sqrt{\Delta d_{50}\theta}}}$
Colby (1957)	$b = 3.1$
Engelund-Hansen (1967)	$b = 5$
Hossain (1985)	$b = 3.25$
Van Rijn (1984), original	$b = 3 + \dfrac{3}{1 - \dfrac{\theta_{cr}}{\theta}(\dfrac{c'}{c})^2}$
Van Rijn (1984), simplified	$b = 3 + \dfrac{2.4}{c\dfrac{\sqrt{\Delta d_{50}\theta}}{u_{cr}} - 1}$
Yang (1973)	$b = 6.397 - 1.227\log\left(\dfrac{w_s d_{50}}{\nu}\right) - 0.942\log\left(\dfrac{\sqrt{g\Delta d_{50}\theta}}{w_s}\right)$

Bed load formula	Expression for exponent 'b'
Meyer-Peter & Mueller (1948)	$b = \dfrac{3}{1 - \dfrac{0.047}{\mu\theta}}$
Van Rijn (1984), original	$b = 1 + \dfrac{3}{1 - \dfrac{\theta_{cr}}{\theta}(\dfrac{c'}{c})^2}$
Van Rijn (1984), simplified	$b = 0.6 + \dfrac{2.4}{c\dfrac{\sqrt{\Delta d_{50}\theta}}{u_{cr}} - 1}$
Parker & Klingeman (1982)	$b = 3\left[\dfrac{\phi_{50} + 1.644}{\phi_{50} - 0.822}\right]$

Theoretical analysis on the exponent of the flow velocity of the various sediment transport equations reveals that the value of the exponent 'b' for alluvial rivers ranges between 3.1 to 8.5 for the total load transport and 3.3 to 10.5 for bed load transport. In this study, the value of 'b' is found as 5.25, which is within the range.

6.3.2 Bed level changes

The definition sketch of bed profile is shown in Fig. 6(a). Consider a uniform flow with a mean flow velocity *u* and mean flow depth *h* in a wide rectangular alluvial channel as shown in the above figure. The equilibrium sediment transport rate under the uniform flow condition is equal to q_{s0} and the bed slope is S_0. Let the sediment supply rate at a section x = 0 be increased at a constant rate Δq_s. The bed level for $x \geq 0$ will rise with time due to increase in the sediment load. The differential equation for bed level obtained by Soni et al. (1980) is

$$\frac{\partial Z}{\partial t} = K\ \frac{\partial^2 Z}{\partial x^2} \qquad (6.1)$$

Here the aggradation coefficient

$$K = \frac{1}{3} \frac{u \frac{\partial q}{\partial u}}{S_0 (1-\lambda)} \left(\frac{u_0}{u} \right)^3 \qquad (6.2)$$

In Eqs. 6.1 and 6.2

Z = depth of deposition at time t at a distance x from the origin

λ = the porosity of the sediment

b = the exponent in the sediment transport law

u_0 = the mean velocity under the initial uniform flow condition

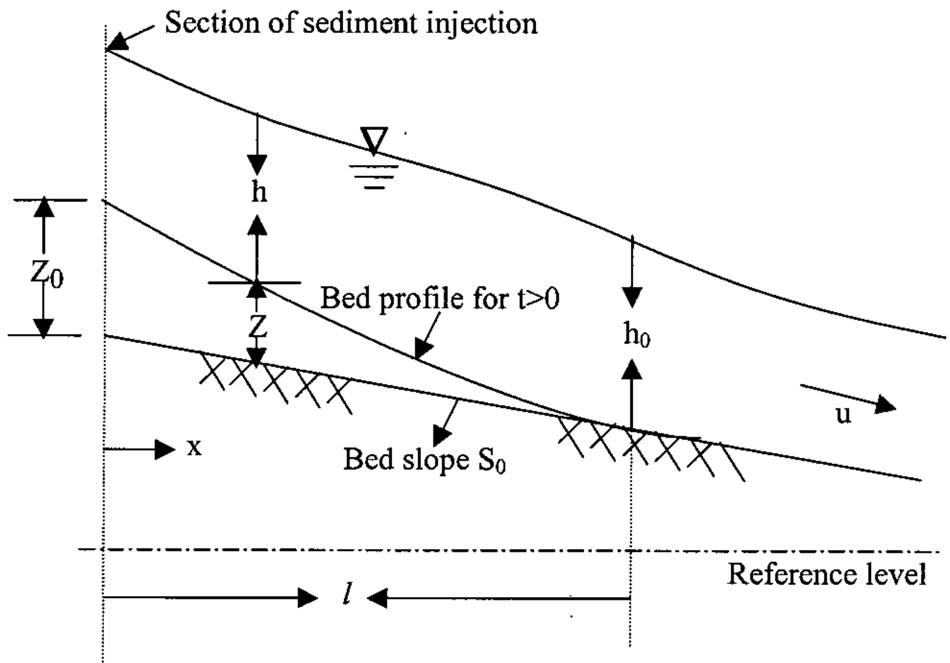

Fig. 6(a) Definition sketch of bed profile

Using the approximation $u \approx u_0$ and combining equation $q_s = au^b$ and the Eq. (6.2) and further designating the equilibrium sediment transport rate as q_{s0}, one gets the theoretical value of the aggradation coefficient, K_0, as

$$K_0 = \frac{1}{3} \frac{b q_{s0}}{S_0 (1-\lambda)} \qquad (6.3)$$

For a constant value of K, Eq. 6.1 can be solved for the following boundary conditions:

$Z(x,0) = 0$; for all x

$Z(0,t) = Z_0$; for all $t>0$

$Z(x,t) = 0$; for $x \rightarrow \infty$ for $t>0$

Substituting $\eta = x/2\sqrt{Kt}$ and $Z/Z_0 = f(\eta)$, Eq. 6.1 can be reduced to the ordinary differential equation: $f'' + 2\eta f' = 0$.

Two different types of plot have been produced after the successful application of the model to the laboratory study. The first type depicts transient bed surface profiles of the channel. While the other type is a dimensionless plot that shows variation of relative aggradation with distance downstream.

Fig. 6.1 through Fig. 6.15 has peen plotted from the model output of 15 different test conditions. Each of the figures shows equilibrium and transient bed profile for 1 hr., 2 hr., 3 hr. and 4 hr. The following results are evident from these plots.

1. Length of aggradation increases spatially with time.

2. The ordinate of the bed profile is decreasing with increase in distance.

3. The depth of aggradation at a location increases with time.

These figures compare the actual data points, observed mean bed surface profiles along with computed profiles from the model. Averaging of the actual data points of these profiles was required because of the presence of ripples and dunes on the bed. The variation of bed formed may be large if smaller sediment size is used. In this case the bed elevation should be taken at close interval of channel length to get the more accurate bed profile. The comparison with the computed profiles shows good result with the average transient profile. Close agreements are found between the experimental and computed values of the bed surface profiles. Experimental and numerical data are given in Table 6.1 through Table 6.15.

6.3.3 Length of aggradation

From Fig. 6(a) it is seen that at a given time the aggradation depth, Z, downstream of the section of increased sediment supply rate, decreases asymptotically in the longitudinal direction. However the region of asymptotic change in Z is taken to end at a section beyond which the change in Z does not exceed some prescribed value. In that case the length of aggradation, *l*, shall be a distance between the section of increased sediment supply rate and the section where the aggradation is assumed to end.

Assuming aggradation ends where $Z/Z_0 = 0.01$, a usual assumption made in problems having asymptotic behavior, e.g., as a boundary layer theory one gets

$$l = 3.2\sqrt{K_0 t} \qquad (6.4)$$

The non dimensional bed profile $[Z/Z_0]$ as a function of non dimensional distance $[x/2\sqrt{(Kt)}]$ for the 9 test runs are shown in Figs. 6.16 to Fig. 6.24. The experimental results show more or less good agreement with the computed values of aggradation. However, the overall performance of the model in this laboratory observation is satisfactory.

6.4 Limitation of this study

The following limitation can be drawn from this study:

- From the bed profiles it is seen that the full length of aggradation does not occur within the channel length. So the downstream boundary condition of constant water depth at the channel end is not satisfied. That is why one should use longer channel than that used herein the study.

CHAPTER SEVEN

CONCLUSIONS AND RECOMMENDATIONS

7.1 Conclusions

In this study the change in bed level of alluvial river is studied with laboratory investigation as well as application of a one-dimensional mathematical model based on MacCormack scheme. The following conclusions can be made after summarizing the present study:

a) In the mathematical model, one-dimensional, unsteady, gradually varied flow equations and the sediment continuity equation are solved numerically by the second-order-accurate, explicit finite difference scheme developed by MacCormack. A simple equation for the sediment discharge as a power function of flow velocity is used.

b) The numerical model was applied to simulate the bed level changes of alluvial channel due to sediment overloading. The computed results were compared with the experimental data. The agreement between them is satisfactory.

c) The sediment transport equation $q_s = au^b$ is calibrated through experimental runs and the value of the coefficient 'a' and 'b' is determined, which are used in the mathematical model. The value of 'a' and 'b' are 0.00205 and 5.25 respectively.

d) Close agreement between the computed results and measured data justifies that the model can applied to any alluvial river problem where there is no significant change in the bed form.

7.2 Recommendations for future study

Based on the present study the following recommendations can be made for future study that may produce better results.

a) This study evaluates the bed level changes due to aggradation caused by sediment over loading. The degradation study not done herein. One can use this model and study the degradation of bed level.

b) The present study does not represent any particular river bed level change. It deals with laboratory cases and the relations developed herein have not been compared to real field situation. This study may be applied for a particular alluvial river to check its accuracy with real field situation.

c) The MacCormack scheme can be applied to develop a two-dimensional model to study the two-dimensional problems and also a three-dimensional model to study three-dimensional problem.

REFERENCES

REFERENCES

1. Alam, M. (1998). "Application of MacCormack scheme to the study of aggadation-degradation in alluvial channels." M.Sc. Engineering thesis work, Department of Water Resources Engineering, BUET, Dhaka.

2. Begin, Z.B. (1981). "Development of longitudinal profiles of alluvial channels in response to base-level lowering." *Earth Surface Processes and Land Forms*, Vol. 6, No. 1, pp.46-68.

3. Bhamidipaty, S.; and Shen, H.W. (1971). " Laboratory study of degradation and aggradation." *Journal of Waterways, Harbor and Coastal Engineering Division*, ASCE., Vol. 97, No. 4, pp. 615-630.

4. Bhallamudi, S.M.; Chaudhry, M. H. (1991). "Numerical modeling of aggradation and degradation in alluvial channels." *Journal of Hydraulic Engineering*, ASCE, Vol. 117, No. HY9, pp. 1145-1164.

5. .Chaudhry, M.H. (1993). *Open Channel Flow.* Prentice-Hall, Englewood- Cliffs, N .J .

6. Dey, K.C. (1995). "Schematised sediment transport predictor for study of alluvial rivers: An application to the Jamuna." M.Sc. Engineering thesis work, Department of Water Resources Engineering, BUET, Dhaka.

7. Depeweg, H.; and Mendez, N. (2002). "Sediment transport applications in irrigation canals." *Journal of Irrigation and Drainage,* Vol. 51, pp. 167-179.

8. .Gill, M.A. (1983a). "Diffusion model for aggrading channels." *Journal of Hydraulic Research*, IAHR, Vol. 21, No. 5, pp. 355-367.

9. Gill, M.A. (1983b). "Diffusion model for degrading channels." *Journal of Hydraulic Research*, IAHR, Vol. 21, No. 5, pp. 369-378.

10. Gill, M.A. (1987). "Nonlinear solution of aggradation and degradation in channels." *Journal of Engineering Mechanics*, IAHR, Vol. 25, No. 5, pp. 537-547.

11. Gill, M.A. (1988). "Hyperbolic model for aggrading channels." *Journal of Hydraulic Research*, ASC, Vol. 114, No. 7, pp. 1245-1255.

12. Hannan, A. (1995). "A laboratory study of sediment distribution at channel bifurcation." M.Sc. Engineering thesis work, Department of Water Resources Engineering, BUET, Dhaka.

13. Hossain, M..M. (1991). "Problems of Erosion and Deposition in the Major Rivers of Bangladesh." *Proceedings of the International Symposium on Special problems of Alluvial Rivers including those of International Rivers*, Seoul, Korea, pp. 247-255.

14. Islam, M. (1993). "Numerical simulation of bed level changes of the Ganges." M. Engineering project work, Department of Water Resources Engineering, BUET, Dhaka.

15. Jain, S.C. (1981). "River bed aggradation due to over loading." *Journal of Hydraulic Engineering*, ASCE, Vol. 107, No. HY1, pp. 120-124.

16. Jaramillo, W.F.; and Jain, S.C. (1984). "Aggradation and degradation of alluvial channel beds." *Journal of Hydraulic Engineering*, ASCE, Vol. 110, No. HY8, pp. 1072-1085.

17. Jain, S.C.; and Park, I. (1986). "River-bed profiles with imposed sediment load." *Journal of Hydraulic Engineering,* ASCE., Vol. 112, No.4, pp. 267-279.

18. Jain, S.C.; and Park, I. (1987). "Numerical simulation of degradation of alluvial channel beds." *Journal of Hydraulic Engineering,* ASCE., Vol. 113,No. 7,pp. 845-859.

19. Jain, S.C.; and Park, I. (1989). " Guide for estimating river bed degradation." *Journal of Hydraulic Engineering*, ASCE, Vol. 115, No. HY3, pp. 356-367.

20. Kamrunnessa (1994), "A study of the geometric and sediment transport characteristics of the River Surma." M. Engineering project work, Department of Water Resources Engineering, BUET, Dhaka.

21. Nahar, Q. (1991), " A numerical approach to study erosion-deposition in a river reach." M.Sc. Engineering thesis work, Department of Water Resources Engineering, BUET, Dhaka.

22. Soni, J.P.; Garde, R.J.; and Raju, K.G.R. (1980). "Aggradation in streams due to overloading." *Journal of the Hydraulics Division, ASCE*, Vol. 106, No. HY1, pp. 117-132.

23. Yen, C.L; Chang, S.Y.; and Lee, H.Y. (1989). "Recovery of channel bed in aggradation-degradation process." *Proceedings, 23rd congress of IAHR,* Ottawa, Canada, pp. B323-B329.

24. Yen, C.L; Chang, S.Y.; and Lee, H.Y. (1992). "Aggradation-degradation process in alluvial channels." *Journal of Hydraulic Engineering*, ASCE, Vol. 118, No. HY12, pp. 1651-1669.

25. Zhang, H.; and Kahawita, R. (1987). "Non linear model for aggradation in alluvial channels." *Journal of Hydraulic Engineering,* ASCE., Vol. 113, No.3, pp. 353-369.

TABLES

Table 5.1: Grain Size Distribution

Sieve Size (mm)	sieve + soil (gm)	Sieve (gm)	Amount Retained (gm)	% retained	Cumulative % retained	% finer
1.18	384.6	384.4	0.2	0.04	0.04	99.96
0.6	375.3	370.6	4.7	0.94	0.98	99.02
0.3	559.9	331	228.9	45.78	46.76	53.24
0.15	555.5	310.3	245.2	49.04	95.8	4.2
0.075	314.1	295.2	18.9	3.78	99.58	0.42
pan	316.7	314.6	2.1	0.42	100	0
		Total	***500***	***100***		

Table 5.2: Data to determine the values of 'a' and 'b' in sediment transport law

Run	Flow velocity(u) m/s	q_s (kg/hr)	q_s (kg/s)	q_s (cu.m/s)
1	0.08	0.03	7.95E-06	6.85E-09
2	0.112	0.04	1.16E-05	1.00E-08
3	0.12	0.18	4.93E-05	4.25E-08
4	0.132	0.53	1.47E-04	1.27E-07
5	0.143	0.15	4.11E-05	3.54E-08
6	0.15	0.33	9.14E-05	7.88E-08
7	0.165	1.82	5.06E-04	4.36E-07
8	0.171	0.53	1.48E-04	1.27E-07
9	0.184	1.23	3.43E-04	2.95E-07
10	0.192	0.94	2.60E-04	2.24E-07
11	0.22	3.14	8.73E-04	7.52E-07
12	0.25	19.28	5.36E-03	4.62E-06
13	0.27	16.79	4.67E-03	4.02E-06
14	0.3	7.80	2.17E-03	1.87E-06
15	0.32	13.26	3.68E-03	3.17E-06
16	0.35	24.38	6.77E-03	5.84E-06

Table 5.3: Input data for experimental and numerical runs

Run No:	NSEC	T (sec.)	CHL (m)	n	So	q (m /s)	y(m)	Sed. Ratio
1	22	14400	11	0.022	0.00272	0.02	0.07	4
2	22	14400	11	0.022	0.00272	0.02	0.072	3
3	22	14400	11	0.022	0.00272	0.02	0.068	2
4	22	14400	11	0.022	0.00272	0.02	0.71	1
5	22	14400	11	0.022	0.00272	0.02	0.07	0.5
6	22	14400	11	0.022	0.00363	0.019	0.06	4
7	22	14400	11	0.022	0.00363	0.019	0.062	3
8	22	14400	11	0.022	0.00363	0.019	0.059	2
9	22	14400	11	0.022	0.00363	0.019	0.06	1
10	22	14400	11	0.022	0.00363	0.019	0.06	0.5
11	22	14400	11	0.022	0.00454	0.018	0.05	4
12	22	14400	11	0.022	0.00454	0.018	0.052	3
13	22	14400	11	0.022	0.00454	0.018	0.05	2
14	22	14400	11	0.022	0.00454	0.018	0.049	1
15	22	14400	11	0.022	0.00454	0.018	0.05	0.5

Table 6.1: Bed elevation (m) for Run 1

	Numerical					Experimental			
X (m)	T=0	T=1hr	T=2 hr	T=3 hr	T=4 hr	T=1hr	T=2 hr	T=3 hr	T=4 hr
0	0.2	0.21258	0.2187	0.22362	0.23017	0.215	0.220	0.226	0.233
0.5	0.19864	0.21083	0.21646	0.22144	0.22816	0.213	0.218	0.223	0.231
1	0.19728	0.20866	0.21449	0.21938	0.22607	0.211	0.216	0.222	0.229
1.5	0.19592	0.20651	0.21244	0.21738	0.22407	0.209	0.214	0.219	0.227
2	0.19456	0.20496	0.21026	0.21526	0.2221	0.207	0.212	0.217	0.225
2.5	0.1932	0.20253	0.20857	0.21345	0.22005	0.205	0.211	0.215	0.221
3	0.19184	0.19995	0.20651	0.21141	0.21823	0.202	0.208	0.213	0.219
3.5	0.19048	0.19901	0.20446	0.20952	0.21613	0.199	0.206	0.211	0.217
4	0.18912	0.19735	0.20297	0.20785	0.21437	0.195	0.204	0.209	0.216
4.5	0.18776	0.19348	0.20066	0.20569	0.21229	0.191	0.199	0.207	0.214
5	0.1864	0.1898	0.19869	0.2041	0.21037	0.189	0.196	0.204	0.212
5.5	0.18504	0.1875	0.19762	0.20227	0.2086	0.186	0.194	0.202	0.209
6	0.18368	0.18591	0.19514	0.20007	0.20624	0.185	0.192	0.200	0.206
6.5	0.18232	0.18454	0.19265	0.19889	0.20483	0.184	0.190	0.199	0.205
7	0.18096	0.18318	0.19223	0.19683	0.20229	0.182	0.187	0.196	0.202
7.5	0.1796	0.18186	0.19068	0.19454	0.20062	0.181	0.186	0.193	0.199
8	0.17824	0.18051	0.18647	0.19386	0.199	0.180	0.184	0.191	0.197
8.5	0.17688	0.17916	0.18263	0.1917	0.19595	0.177	0.181	0.189	0.194
9	0.17552	0.17778	0.18033	0.18861	0.19518	0.176	0.179	0.186	0.192
9.5	0.17416	0.17641	0.17872	0.18866	0.19249	0.175	0.177	0.184	0.190
10	0.1728	0.17498	0.17731	0.18737	0.19008	0.173	0.176	0.182	0.188
10.5	0.17144	0.17355	0.17587	0.1832	0.18835	0.172	0.175	0.180	0.186
11	0.17008	0.17212	0.17443	0.17902	0.18663	0.171	0.173	0.176	0.184

Table 6.2: Bed elevation (m) for Run 2

	Numerical					Experimental			
X (m)	T=0	T=1hr	T=2 hr	T=3 hr	T=4 hr	T=1hr	T=2 hr	T=3 hr	T=4 hr
0	0.2	0.20753	0.21117	0.21468	0.21813	0.209	0.212	0.215	0.220
0.5	0.19864	0.20571	0.20955	0.21299	0.21636	0.207	0.211	0.214	0.217
1	0.19728	0.20421	0.20786	0.21126	0.21463	0.206	0.209	0.212	0.215
1.5	0.19592	0.20228	0.20613	0.20967	0.21286	0.204	0.207	0.210	0.213
2	0.19456	0.20047	0.20463	0.20792	0.21131	0.202	0.206	0.209	0.211
2.5	0.1932	0.19926	0.20291	0.20624	0.20963	0.201	0.204	0.206	0.210
3	0.19184	0.19759	0.20104	0.20481	0.20796	0.198	0.202	0.205	0.208
3.5	0.19048	0.19496	0.19968	0.20304	0.20647	0.195	0.201	0.203	0.206
4	0.18912	0.19232	0.19822	0.20141	0.20474	0.192	0.199	0.201	0.204
4.5	0.18776	0.19027	0.19614	0.20007	0.20321	0.189	0.196	0.199	0.203
5	0.1864	0.18869	0.19447	0.19829	0.20182	0.188	0.194	0.197	0.201
5.5	0.18504	0.18729	0.19356	0.19656	0.19999	0.186	0.192	0.196	0.199
6	0.18368	0.18593	0.19205	0.19548	0.19858	0.185	0.190	0.194	0.199
6.5	0.18232	0.18458	0.18937	0.1938	0.19727	0.184	0.187	0.192	0.196
7	0.18096	0.18322	0.18662	0.19163	0.19525	0.182	0.185	0.190	0.194
7.5	0.1796	0.18187	0.18448	0.19044	0.1939	0.181	0.183	0.187	0.192
8	0.17824	0.18047	0.18289	0.1897	0.19286	0.179	0.182	0.186	0.191
8.5	0.17688	0.17906	0.18144	0.18754	0.19067	0.178	0.181	0.184	0.189
9	0.17552	0.17766	0.18006	0.18434	0.18871	0.177	0.179	0.181	0.187
9.5	0.17416	0.17623	0.17859	0.18164	0.18833	0.175	0.178	0.181	0.185
10	0.1728	0.17482	0.17708	0.17967	0.18679	0.174	0.176	0.179	0.183
10.5	0.17144	0.17339	0.17555	0.178	0.18368	0.172	0.175	0.177	0.180
11	0.17008	0.17196	0.17402	0.17634	0.18057	0.171	0.173	0.175	0.177

Table 6.3: Bed elevation (m) for Run 3

	Numerical					Experimental			
X (m)	T=0	T=1hr	T=2 hr	T=3 hr	T=4 hr	T=1hr	T=2 hr	T=3 hr	T=4 hr
0	0.2	0.20656	0.20986	0.21294	0.21666	0.207	0.211	0.215	0.219
0.5	0.19864	0.20466	0.20815	0.21129	0.2149	0.205	0.209	0.213	0.217
1	0.19728	0.20307	0.2065	0.2096	0.21317	0.204	0.207	0.211	0.215
1.5	0.19592	0.20135	0.20478	0.20795	0.21147	0.202	0.206	0.209	0.212
2	0.19456	0.19948	0.20316	0.20635	0.20974	0.200	0.204	0.208	0.211
2.5	0.1932	0.19797	0.2016	0.20467	0.20811	0.198	0.202	0.206	0.209
3	0.19184	0.19656	0.19988	0.20305	0.20641	0.197	0.201	0.205	0.208
3.5	0.19048	0.19464	0.19819	0.20154	0.20477	0.195	0.199	0.202	0.206
4	0.18912	0.19236	0.19676	0.19989	0.2032	0.193	0.198	0.201	0.204
4.5	0.18776	0.19027	0.1952	0.19828	0.20155	0.191	0.196	0.199	0.202
5	0.1864	0.18854	0.19335	0.19686	0.19999	0.189	0.194	0.198	0.201
5.5	0.18504	0.18707	0.19179	0.19521	0.19852	0.187	0.192	0.195	0.199
6	0.18368	0.18575	0.19059	0.19357	0.19685	0.186	0.189	0.194	0.197
6.5	0.18232	0.18441	0.18908	0.19225	0.19538	0.184	0.188	0.192	0.195
7	0.18096	0.18307	0.18697	0.19076	0.19397	0.183	0.186	0.189	0.192
7.5	0.1796	0.18174	0.18476	0.18894	0.19227	0.181	0.184	0.188	0.191
8	0.17824	0.18041	0.18292	0.18741	0.1907	0.180	0.183	0.186	0.189
8.5	0.17688	0.17909	0.18135	0.18631	0.18951	0.178	0.181	0.185	0.188
9	0.17552	0.1778	0.17995	0.18484	0.18776	0.176	0.180	0.183	0.186
9.5	0.17416	0.17644	0.17859	0.1827	0.18592	0.175	0.178	0.181	0.184
10	0.1728	0.17509	0.17725	0.18038	0.18483	0.173	0.177	0.180	0.183
10.5	0.17144	0.17372	0.17589	0.17853	0.1833	0.172	0.175	0.178	0.182
11	0.17008	0.17234	0.17454	0.17667	0.18177	0.170	0.174	0.176	0.180

Table 6.4: Bed elevation (m) for Run 4

	Numerical					Experimental			
X (m)	T=0	T=1hr	T=2 hr	T=3 hr	T=4 hr	T=1hr	T=2 hr	T=3 hr	T=4 hr
0	0.2	0.19889	0.20034	0.20204	0.2037	0.199	0.201	0.202	0.204
0.5	0.19864	0.19794	0.1992	0.20077	0.20247	0.198	0.200	0.201	0.203
1	0.19728	0.19666	0.19793	0.19952	0.2012	0.197	0.198	0.200	0.202
1.5	0.19592	0.19544	0.19673	0.19827	0.19995	0.195	0.197	0.198	0.200
2	0.19456	0.1945	0.19558	0.19703	0.19873	0.195	0.196	0.197	0.199
2.5	0.1932	0.19375	0.19439	0.19578	0.19747	0.194	0.195	0.196	0.198
3	0.19184	0.19295	0.19316	0.19456	0.19621	0.193	0.193	0.195	0.196
3.5	0.19048	0.19202	0.19195	0.19342	0.19505	0.192	0.192	0.193	0.195
4	0.18912	0.19097	0.19091	0.19228	0.19372	0.191	0.191	0.192	0.194
4.5	0.18776	0.18979	0.18999	0.19107	0.19259	0.190	0.190	0.191	0.192
5	0.1864	0.18851	0.18913	0.18984	0.19138	0.189	0.189	0.190	0.191
5.5	0.18504	0.18718	0.18828	0.18869	0.19018	0.187	0.186	0.189	0.188
6	0.18368	0.18584	0.18739	0.18764	0.189	0.186	0.185	0.188	0.187
6.5	0.18232	0.18452	0.18636	0.18671	0.18777	0.185	0.184	0.187	0.186
7	0.18096	0.18321	0.18523	0.18587	0.1866	0.183	0.183	0.186	0.184
7.5	0.1796	0.18186	0.18398	0.18498	0.18554	0.182	0.182	0.185	0.183
8	0.17824	0.18051	0.18264	0.18412	0.18457	0.181	0.180	0.184	0.182
8.5	0.17688	0.17914	0.18127	0.18315	0.18363	0.179	0.179	0.183	0.181
9	0.17552	0.17777	0.17993	0.18196	0.18289	0.178	0.177	0.182	0.180
9.5	0.17416	0.17632	0.1786	0.18067	0.18199	0.176	0.176	0.181	0.179
10	0.1728	0.17489	0.17722	0.17936	0.18104	0.175	0.175	0.179	0.178
10.5	0.17144	0.1735	0.17573	0.17791	0.17983	0.173	0.173	0.178	0.177
11	0.17008	0.1721	0.17424	0.17647	0.17863	0.172	0.172	0.176	0.176

Table 6.5: Bed elevation (m) for Run 5

	Numerical					Experimental			
X (m)	T=0	T=1hr	T=2 hr	T=3 hr	T=4 hr	T=1hr	T=2 hr	T=3 hr	T=4 hr
0	0.2	0.19622	0.19709	0.19806	0.19927	0.196	0.199	0.202	0.200
0.5	0.19864	0.1953	0.19582	0.19688	0.19822	0.195	0.198	0.201	0.199
1	0.19728	0.19411	0.19471	0.19585	0.19708	0.194	0.197	0.200	0.198
1.5	0.19592	0.19342	0.19378	0.19472	0.19595	0.193	0.196	0.198	0.196
2	0.19456	0.19309	0.19275	0.19361	0.1948	0.193	0.195	0.197	0.195
2.5	0.1932	0.19279	0.19166	0.19259	0.19368	0.193	0.194	0.196	0.194
3	0.19184	0.19233	0.19072	0.19158	0.1926	0.192	0.192	0.195	0.193
3.5	0.19048	0.19164	0.18999	0.19049	0.19147	0.192	0.191	0.193	0.192
4	0.18912	0.19071	0.1894	0.18943	0.19046	0.191	0.190	0.192	0.191
4.5	0.18776	0.18963	0.18885	0.18842	0.18945	0.190	0.189	0.191	0.189
5	0.1864	0.18843	0.1883	0.18761	0.18839	0.188	0.188	0.190	0.188
5.5	0.18504	0.18715	0.18763	0.18688	0.18727	0.187	0.186	0.189	0.185
6	0.18368	0.18582	0.1869	0.18626	0.18631	0.186	0.185	0.188	0.184
6.5	0.18232	0.18449	0.18602	0.18564	0.18545	0.184	0.184	0.187	0.183
7	0.18096	0.18319	0.185	0.18502	0.18471	0.183	0.183	0.186	0.183
7.5	0.1796	0.18185	0.18387	0.18434	0.18404	0.182	0.181	0.185	0.182
8	0.17824	0.18051	0.18262	0.18356	0.18342	0.181	0.180	0.184	0.181
8.5	0.17688	0.17917	0.18128	0.18274	0.18275	0.179	0.179	0.183	0.180
9	0.17552	0.1778	0.17992	0.18178	0.18209	0.178	0.177	0.182	0.179
9.5	0.17416	0.17642	0.17858	0.18059	0.18136	0.176	0.176	0.181	0.179
10	0.1728	0.17498	0.17725	0.17936	0.18063	0.175	0.175	0.179	0.178
10.5	0.17144	0.17356	0.17584	0.17796	0.1796	0.174	0.173	0.178	0.177
11	0.17008	0.17213	0.17444	0.17656	0.17856	0.172	0.172	0.176	0.176

Table 6.6: Bed elevation (m) for Run 6

	Numerical					Experimental			
X (m)	T=0	T=1hr	T=2 hr	T=3 hr	T=4 hr	T=1hr	T=2 hr	T=3 hr	T=4 hr
0	0.2	0.21863	0.22875	0.23896	0.24921	0.222	0.232	0.242	0.253
0.5	0.19819	0.21566	0.22581	0.23601	0.24626	0.219	0.229	0.239	0.250
1	0.19637	0.21276	0.2229	0.23311	0.24336	0.216	0.226	0.236	0.247
1.5	0.19456	0.20991	0.22006	0.23026	0.24051	0.212	0.222	0.232	0.244
2	0.19274	0.2071	0.21727	0.22747	0.23772	0.209	0.219	0.229	0.242
2.5	0.19093	0.20439	0.21453	0.22473	0.23498	0.206	0.216	0.226	0.238
3	0.18911	0.20168	0.21185	0.22204	0.23229	0.203	0.213	0.224	0.236
3.5	0.1873	0.19906	0.2092	0.21941	0.22965	0.199	0.211	0.221	0.232
4	0.18548	0.19654	0.20664	0.21682	0.22707	0.197	0.208	0.218	0.230
4.5	0.18366	0.19391	0.20408	0.21429	0.22453	0.194	0.204	0.216	0.227
5	0.18185	0.19151	0.20162	0.21179	0.22206	0.190	0.200	0.213	0.225
5.5	0.18003	0.18917	0.19919	0.20936	0.2196	0.187	0.196	0.208	0.221
6	0.17822	0.18654	0.19675	0.20697	0.21722	0.185	0.194	0.204	0.218
6.5	0.1764	0.18427	0.19449	0.20459	0.21485	0.182	0.191	0.201	0.214
7	0.17459	0.18231	0.19203	0.2023	0.21254	0.180	0.188	0.198	0.209
7.5	0.17277	0.17968	0.18987	0.19998	0.21023	0.177	0.186	0.196	0.206
8	0.17096	0.17659	0.18755	0.19775	0.20798	0.175	0.183	0.194	0.204
8.5	0.16914	0.17393	0.18514	0.19545	0.20572	0.172	0.181	0.191	0.201
9	0.16733	0.17188	0.18316	0.19325	0.20348	0.170	0.179	0.189	0.199
9.5	0.16551	0.1701	0.18052	0.19092	0.20116	0.168	0.176	0.186	0.196
10	0.1637	0.16845	0.17827	0.18862	0.19889	0.165	0.173	0.183	0.194
10.5	0.16188	0.16674	0.17599	0.18614	0.1964	0.164	0.170	0.181	0.191
11	0.16007	0.16504	0.17371	0.18365	0.19391	0.162	0.168	0.178	0.188

Table 6.7: Bed elevation (m) for Run 7

	Numerical					Experimental			
X (m)	T=0	T=1hr	T=2 hr	T=3 hr	T=4 hr	T=1hr	T=2 hr	T=3 hr	T=4 hr
0	0.2	0.21004	0.21642	0.22288	0.22933	0.213	0.219	0.226	0.233
0.5	0.19819	0.20767	0.21405	0.22052	0.22695	0.210	0.217	0.224	0.230
1	0.19637	0.20533	0.21172	0.21818	0.22462	0.208	0.215	0.221	0.228
1.5	0.19456	0.20302	0.20942	0.21588	0.22232	0.205	0.211	0.217	0.226
2	0.19274	0.20076	0.20717	0.21363	0.22006	0.203	0.209	0.215	0.224
2.5	0.19093	0.19853	0.20493	0.21139	0.21783	0.200	0.207	0.213	0.221
3	0.18911	0.19629	0.20274	0.2092	0.21563	0.196	0.204	0.211	0.219
3.5	0.1873	0.19415	0.20059	0.20704	0.21348	0.194	0.202	0.209	0.215
4	0.18548	0.19206	0.19845	0.2049	0.21134	0.192	0.198	0.207	0.214
4.5	0.18366	0.18987	0.19637	0.20283	0.20925	0.190	0.196	0.204	0.212
5	0.18185	0.18777	0.1943	0.20073	0.20718	0.187	0.193	0.202	0.210
5.5	0.18003	0.18585	0.19223	0.19872	0.20514	0.185	0.191	0.199	0.207
6	0.17822	0.18385	0.19028	0.19668	0.20314	0.183	0.189	0.195	0.206
6.5	0.1764	0.18157	0.18826	0.19469	0.20113	0.180	0.187	0.193	0.204
7	0.17459	0.17929	0.18627	0.19277	0.19918	0.178	0.185	0.191	0.198
7.5	0.17277	0.17724	0.1844	0.19072	0.1972	0.175	0.182	0.189	0.195
8	0.17096	0.1754	0.18245	0.18888	0.19528	0.173	0.181	0.187	0.193
8.5	0.16914	0.17371	0.18038	0.18684	0.19331	0.172	0.179	0.184	0.191
9	0.16733	0.17204	0.17859	0.18492	0.19139	0.169	0.177	0.182	0.189
9.5	0.16551	0.17036	0.17684	0.18296	0.18937	0.166	0.175	0.180	0.187
10	0.1637	0.16866	0.17451	0.18091	0.18741	0.164	0.172	0.178	0.184
10.5	0.16188	0.16681	0.17209	0.17878	0.18529	0.162	0.169	0.176	0.182
11	0.16007	0.16495	0.16968	0.17666	0.18317	0.160	0.167	0.174	0.180

Table 6.8: Bed elevation (m) for Run 8

	Numerical					Experimental			
X (m)	T=0	T=1hr	T=2 hr	T=3 hr	T=4 hr	T=1hr	T=2 hr	T=3 hr	T=4 hr
0	0.2	0.20869	0.21425	0.21982	0.22537	0.209	0.216	0.219	0.226
0.5	0.19819	0.20636	0.21193	0.21749	0.22304	0.207	0.213	0.216	0.224
1	0.19637	0.20407	0.20964	0.21521	0.22076	0.205	0.211	0.214	0.222
1.5	0.19456	0.2018	0.20738	0.21295	0.2185	0.204	0.208	0.212	0.219
2	0.19274	0.19958	0.20517	0.21072	0.21627	0.201	0.206	0.209	0.217
2.5	0.19093	0.19739	0.20298	0.20853	0.21408	0.198	0.203	0.207	0.213
3	0.18911	0.1952	0.20081	0.20636	0.21191	0.195	0.201	0.205	0.211
3.5	0.1873	0.19307	0.19869	0.20424	0.20979	0.193	0.199	0.204	0.209
4	0.18548	0.19101	0.19659	0.20214	0.20769	0.191	0.197	0.202	0.207
4.5	0.18366	0.18891	0.19453	0.20008	0.20563	0.189	0.195	0.200	0.205
5	0.18185	0.18682	0.19249	0.19804	0.20359	0.186	0.191	0.198	0.203
5.5	0.18003	0.18486	0.19047	0.19604	0.20159	0.184	0.189	0.196	0.201
6	0.17822	0.18294	0.18848	0.19406	0.19961	0.182	0.187	0.193	0.199
6.5	0.1764	0.1809	0.18655	0.19209	0.19765	0.180	0.185	0.191	0.197
7	0.17459	0.17878	0.18459	0.19018	0.19573	0.178	0.183	0.189	0.195
7.5	0.17277	0.17674	0.18267	0.18827	0.19382	0.174	0.181	0.186	0.192
8	0.17096	0.17488	0.18081	0.18637	0.19192	0.172	0.179	0.184	0.190
8.5	0.16914	0.17314	0.17895	0.18451	0.19006	0.170	0.177	0.182	0.188
9	0.16733	0.17149	0.17699	0.18263	0.18818	0.168	0.174	0.180	0.185
9.5	0.16551	0.16984	0.17522	0.18078	0.18633	0.166	0.172	0.178	0.183
10	0.1637	0.16824	0.17344	0.17892	0.18447	0.164	0.170	0.176	0.181
10.5	0.16188	0.16659	0.17151	0.17704	0.18259	0.162	0.168	0.173	0.179
11	0.16007	0.16494	0.16957	0.17515	0.1807	0.160	0.166	0.171	0.177

Table 6.9: Bed elevation (m) for Run 9

	Numerical					Experimental			
X (m)	T=0	T=1hr	T=2 hr	T=3 hr	T=4 hr	T=1hr	T=2 hr	T=3 hr	T=4 hr
0	0.2	0.20049	0.20313	0.20571	0.20832	0.199	0.205	0.202	0.211
0.5	0.19819	0.19876	0.20138	0.20397	0.20657	0.198	0.203	0.201	0.209
1	0.19637	0.19705	0.19965	0.20225	0.20486	0.197	0.201	0.200	0.207
1.5	0.19456	0.19535	0.19795	0.20054	0.20314	0.195	0.200	0.198	0.205
2	0.19274	0.19366	0.19625	0.19885	0.20146	0.195	0.198	0.197	0.203
2.5	0.19093	0.19204	0.19459	0.19717	0.19978	0.194	0.196	0.196	0.201
3	0.18911	0.19041	0.19292	0.19553	0.19813	0.193	0.193	0.195	0.199
3.5	0.1873	0.18878	0.19127	0.19389	0.19648	0.192	0.191	0.193	0.197
4	0.18548	0.18716	0.18965	0.19227	0.19486	0.191	0.190	0.192	0.195
4.5	0.18366	0.18559	0.18803	0.19064	0.19323	0.190	0.188	0.191	0.193
5	0.18185	0.18404	0.18645	0.18907	0.19165	0.189	0.186	0.190	0.191
5.5	0.18003	0.18255	0.18488	0.18749	0.19007	0.187	0.183	0.189	0.188
6	0.17822	0.18106	0.18332	0.18593	0.18851	0.186	0.181	0.188	0.187
6.5	0.1764	0.17954	0.18178	0.18437	0.18697	0.185	0.180	0.187	0.185
7	0.17459	0.17801	0.18025	0.18286	0.18542	0.183	0.178	0.186	0.183
7.5	0.17277	0.17646	0.17872	0.18132	0.1839	0.182	0.176	0.185	0.182
8	0.17096	0.17487	0.17722	0.17982	0.1824	0.181	0.175	0.184	0.180
8.5	0.16914	0.17327	0.17575	0.17831	0.18091	0.179	0.173	0.183	0.178
9	0.16733	0.17169	0.17431	0.17685	0.17943	0.178	0.172	0.182	0.177
9.5	0.16551	0.17004	0.17287	0.17538	0.17796	0.176	0.170	0.181	0.175
10	0.1637	0.16844	0.17149	0.17389	0.1765	0.175	0.169	0.179	0.174
10.5	0.16188	0.16674	0.17005	0.17244	0.17505	0.173	0.167	0.178	0.172
11	0.16007	0.16504	0.16861	0.171	0.1736	0.172	0.166	0.176	0.171

Table 6.10: Bed elevation (m) for Run 10

	Numerical					Experimental			
X (m)	T=0	T=1hr	T=2 hr	T=3 hr	T=4 hr	T=1hr	T=2 hr	T=3 hr	T=4 hr
0	0.2	0.19648	0.19783	0.1992	0.20042	0.196	0.200	0.202	0.202
0.5	0.19819	0.19504	0.19636	0.19776	0.19898	0.195	0.198	0.201	0.201
1	0.19637	0.19363	0.1949	0.19632	0.19755	0.194	0.197	0.200	0.199
1.5	0.19456	0.19228	0.19347	0.19489	0.19612	0.193	0.195	0.198	0.198
2	0.19274	0.19096	0.19206	0.19349	0.19471	0.193	0.194	0.197	0.196
2.5	0.19093	0.18961	0.19065	0.19208	0.1933	0.193	0.193	0.196	0.194
3	0.18911	0.18828	0.18924	0.19068	0.19191	0.192	0.190	0.195	0.192
3.5	0.1873	0.18699	0.18785	0.18928	0.19052	0.192	0.189	0.193	0.191
4	0.18548	0.18574	0.18647	0.18791	0.18915	0.191	0.187	0.192	0.189
4.5	0.18366	0.18454	0.18513	0.18655	0.18779	0.190	0.185	0.191	0.188
5	0.18185	0.18331	0.18382	0.18519	0.18645	0.188	0.183	0.190	0.186
5.5	0.18003	0.18206	0.1825	0.18384	0.1851	0.187	0.181	0.189	0.183
6	0.17822	0.18074	0.1812	0.18249	0.18381	0.186	0.179	0.188	0.182
6.5	0.1764	0.17935	0.17986	0.18112	0.18246	0.184	0.178	0.187	0.180
7	0.17459	0.17791	0.17861	0.17983	0.18115	0.183	0.176	0.186	0.179
7.5	0.17277	0.1764	0.17737	0.17851	0.17983	0.182	0.175	0.185	0.177
8	0.17096	0.17485	0.17615	0.17721	0.17853	0.181	0.174	0.184	0.176
8.5	0.16914	0.17327	0.17493	0.17594	0.17724	0.179	0.172	0.183	0.175
9	0.16733	0.17169	0.17372	0.17472	0.17597	0.178	0.171	0.182	0.173
9.5	0.16551	0.17005	0.17248	0.17346	0.17472	0.176	0.170	0.181	0.172
10	0.1637	0.16844	0.17124	0.17222	0.17342	0.175	0.169	0.179	0.171
10.5	0.16188	0.16674	0.16989	0.17101	0.17218	0.174	0.167	0.178	0.170
11	0.16007	0.16504	0.16854	0.16981	0.17093	0.172	0.166	0.176	0.168

Table 6.11: Bed elevation (m) for Run 11

	Numerical					Experimental			
X (m)	T=0	T=1hr	T=2 hr	T=3 hr	T=4 hr	T=1hr	T=2 hr	T=3 hr	T=4 hr
0	0.2	0.23723	0.25761	0.2776	0.2976	0.242	0.263	0.276	0.296
0.5	0.19773	0.23258	0.25295	0.27294	0.29295	0.237	0.256	0.271	0.291
1	0.19546	0.22803	0.24839	0.26838	0.28838	0.233	0.251	0.266	0.286
1.5	0.19319	0.22359	0.24393	0.26392	0.28393	0.228	0.246	0.262	0.282
2	0.19092	0.21925	0.23957	0.25956	0.27957	0.223	0.241	0.256	0.277
2.5	0.18865	0.21503	0.23532	0.2553	0.27531	0.219	0.237	0.252	0.273
3	0.18638	0.21091	0.23116	0.25114	0.27115	0.212	0.233	0.249	0.269
3.5	0.18411	0.2069	0.22711	0.24709	0.2671	0.206	0.229	0.245	0.264
4	0.18184	0.20299	0.22316	0.24314	0.26314	0.201	0.225	0.241	0.260
4.5	0.17957	0.1992	0.21932	0.23929	0.2593	0.197	0.219	0.237	0.256
5	0.1773	0.19551	0.21557	0.23554	0.25555	0.194	0.214	0.234	0.254
5.5	0.17503	0.19193	0.21193	0.2319	0.25191	0.191	0.210	0.229	0.249
6	0.17276	0.18845	0.2084	0.22836	0.24836	0.186	0.205	0.225	0.245
6.5	0.17049	0.18509	0.20496	0.22492	0.24492	0.183	0.201	0.221	0.241
7	0.16822	0.1818	0.20163	0.22158	0.24158	0.179	0.198	0.218	0.238
7.5	0.16595	0.17865	0.19838	0.21834	0.23834	0.176	0.194	0.214	0.233
8	0.16368	0.17554	0.19524	0.21519	0.23519	0.173	0.191	0.211	0.230
8.5	0.16141	0.17255	0.19218	0.21213	0.23213	0.169	0.187	0.207	0.226
9	0.15914	0.16965	0.1892	0.20915	0.22914	0.165	0.184	0.204	0.223
9.5	0.15687	0.16679	0.18628	0.20623	0.22622	0.162	0.180	0.201	0.219
10	0.1546	0.16399	0.18343	0.20336	0.22336	0.159	0.177	0.197	0.216
10.5	0.15233	0.16126	0.18057	0.2005	0.22049	0.156	0.174	0.194	0.213
11	0.15006	0.15853	0.17771	0.19763	0.21763	0.154	0.171	0.191	0.210

Table 6.12: Bed elevation (m) for Run 12

	Numerical					Experimental			
X (m)	T=0	T=1hr	T=2 hr	T=3 hr	T=4 hr	T=1hr	T=2 hr	T=3 hr	T=4 hr
0	0.2	0.22119	0.23361	0.24588	0.25815	0.224	0.237	0.250	0.262
0.5	0.19773	0.21758	0.23	0.24227	0.25454	0.220	0.233	0.246	0.258
1	0.19546	0.21403	0.22645	0.23872	0.25099	0.216	0.229	0.242	0.254
1.5	0.19319	0.21056	0.22297	0.23524	0.24751	0.213	0.225	0.239	0.251
2	0.19092	0.20716	0.21956	0.23183	0.2441	0.209	0.221	0.235	0.248
2.5	0.18865	0.20383	0.21622	0.22849	0.24076	0.205	0.218	0.231	0.244
3	0.18638	0.20057	0.21295	0.22522	0.23749	0.201	0.215	0.228	0.241
3.5	0.18411	0.19739	0.20975	0.22202	0.23429	0.196	0.211	0.224	0.236
4	0.18184	0.19428	0.20661	0.21888	0.23115	0.193	0.207	0.221	0.234
4.5	0.17957	0.19124	0.20355	0.21582	0.22809	0.190	0.204	0.217	0.231
5	0.1773	0.18827	0.20055	0.21282	0.22509	0.187	0.199	0.214	0.228
5.5	0.17503	0.18537	0.19762	0.20989	0.22216	0.184	0.196	0.210	0.223
6	0.17276	0.18254	0.19476	0.20703	0.2193	0.181	0.193	0.206	0.218
6.5	0.17049	0.17978	0.19196	0.20423	0.2165	0.179	0.190	0.203	0.214
7	0.16822	0.17707	0.18923	0.20149	0.21376	0.176	0.186	0.199	0.211
7.5	0.16595	0.17446	0.18655	0.19881	0.21108	0.172	0.183	0.196	0.208
8	0.16368	0.17188	0.18394	0.1962	0.20847	0.169	0.180	0.193	0.205
8.5	0.16141	0.16934	0.18137	0.19363	0.2059	0.167	0.177	0.190	0.202
9	0.15914	0.1669	0.17885	0.19112	0.20339	0.162	0.174	0.187	0.199
9.5	0.15687	0.16456	0.17637	0.18864	0.20091	0.160	0.172	0.184	0.196
10	0.1546	0.16204	0.17392	0.18619	0.19846	0.157	0.169	0.181	0.193
10.5	0.15233	0.15964	0.17147	0.18373	0.196	0.155	0.165	0.178	0.190
11	0.15006	0.15724	0.16902	0.18128	0.19355	0.152	0.163	0.175	0.187

Table 6.13: Bed elevation (m) for Run 13

	Numerical					Experimental			
X (m)	T=0	T=1hr	T=2 hr	T=3 hr	T=4 hr	T=1hr	T=2 hr	T=3 hr	T=4 hr
0	0.2	0.21788	0.22809	0.23817	0.24826	0.220	0.231	0.240	0.246
0.5	0.19773	0.21444	0.22465	0.23473	0.24482	0.217	0.228	0.236	0.243
1	0.19546	0.21105	0.22126	0.23134	0.24143	0.213	0.224	0.233	0.239
1.5	0.19319	0.20773	0.21793	0.22802	0.23811	0.210	0.220	0.230	0.236
2	0.19092	0.20446	0.21466	0.22475	0.23484	0.207	0.216	0.226	0.232
2.5	0.18865	0.20126	0.21145	0.22154	0.23163	0.202	0.213	0.221	0.229
3	0.18638	0.19813	0.2083	0.21838	0.22847	0.198	0.210	0.218	0.225
3.5	0.18411	0.19505	0.20521	0.21529	0.22538	0.193	0.207	0.216	0.226
4	0.18184	0.19204	0.20217	0.21225	0.22234	0.190	0.202	0.214	0.223
4.5	0.17957	0.18909	0.1992	0.20927	0.21936	0.186	0.199	0.211	0.219
5	0.1773	0.1862	0.19628	0.20635	0.21644	0.183	0.194	0.208	0.216
5.5	0.17503	0.18337	0.19342	0.20349	0.21358	0.180	0.191	0.203	0.212
6	0.17276	0.18061	0.19061	0.20069	0.21078	0.177	0.188	0.200	0.209
6.5	0.17049	0.1779	0.18787	0.19794	0.20803	0.174	0.185	0.196	0.206
7	0.16822	0.17525	0.18518	0.19525	0.20534	0.171	0.182	0.193	0.203
7.5	0.16595	0.17267	0.18255	0.19261	0.2027	0.171	0.179	0.190	0.200
8	0.16368	0.17014	0.17996	0.19003	0.20012	0.167	0.176	0.187	0.198
8.5	0.16141	0.16767	0.17744	0.18751	0.1976	0.164	0.173	0.184	0.195
9	0.15914	0.16521	0.17496	0.18502	0.19511	0.160	0.171	0.181	0.193
9.5	0.15687	0.1629	0.17254	0.1826	0.19269	0.157	0.168	0.178	0.190
10	0.1546	0.16054	0.17014	0.1802	0.19029	0.155	0.165	0.175	0.188
10.5	0.15233	0.15827	0.1678	0.17786	0.18795	0.152	0.162	0.172	0.185
11	0.15006	0.15601	0.16547	0.17552	0.18561	0.150	0.159	0.170	0.183

Table 6.14: Bed elevation (m) for Run 14

	Numerical					Experimental			
X (m)	T=0	T=1hr	T=2 hr	T=3 hr	T=4 hr	T=1hr	T=2 hr	T=3 hr	T=4 hr
0	0.2	0.20921	0.21485	0.2204	0.22595	0.199	0.213	0.202	0.223
0.5	0.19773	0.20633	0.21197	0.21752	0.22307	0.198	0.210	0.201	0.220
1	0.19546	0.20348	0.20913	0.21468	0.22023	0.197	0.207	0.200	0.217
1.5	0.19319	0.20068	0.20633	0.21188	0.21742	0.195	0.204	0.198	0.214
2	0.19092	0.19791	0.20356	0.20911	0.21465	0.195	0.202	0.197	0.212
2.5	0.18865	0.19518	0.20083	0.20638	0.21192	0.194	0.199	0.196	0.210
3	0.18638	0.19249	0.19813	0.20368	0.20923	0.193	0.196	0.195	0.207
3.5	0.18411	0.18984	0.19547	0.20102	0.20656	0.192	0.193	0.193	0.205
4	0.18184	0.18722	0.19285	0.1984	0.20394	0.191	0.191	0.192	0.202
4.5	0.17957	0.18465	0.19026	0.19581	0.20135	0.190	0.188	0.191	0.199
5	0.1773	0.18211	0.18771	0.19326	0.19881	0.189	0.186	0.190	0.197
5.5	0.17503	0.17962	0.1852	0.19075	0.19629	0.187	0.183	0.189	0.194
6	0.17276	0.17716	0.18272	0.18827	0.19382	0.186	0.180	0.188	0.191
6.5	0.17049	0.17474	0.18028	0.18583	0.19138	0.185	0.177	0.187	0.188
7	0.16822	0.17236	0.17788	0.18343	0.18898	0.183	0.174	0.186	0.186
7.5	0.16595	0.17001	0.17552	0.18107	0.18662	0.182	0.171	0.185	0.183
8	0.16368	0.16771	0.17319	0.17874	0.18429	0.181	0.168	0.184	0.180
8.5	0.16141	0.16544	0.1709	0.17645	0.182	0.179	0.165	0.183	0.178
9	0.15914	0.1632	0.16863	0.17418	0.17973	0.178	0.162	0.182	0.175
9.5	0.15687	0.16103	0.16642	0.17197	0.17752	0.176	0.160	0.181	0.173
10	0.1546	0.15885	0.16422	0.16977	0.17531	0.175	0.157	0.179	0.170
10.5	0.15233	0.15675	0.16207	0.16762	0.17317	0.173	0.154	0.178	0.167
11	0.15006	0.15464	0.15993	0.16548	0.17103	0.172	0.152	0.176	0.165

Table 6.15: Bed elevation (m) for Run 15

	Numerical					Experimental			
X (m)	T=0	T=1hr	T=2 hr	T=3 hr	T=4 hr	T=1hr	T=2 hr	T=3 hr	T=4 hr
0	0.2	0.2011	0.20355	0.20607	0.20859	0.196	0.202	0.202	0.206
0.5	0.19773	0.19886	0.20129	0.20381	0.20634	0.195	0.199	0.201	0.204
1	0.19546	0.19662	0.19905	0.20157	0.20409	0.194	0.197	0.200	0.201
1.5	0.19319	0.1944	0.19683	0.19935	0.20187	0.193	0.195	0.198	0.199
2	0.19092	0.1922	0.19463	0.19715	0.19967	0.193	0.193	0.197	0.197
2.5	0.18865	0.19002	0.19244	0.19496	0.19748	0.193	0.190	0.196	0.194
3	0.18638	0.18785	0.19028	0.1928	0.19532	0.192	0.188	0.195	0.193
3.5	0.18411	0.18569	0.18812	0.19064	0.19317	0.192	0.186	0.193	0.191
4	0.18184	0.18355	0.186	0.18852	0.19104	0.191	0.184	0.192	0.189
4.5	0.17957	0.18143	0.18388	0.18641	0.18893	0.190	0.182	0.191	0.187
5	0.1773	0.17933	0.18179	0.18431	0.18683	0.188	0.179	0.190	0.185
5.5	0.17503	0.17725	0.17972	0.18224	0.18476	0.187	0.177	0.189	0.183
6	0.17276	0.17517	0.17766	0.18018	0.18271	0.186	0.175	0.188	0.181
6.5	0.17049	0.17313	0.17563	0.17815	0.18067	0.184	0.173	0.187	0.179
7	0.16822	0.17109	0.1736	0.17612	0.17865	0.183	0.171	0.186	0.176
7.5	0.16595	0.16906	0.1716	0.17412	0.17664	0.182	0.169	0.185	0.174
8	0.16368	0.16706	0.16961	0.17213	0.17465	0.181	0.166	0.184	0.171
8.5	0.16141	0.16506	0.16765	0.17017	0.17269	0.179	0.164	0.183	0.169
9	0.15914	0.16309	0.16569	0.16821	0.17074	0.178	0.162	0.182	0.167
9.5	0.15687	0.16114	0.16377	0.16629	0.16881	0.176	0.160	0.181	0.164
10	0.1546	0.15919	0.16186	0.16438	0.1669	0.175	0.157	0.179	0.162
10.5	0.15233	0.15727	0.15997	0.16249	0.16502	0.174	0.155	0.178	0.160
11	0.15006	0.15535	0.15809	0.16061	0.16313	0.172	0.153	0.176	0.158

FIGURES

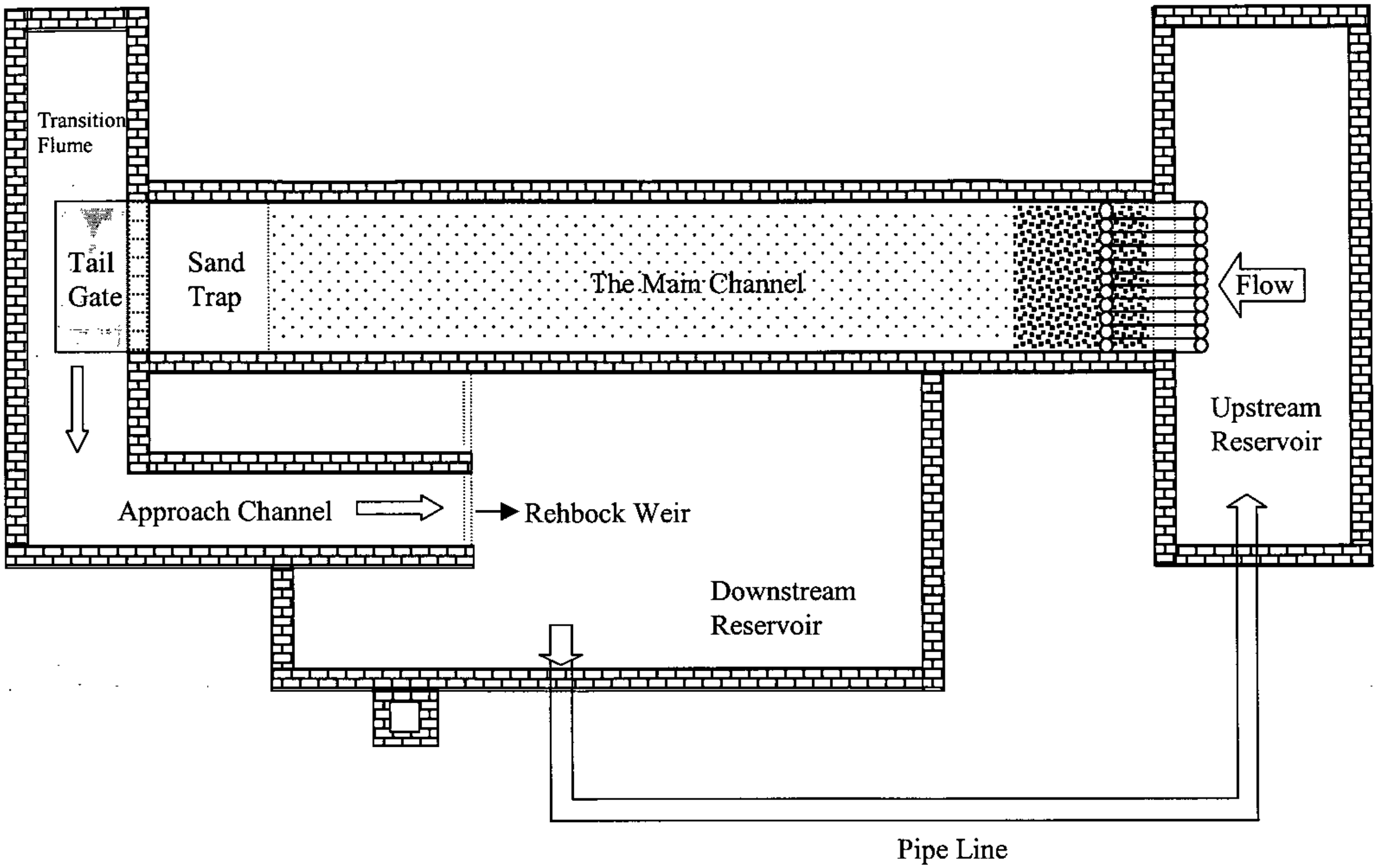

Fig. 4.1 General layout plan of the set-up

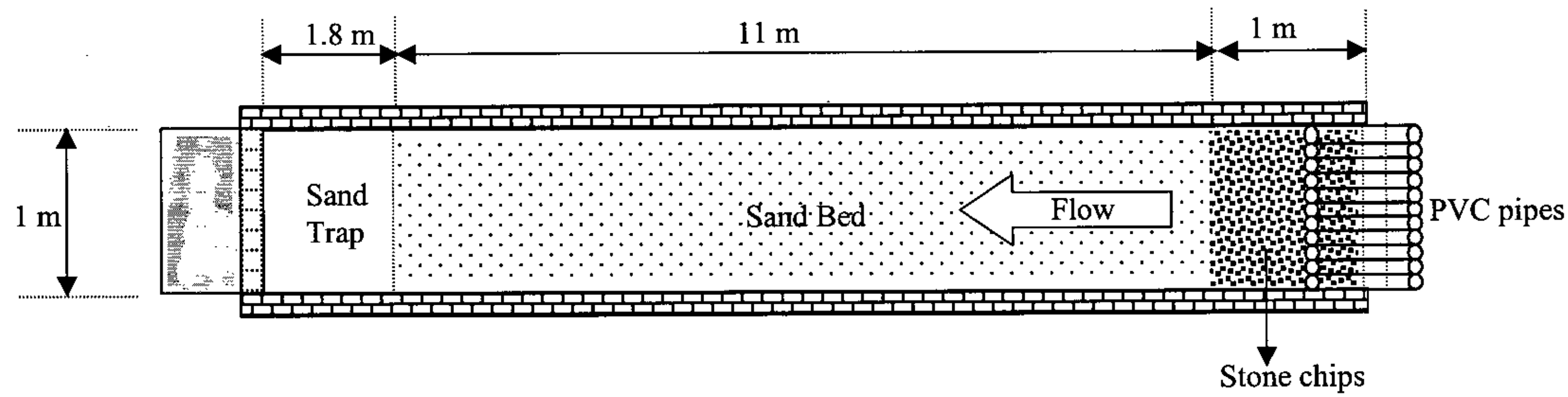

Fig. 4.2 Detail of the temporary part

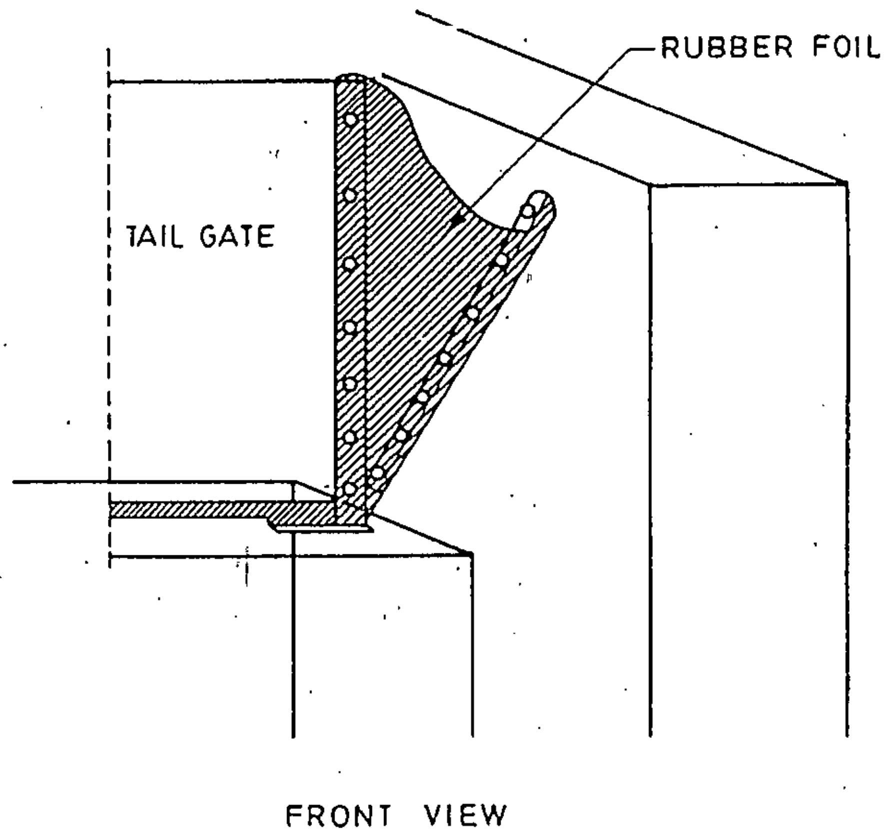

Fig. 4.3 Front view of the Tail Gate

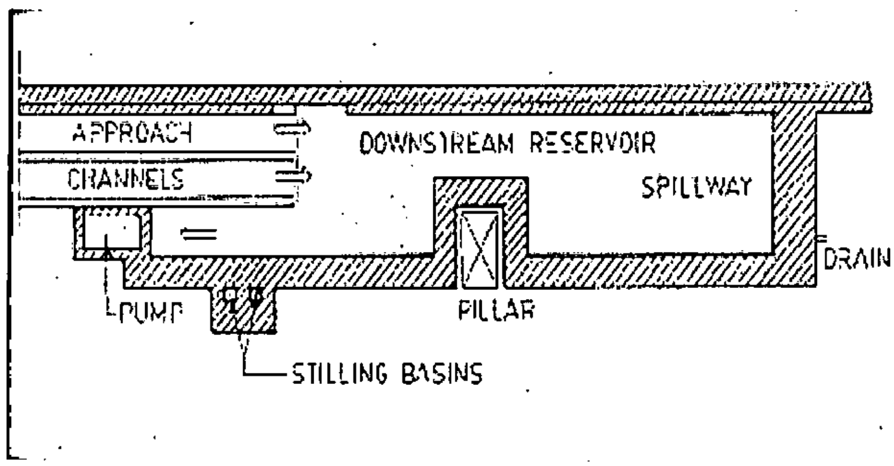

Fig. 4.4 Downstream Reservoir

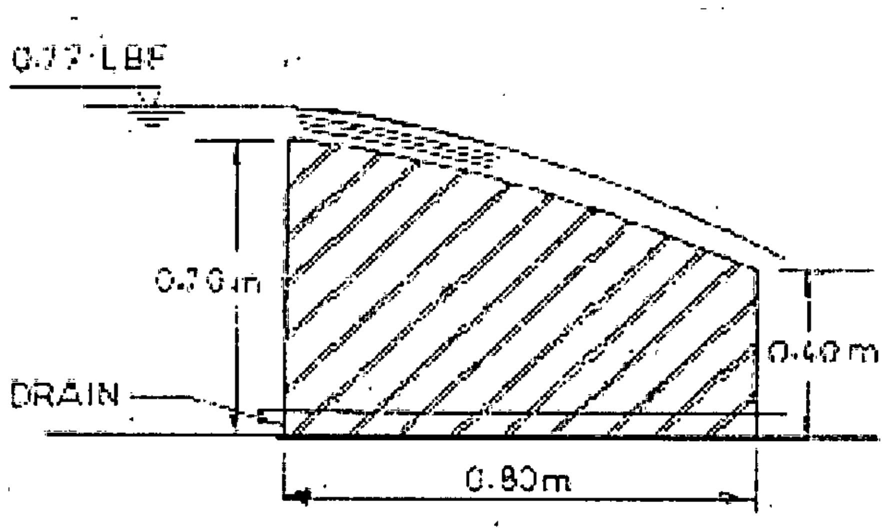

Fig. 4.5 Cross-section of the Spillway

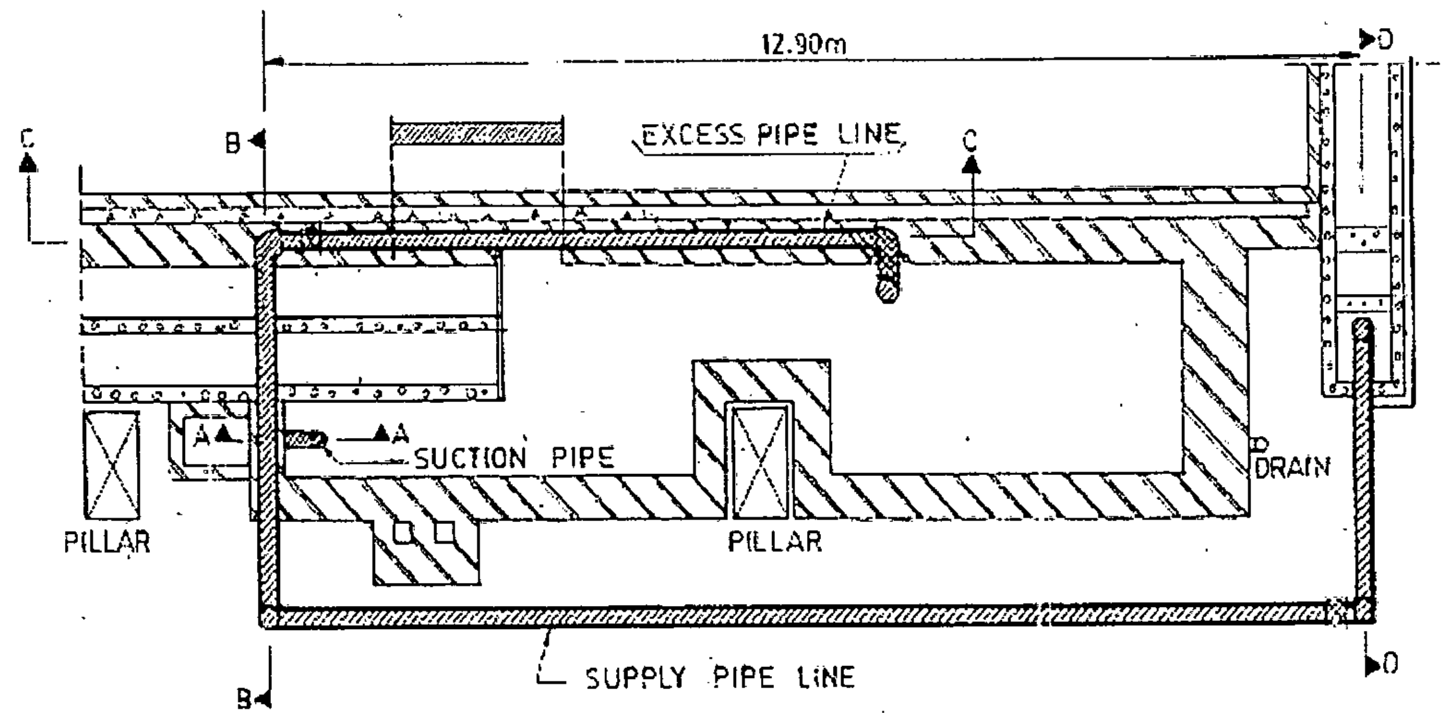

Fig. 4.6 Layout of the pipeline

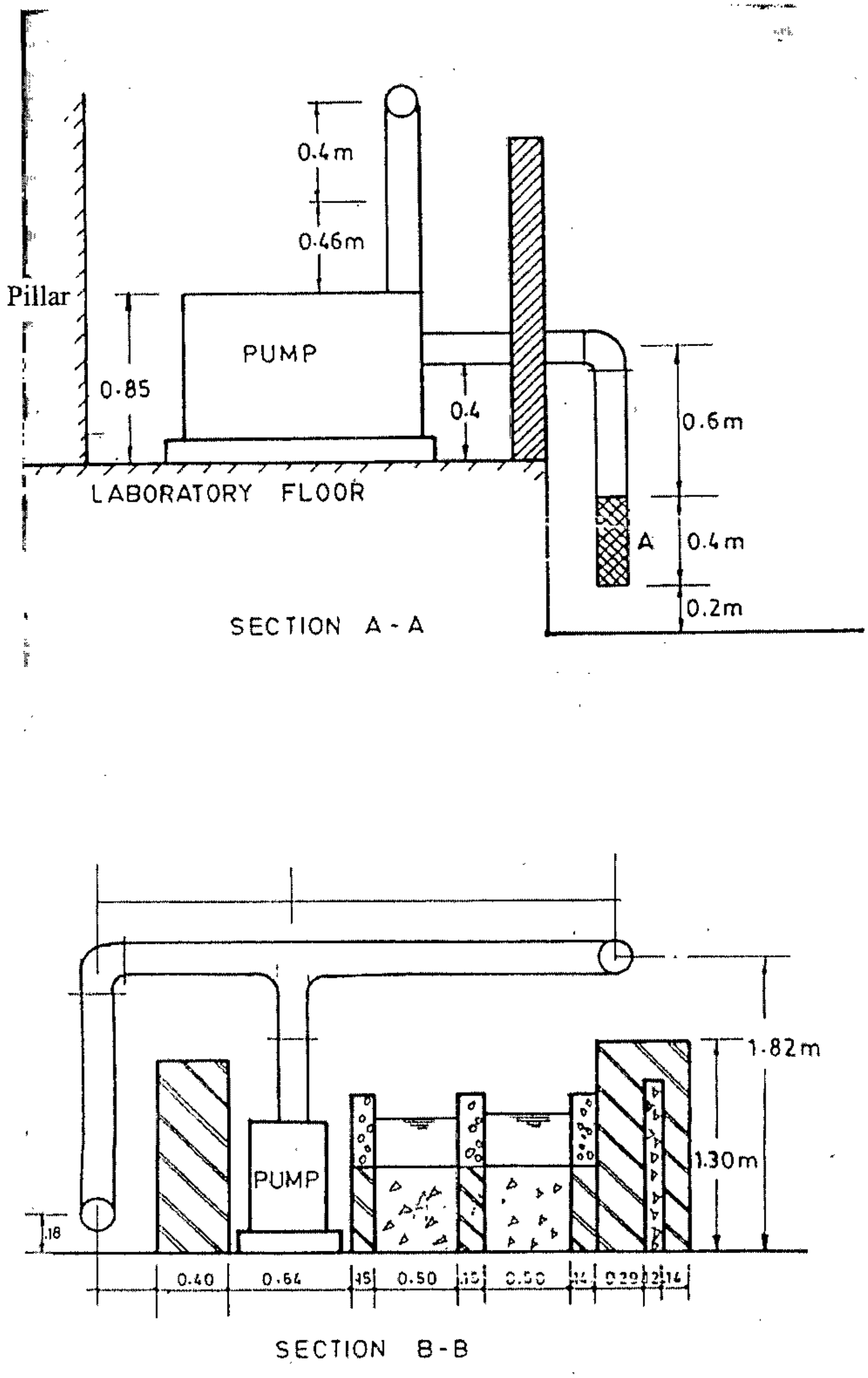

Fig. 4.7 Section A-A and B-B of the Pipeline

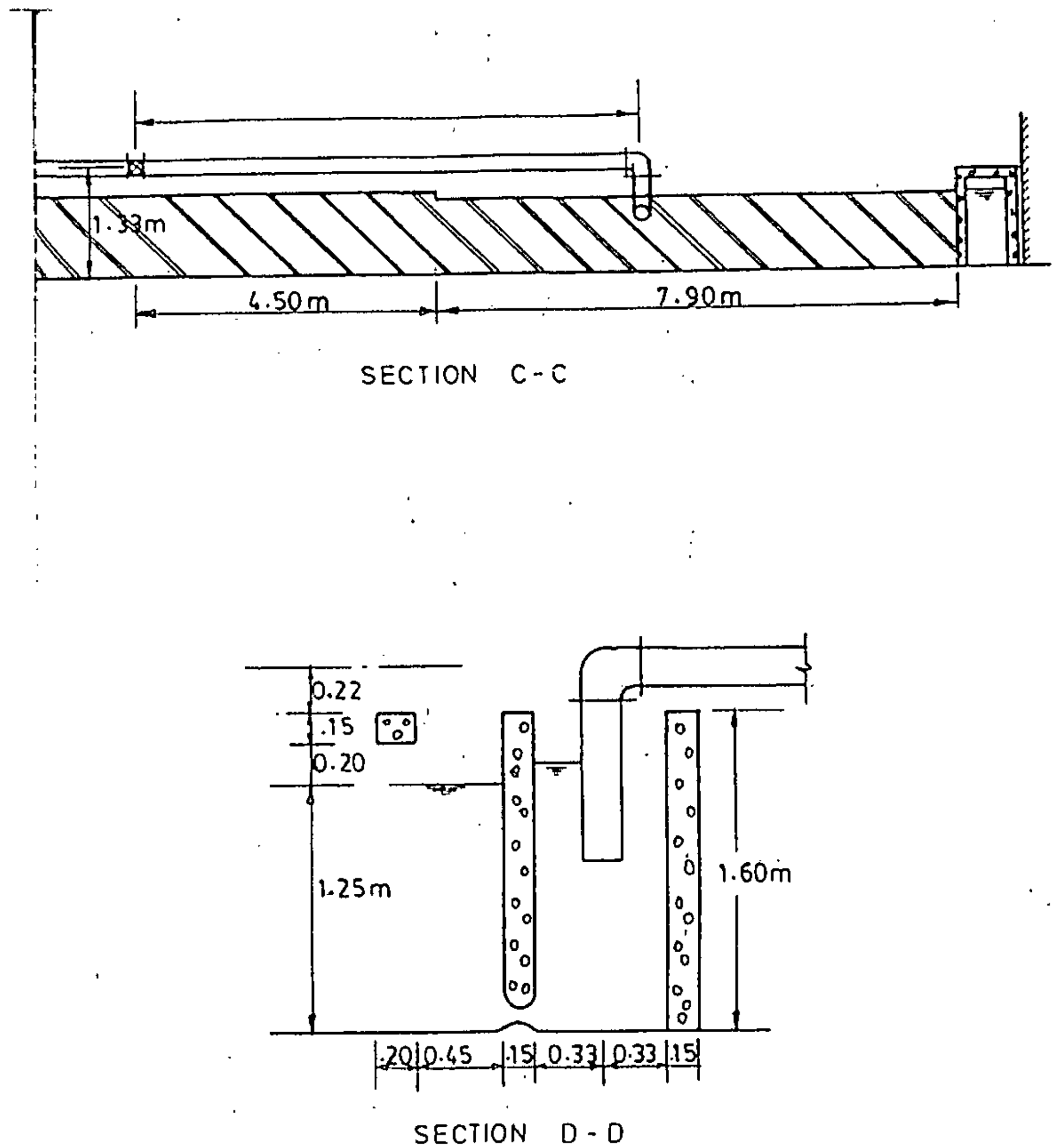

Fig. 4. 8 Section C-C and D-D of the Pipeline

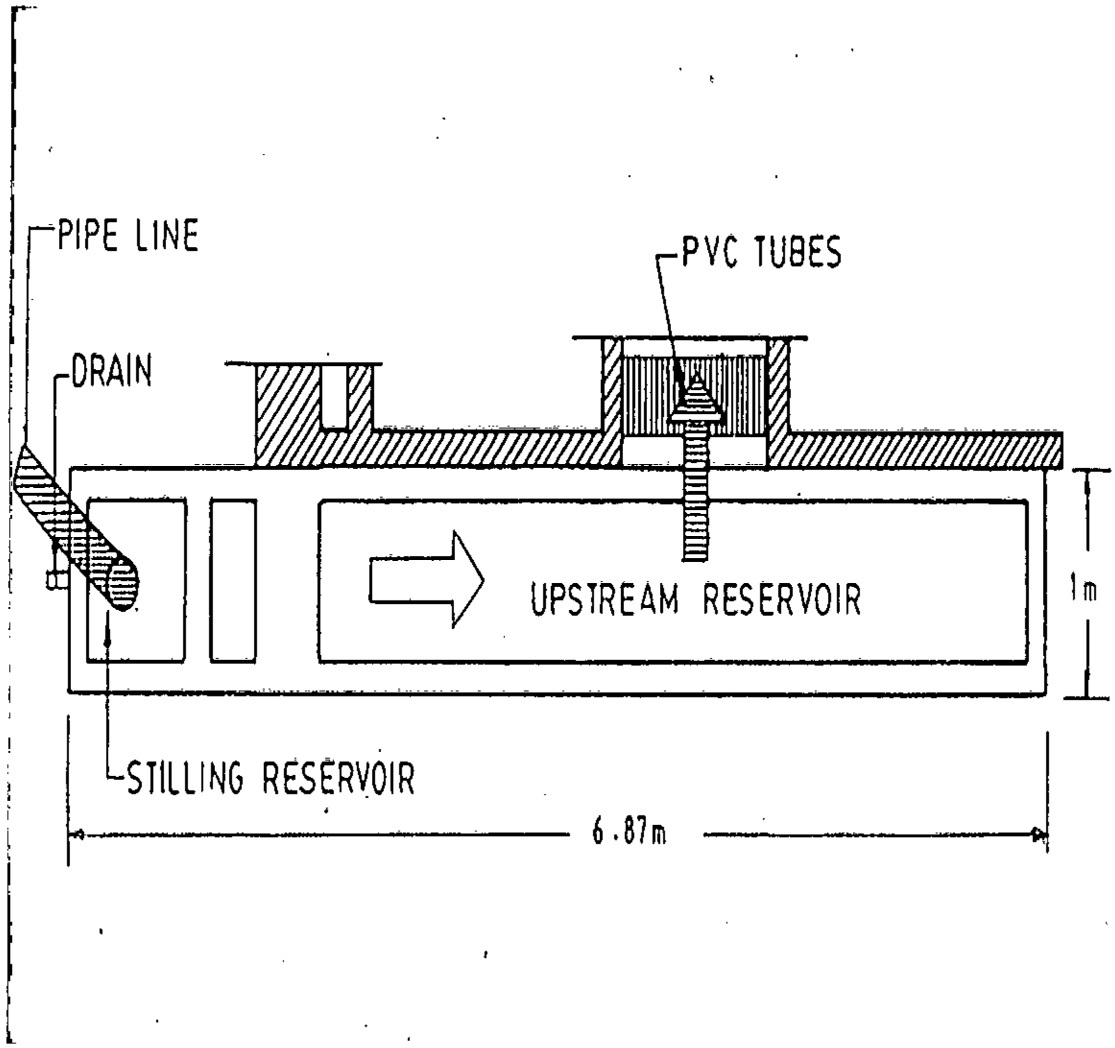

Fig. 4.9 Detail of the Upstream Reservoir

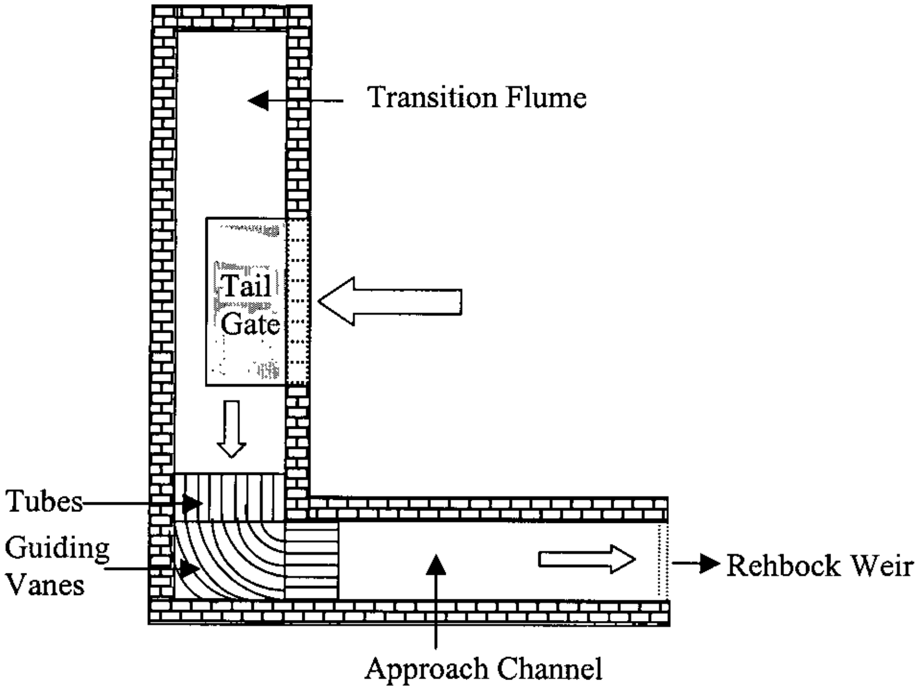

Fig. 4.10 Detail of the regulating and measuring system

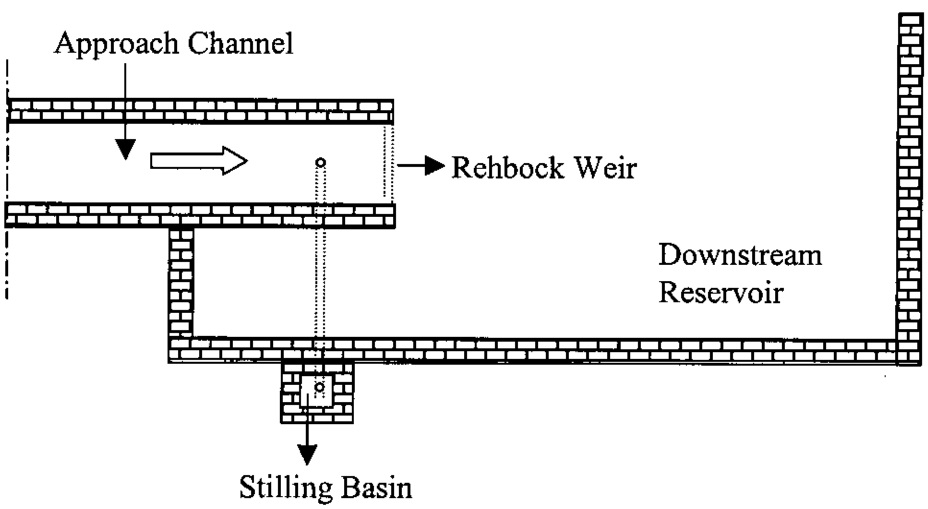

Fig. 4.11 The Approach Channel and the Rehbock Weir

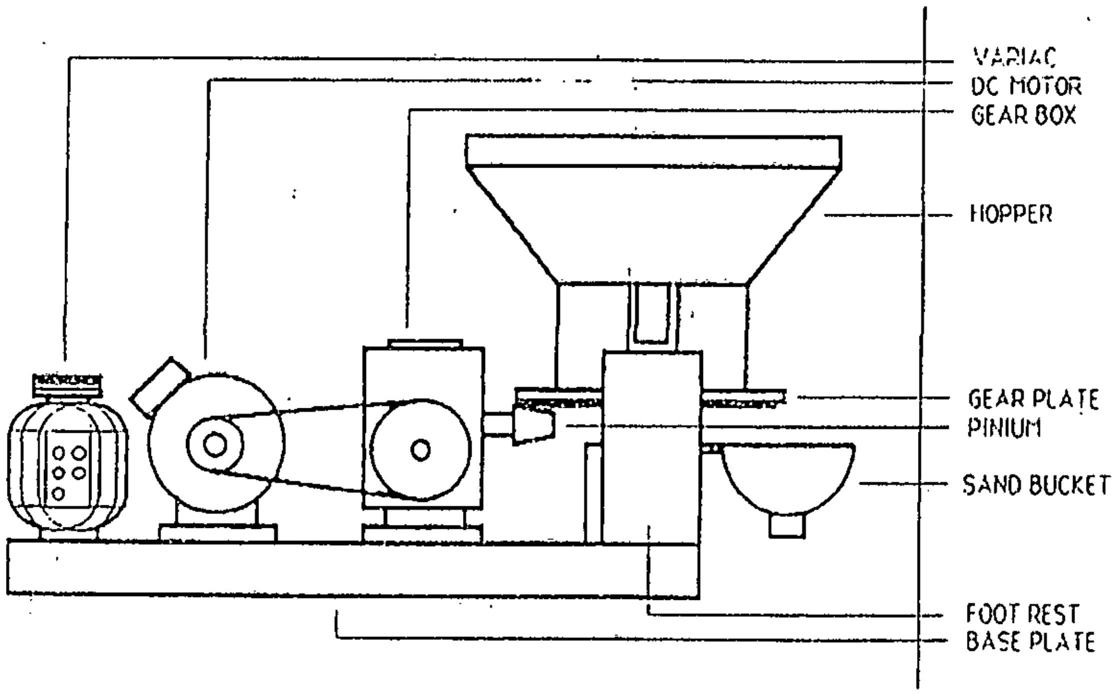

Fig. 4.12 Diagrammatic view of Sand Feeder

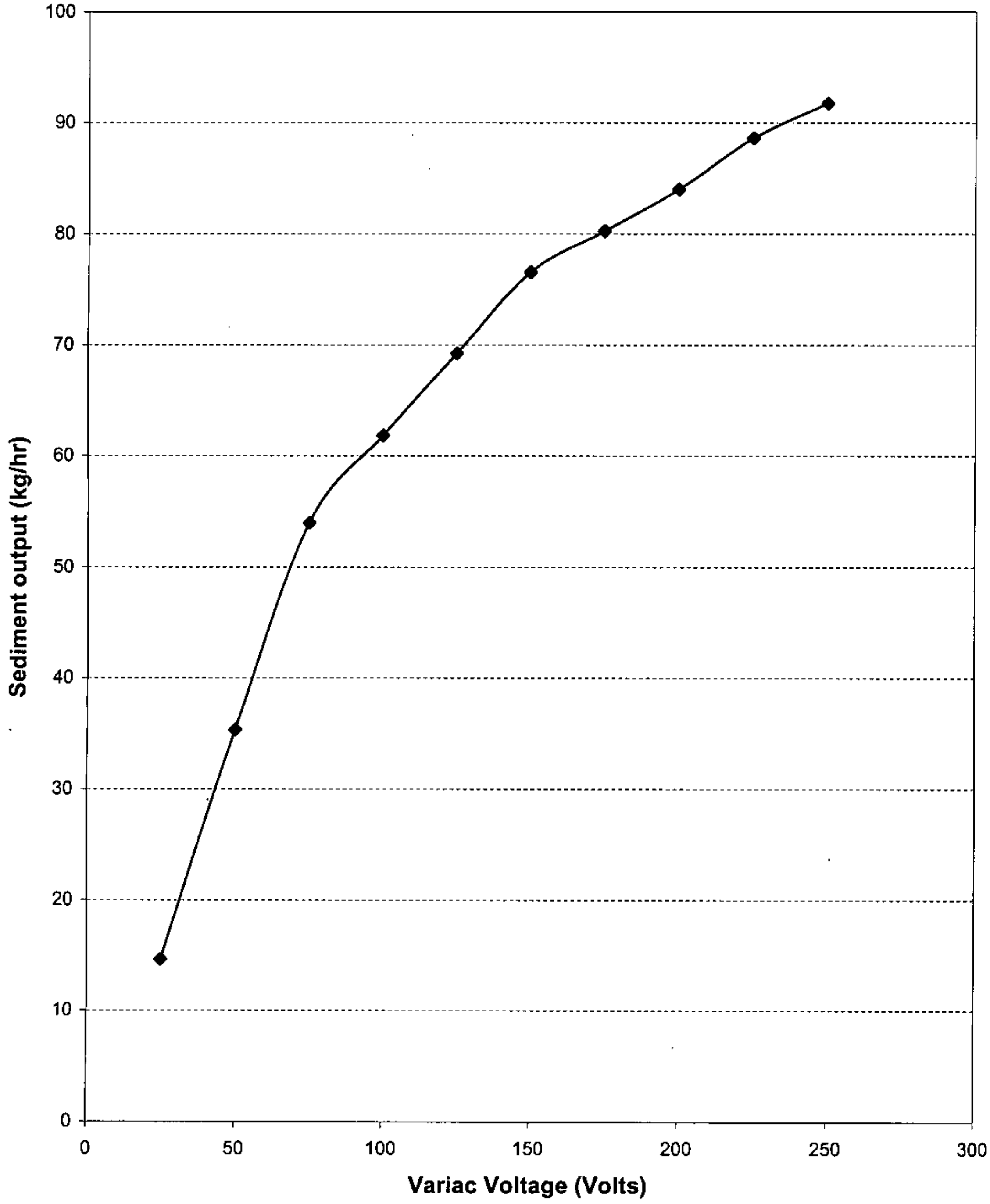

Fig. 4.13(a) Calibration curve for sand feeder no. 1

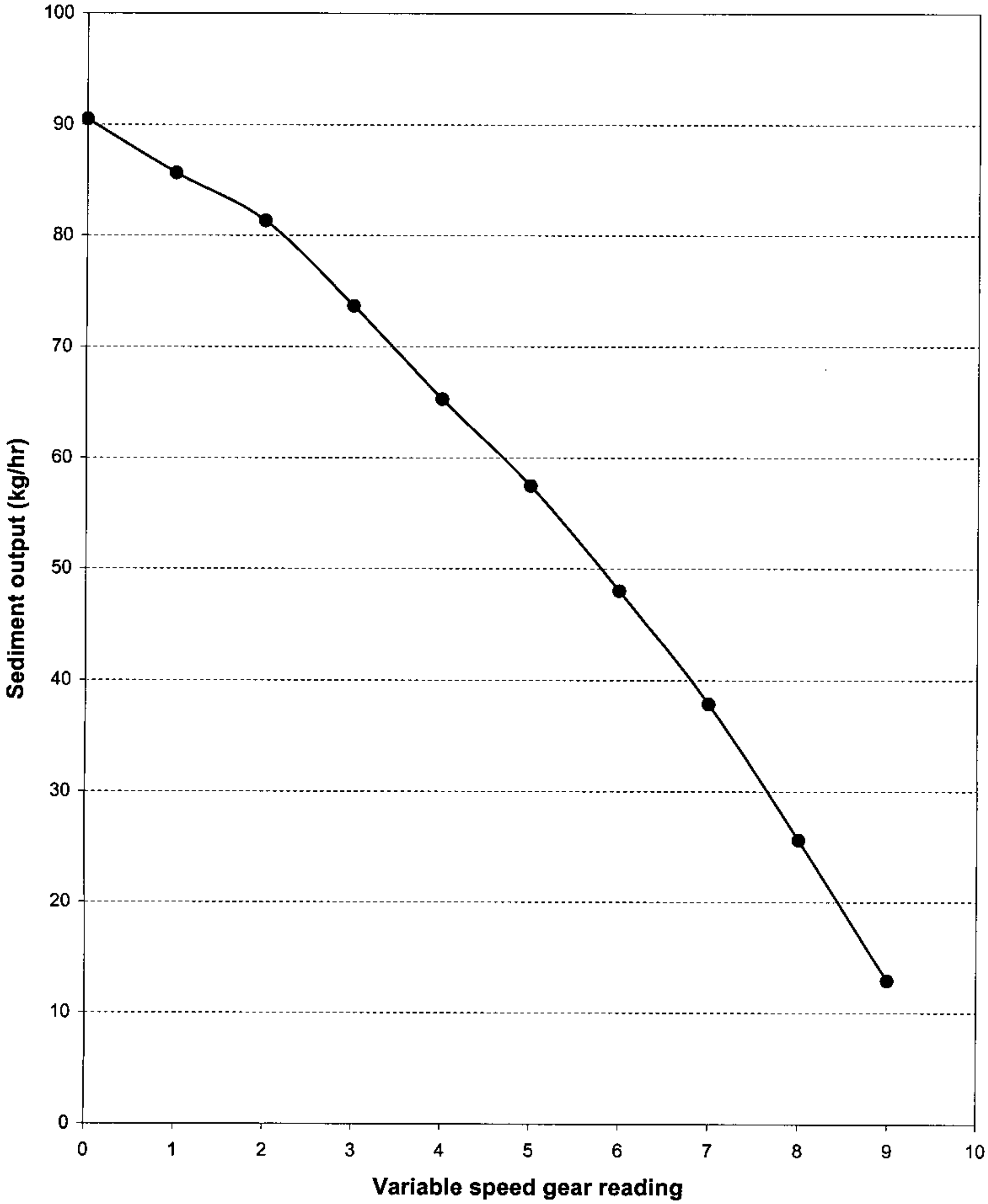

Fig. 4.13(b) Calibration curve for sand feeder no. 2

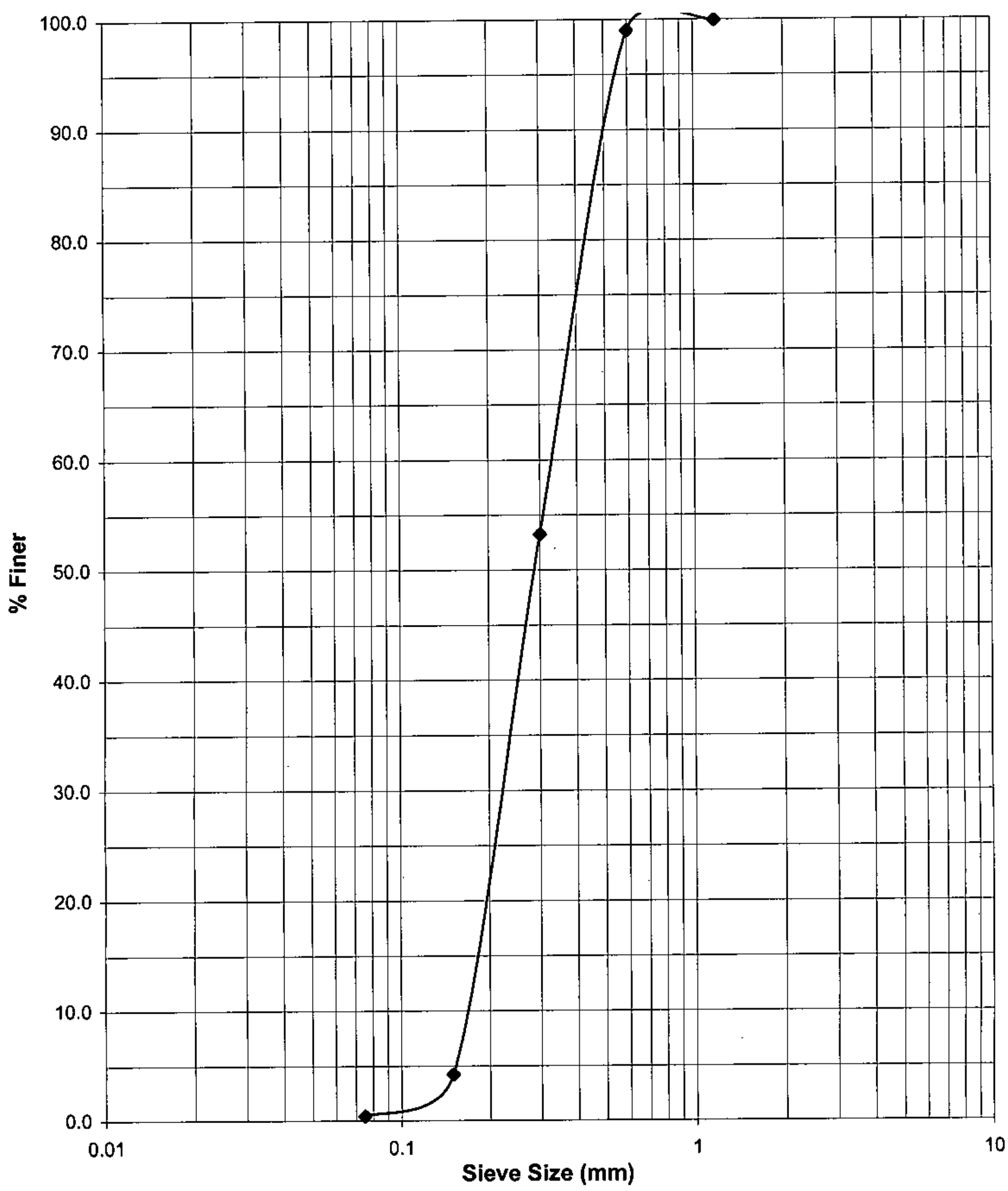

Fig. 4.14 Gradation of Bed Material

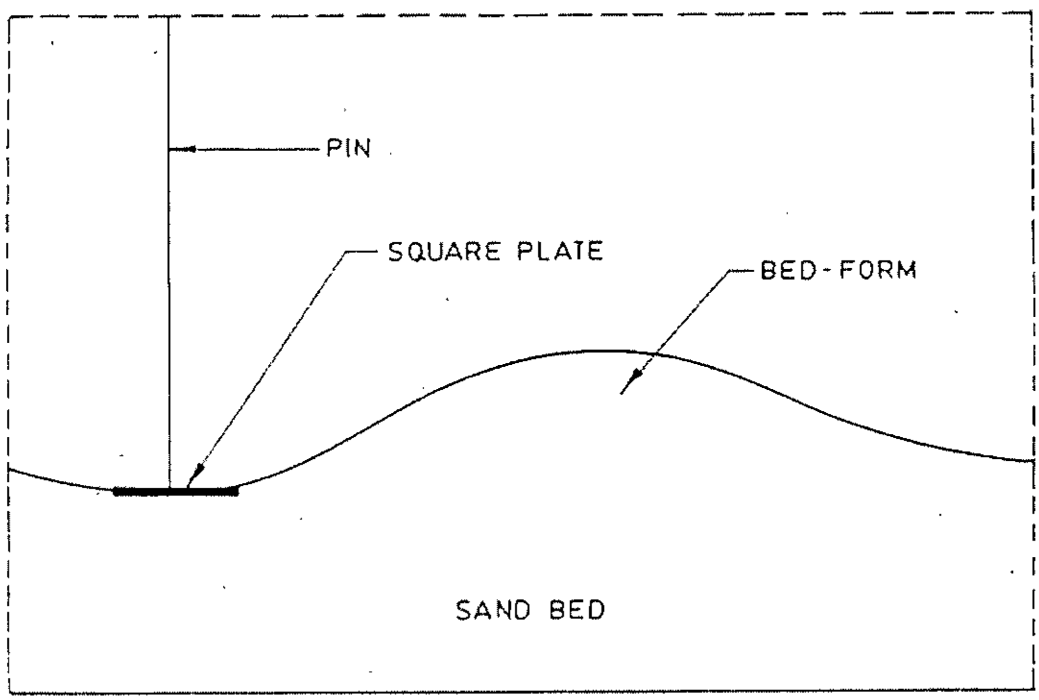

Fig. 4. 15 Detail of the special pin

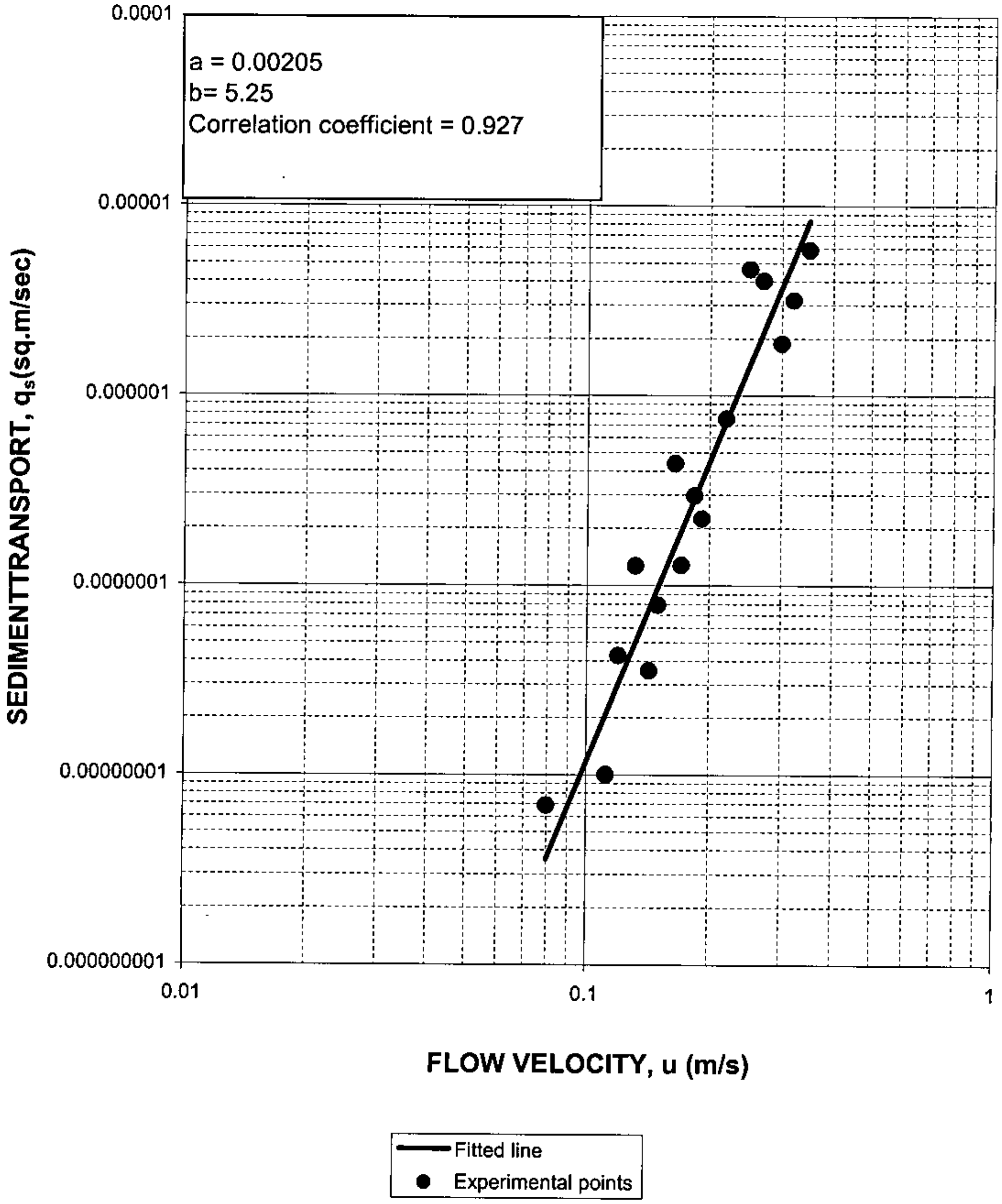

Fig. 5.1 Determination of 'a' and ' b' for sediment transport formula (q_s=a*u^b)

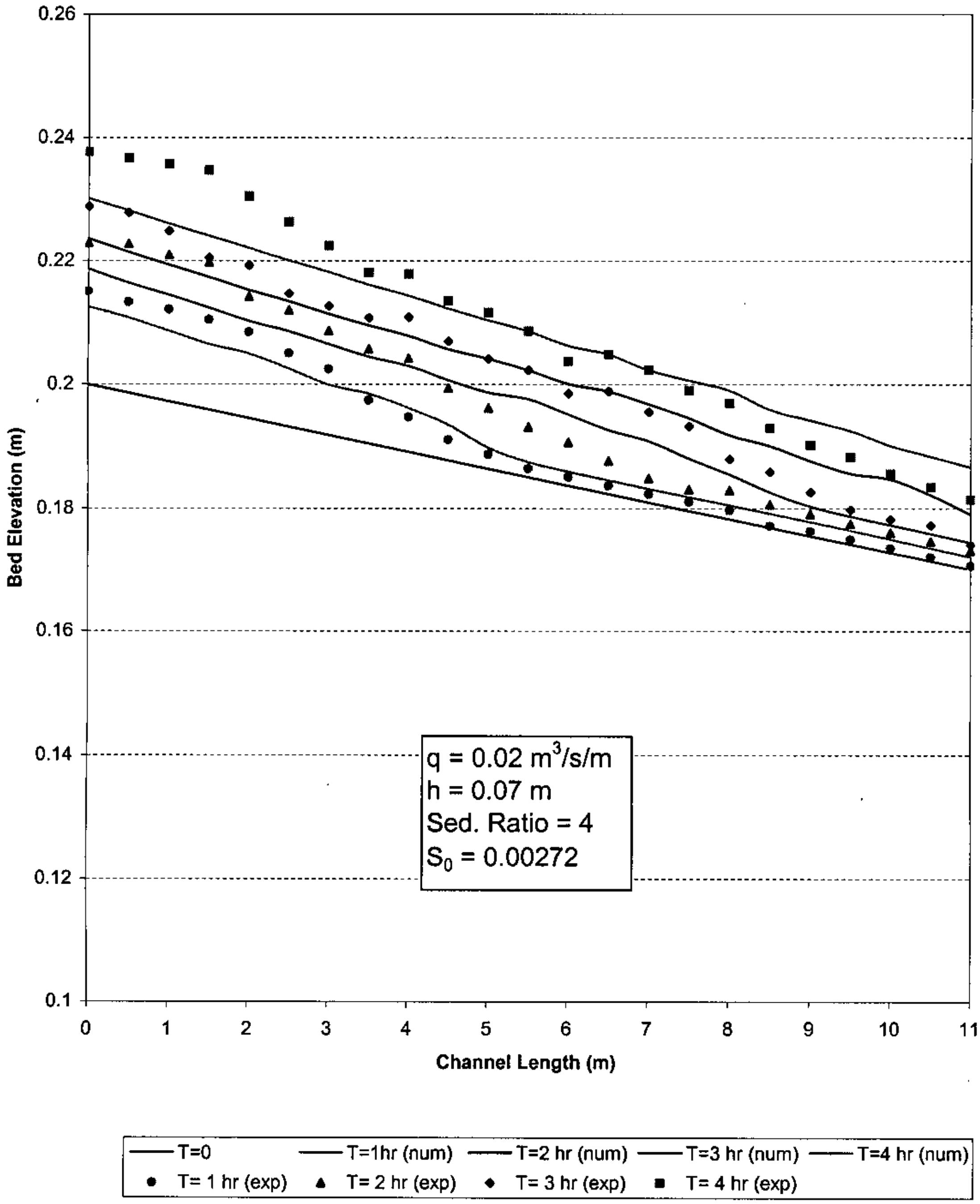

Fig. 6.1 Bed surface profles (Run 1)

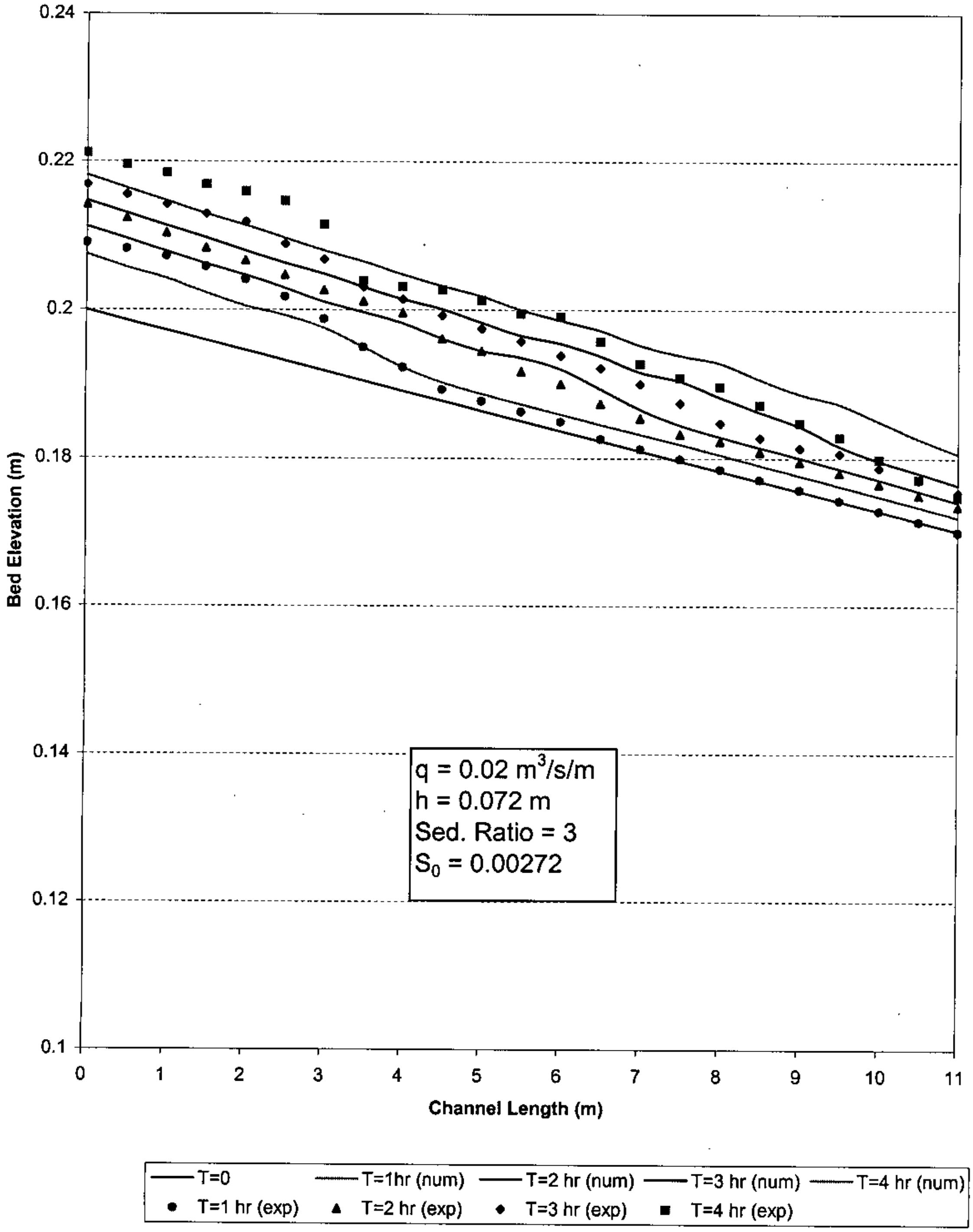

Fig. 6.2 Bed surface profiles (Run 2)

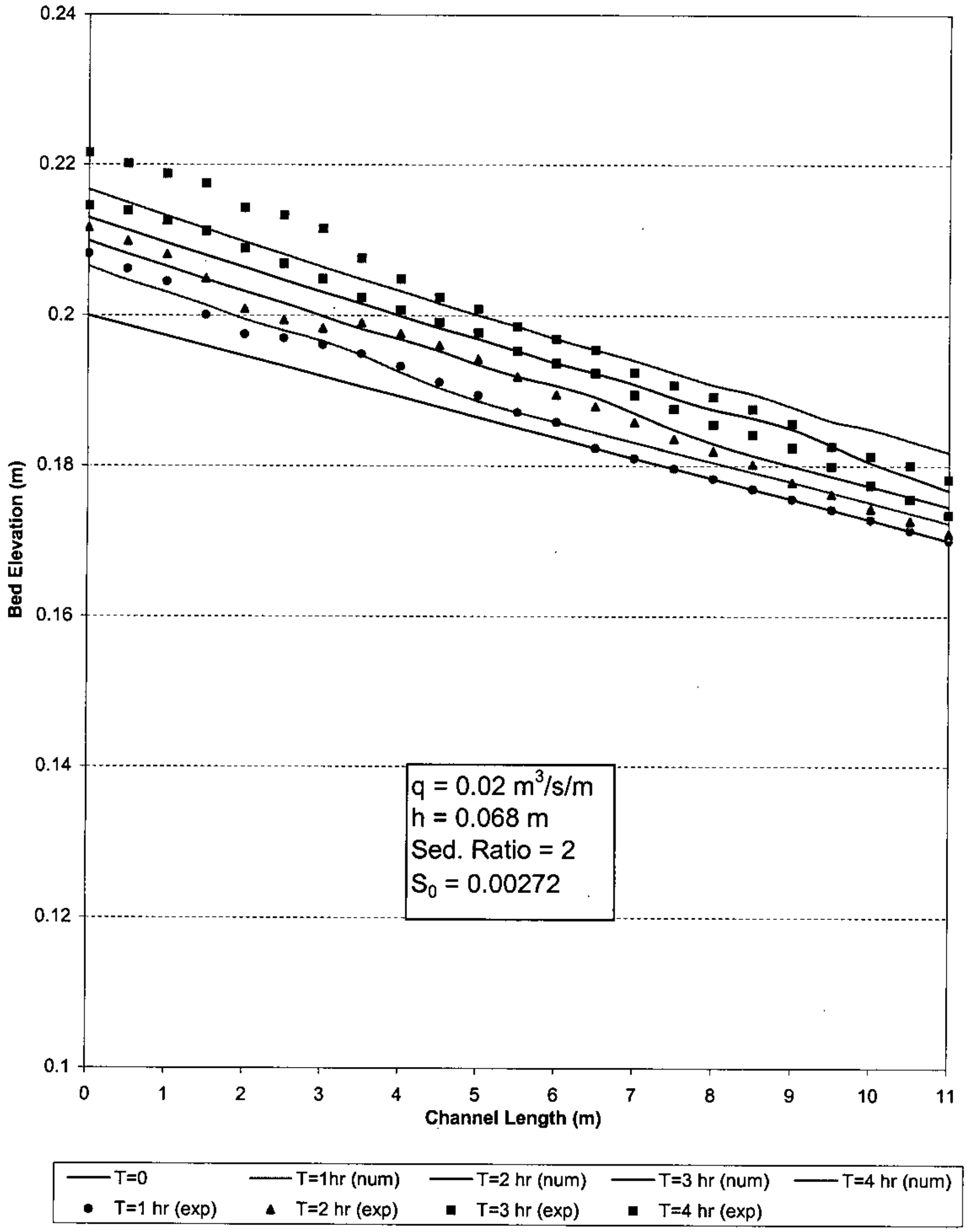

Fig. 6.3 Bed surface profiles (Run 3)

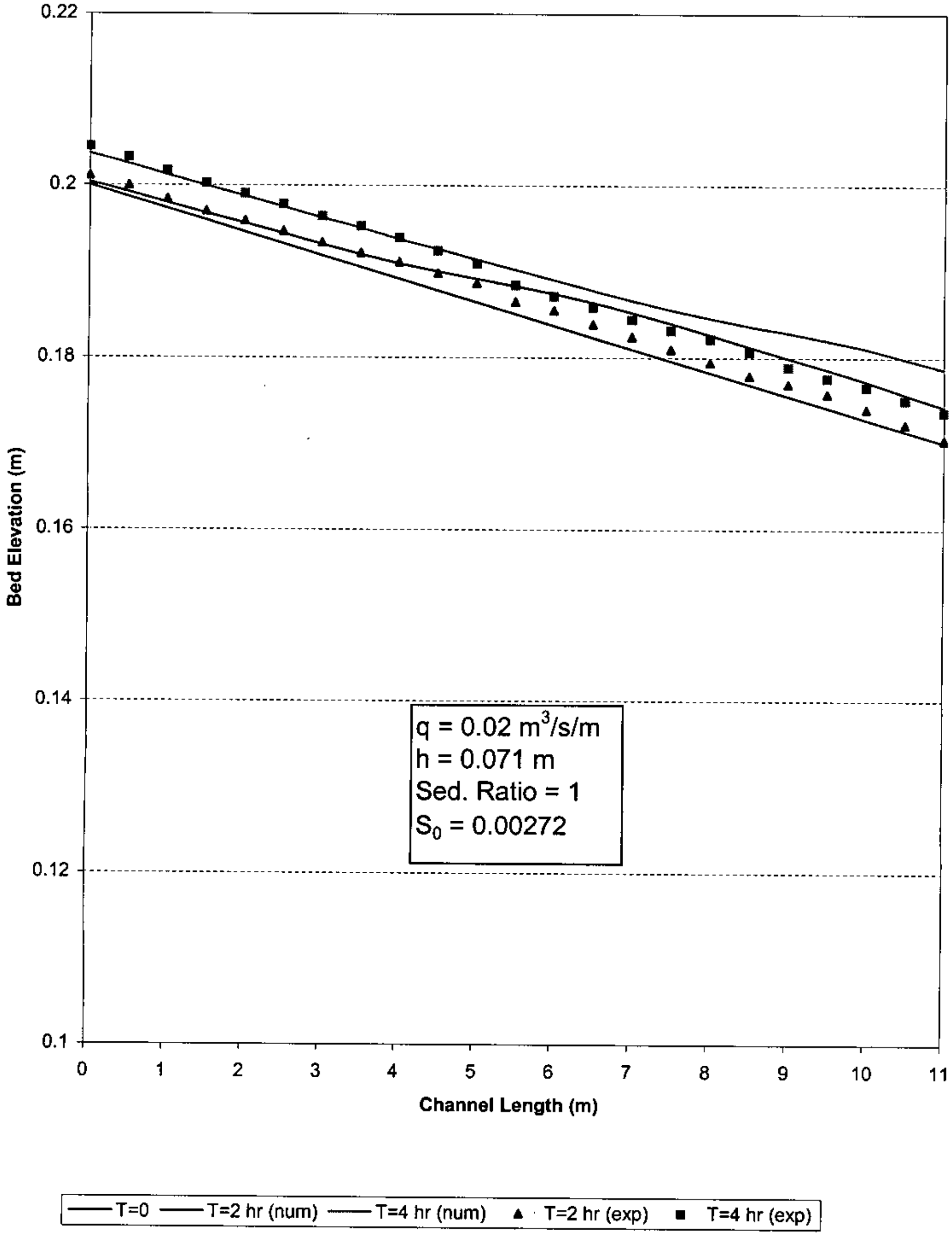

Fig. 6.4 Bed surface profiles (Run 4)

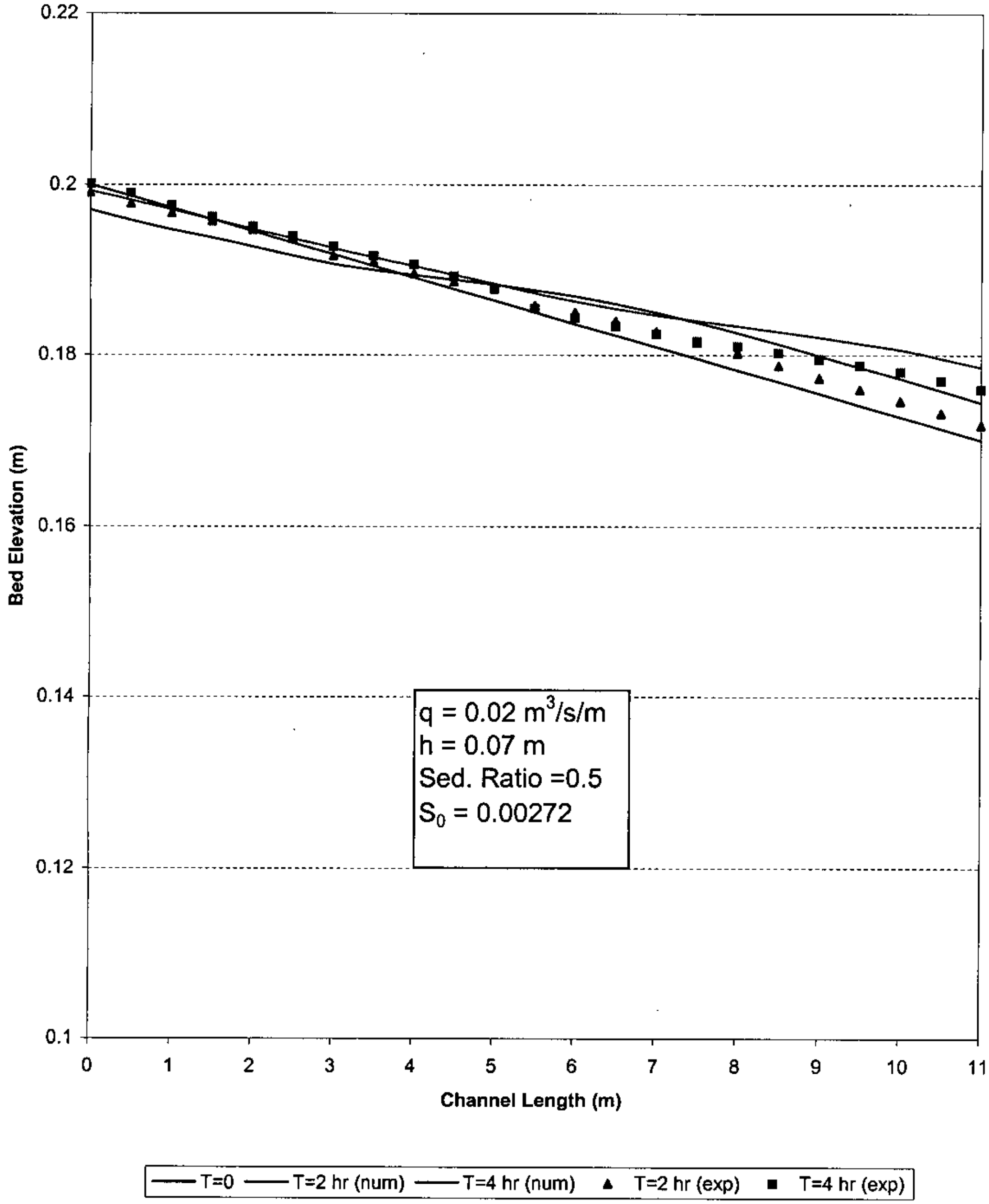

Fig. 6.5 Bed surface profiles (Run 5)

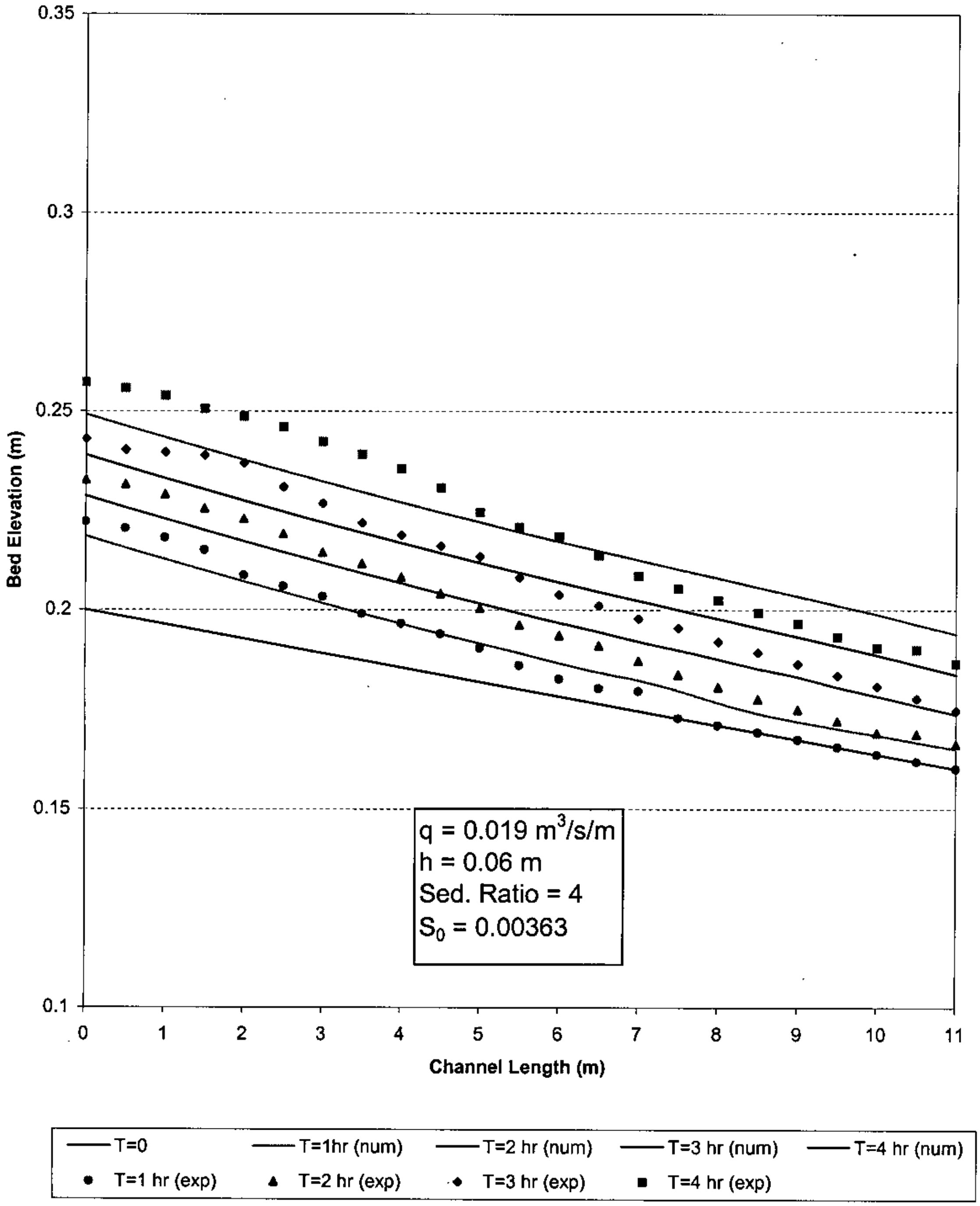

Fig. 6.6 Bed surface profiles (Run 6)

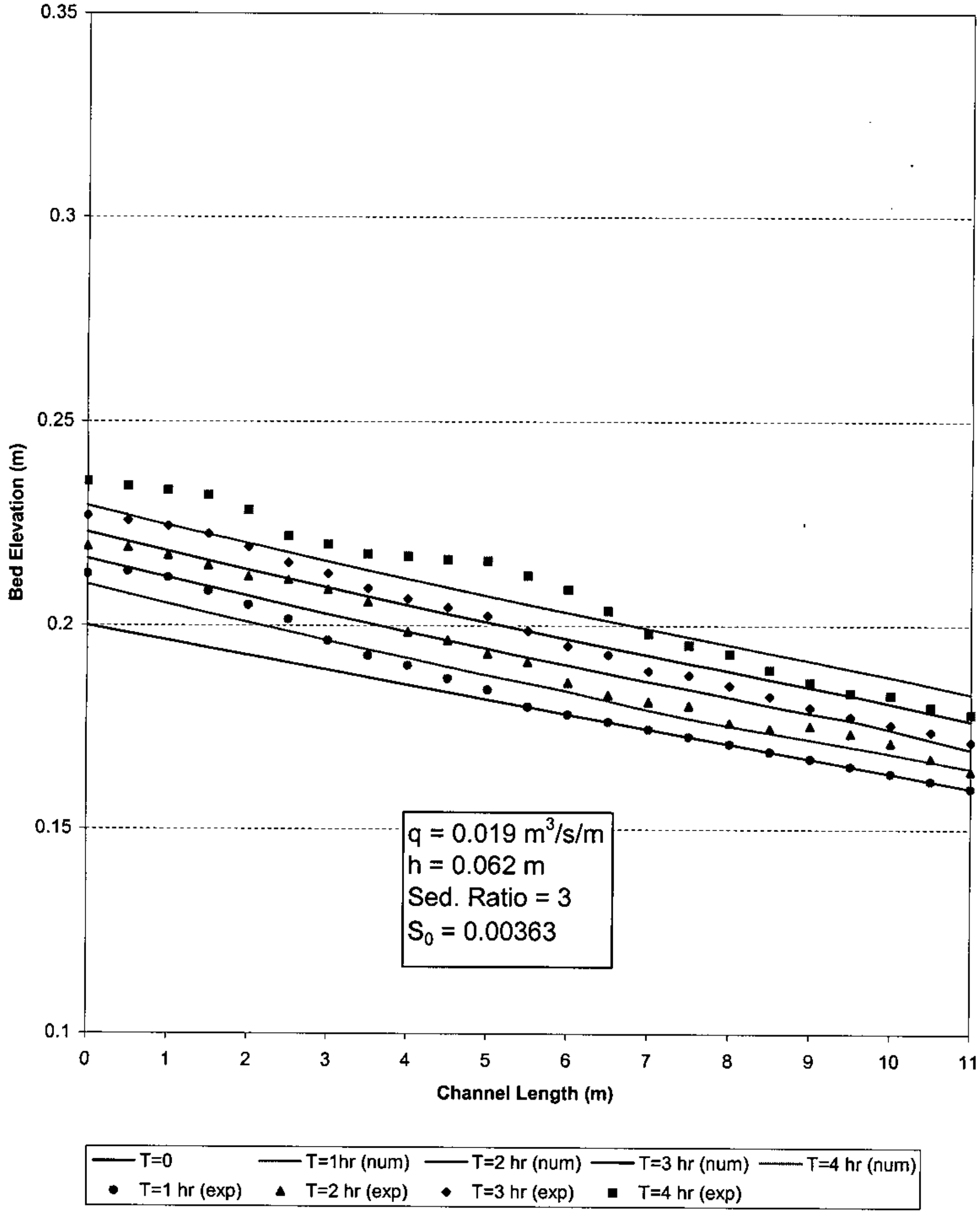

Fig. 6.7 Bed surface profiles (Run 7)

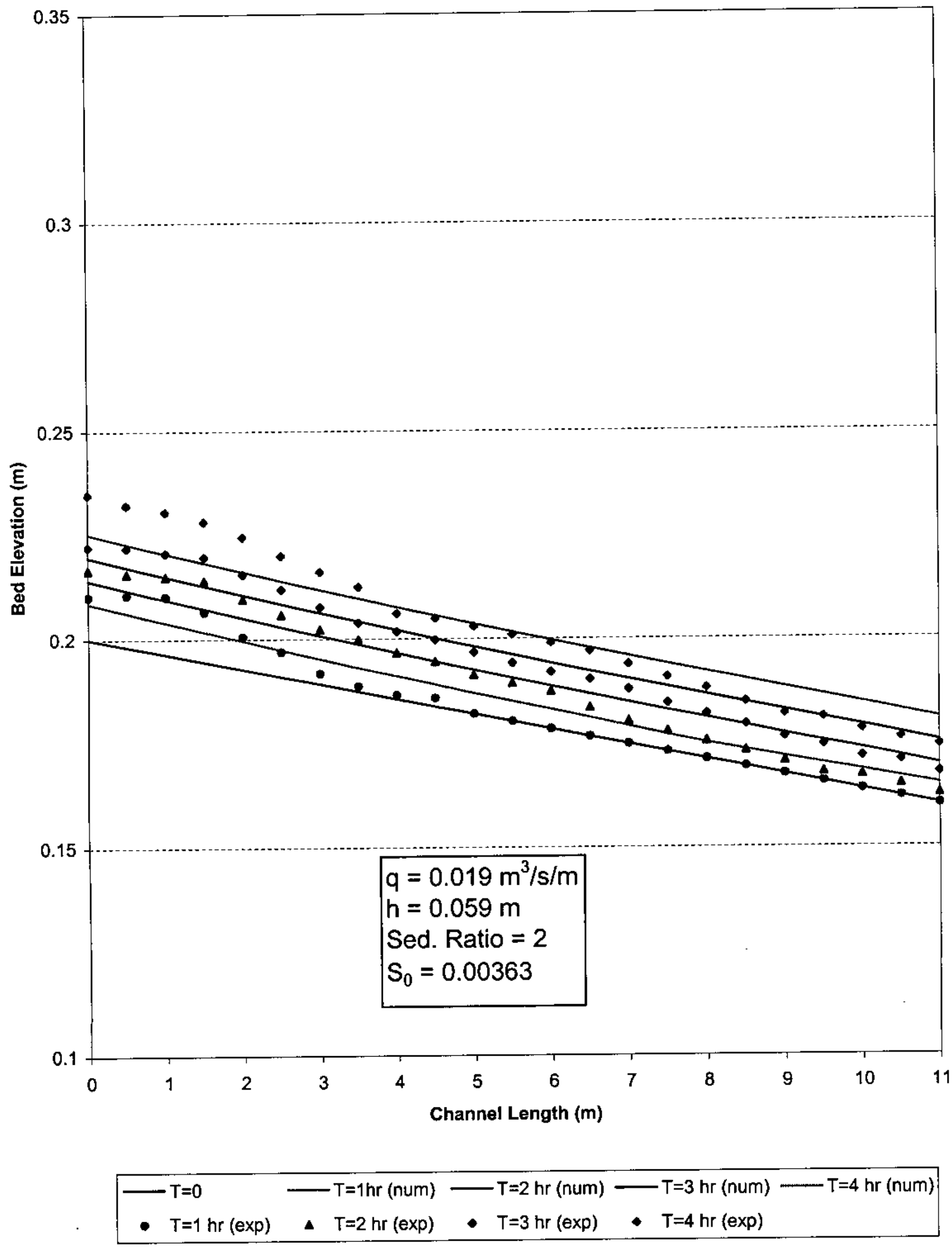

Fig. 6.8 Bed surface profiles (Run 8)

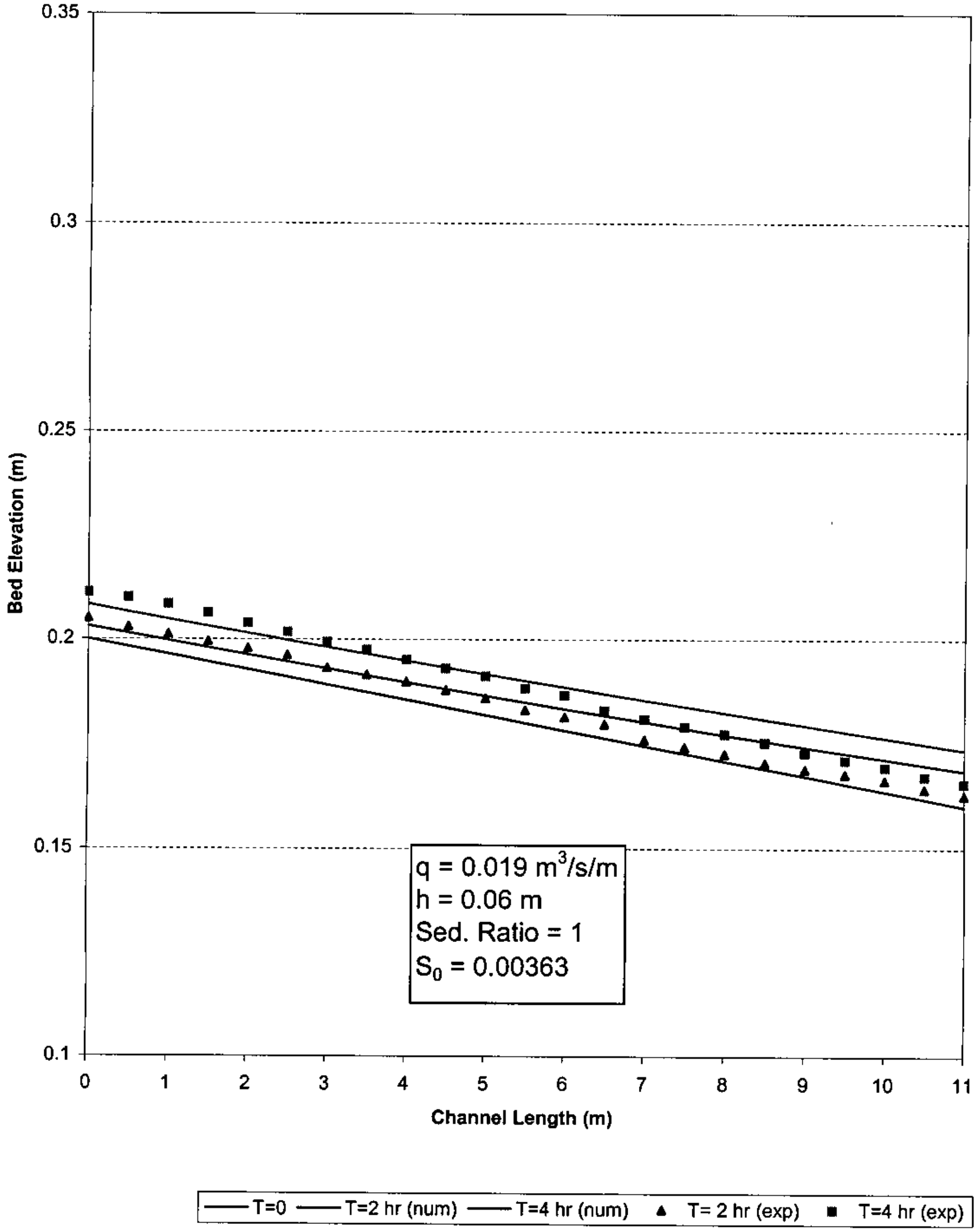

Fig. 6.9 Bed surface profiles (Run 9)

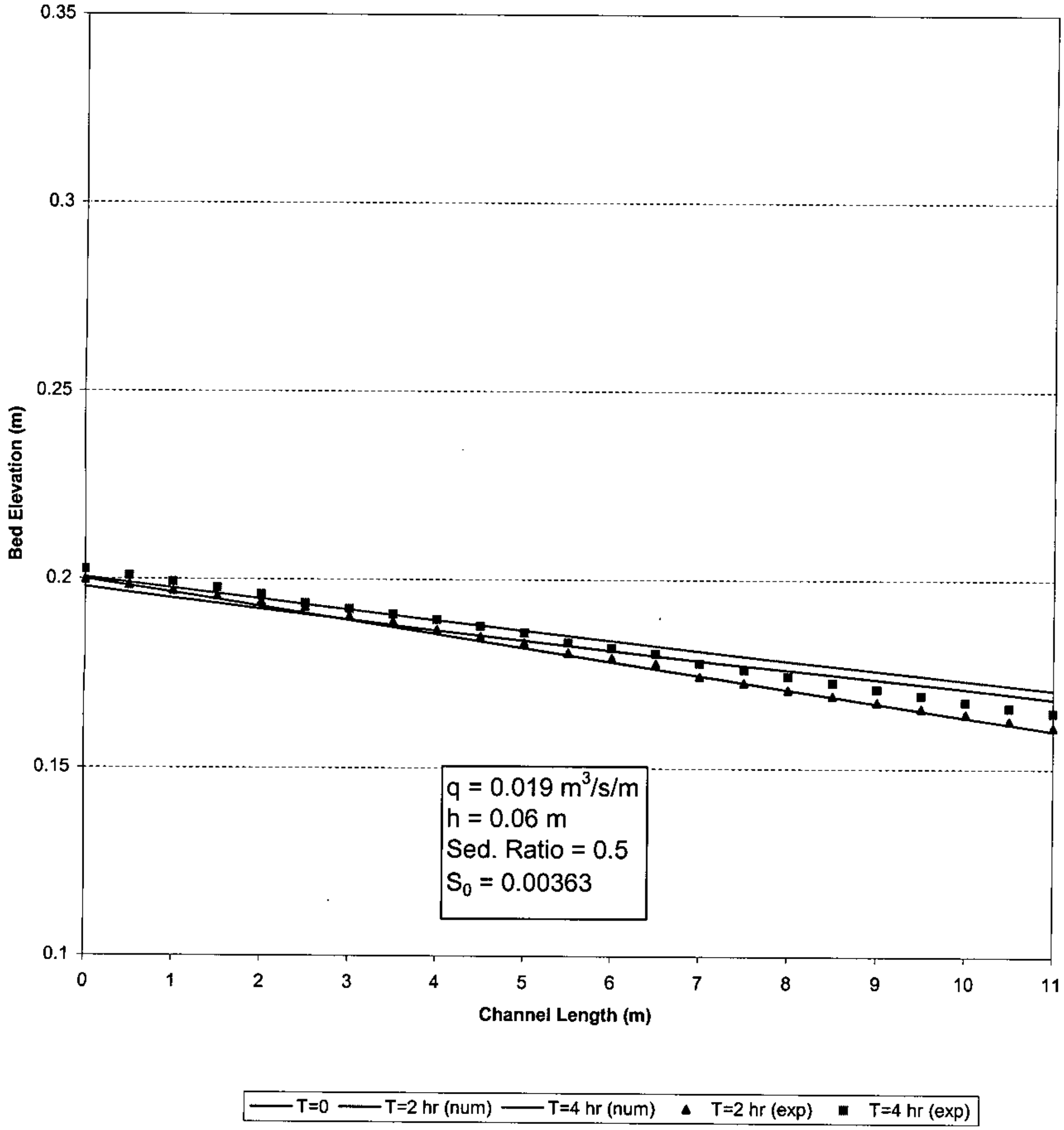

Fig. 6.10 Bed surface profiles (Run 10)

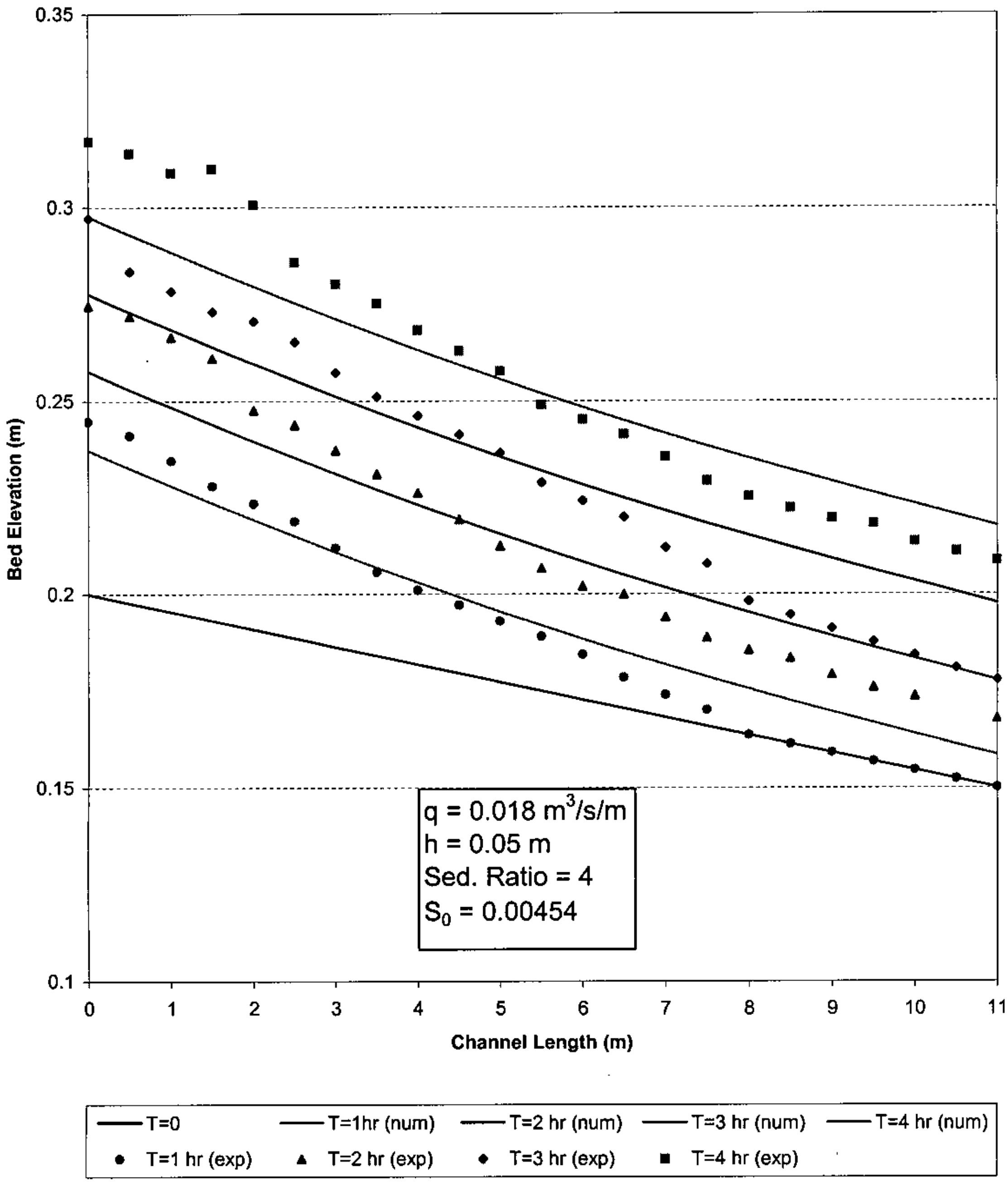

Fig. 6.11 Bed surface profiles (Run 11)

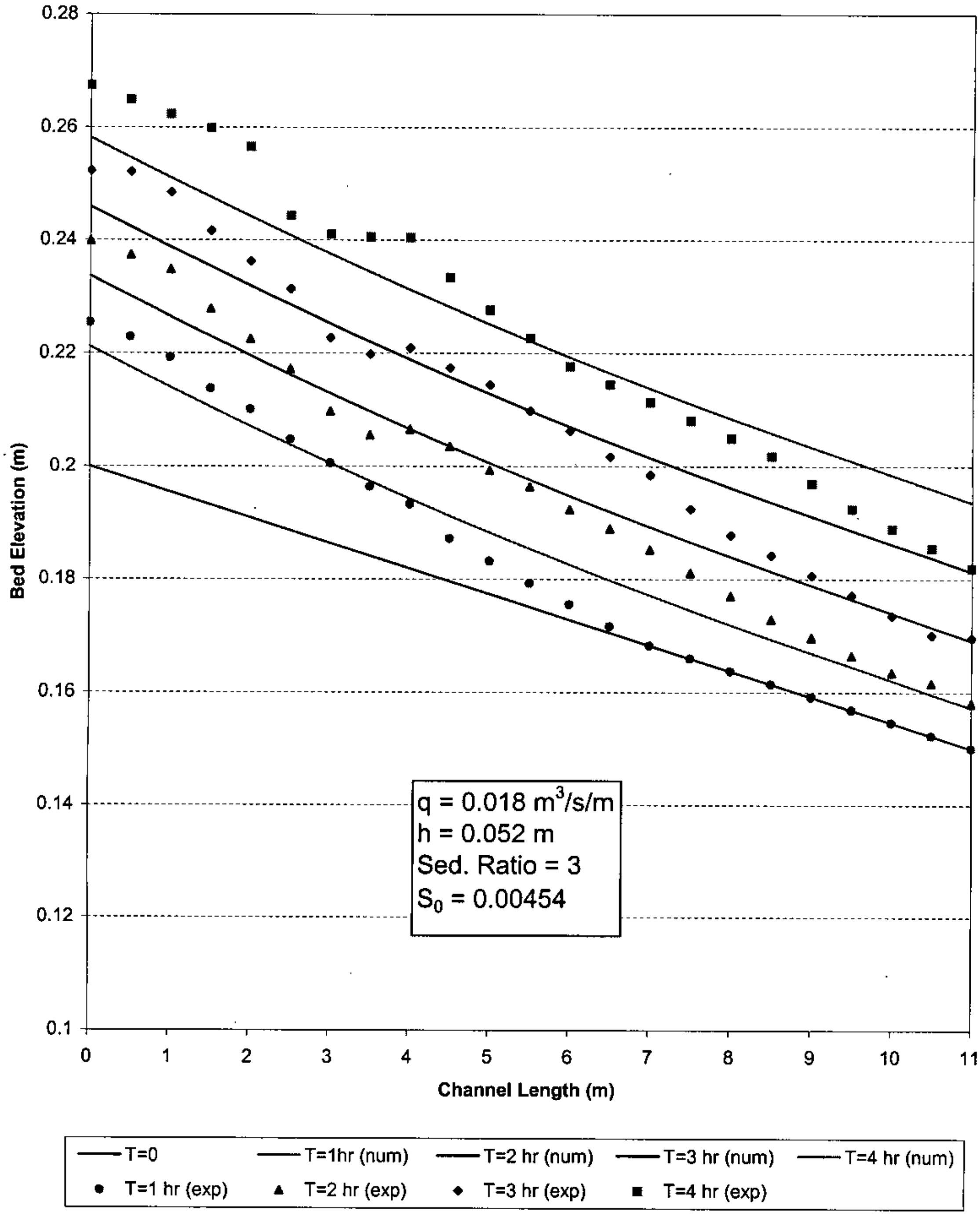

Fig. 6.12 Bed surface profiles (Run 12)

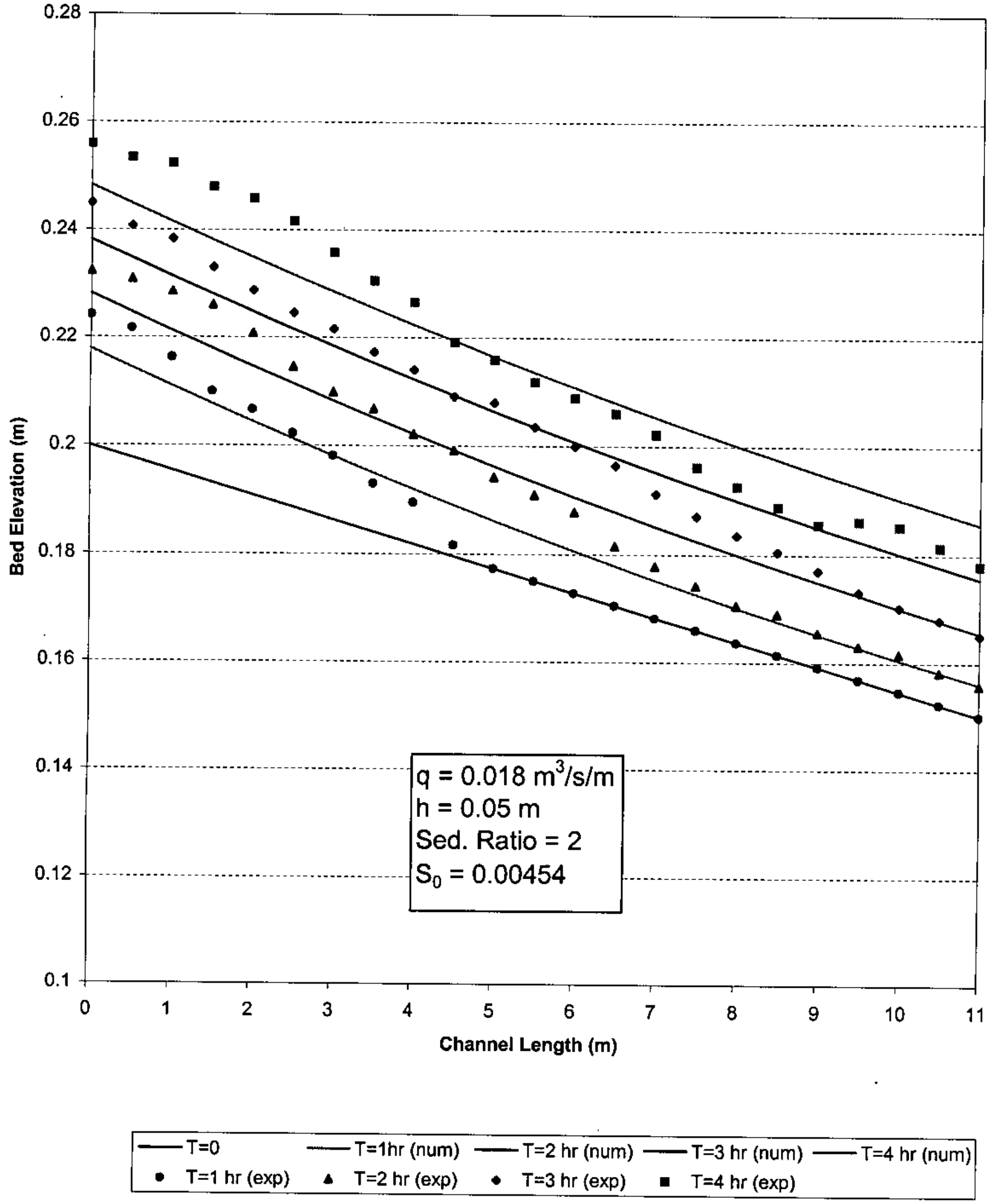

Fig. 6.13 Bed surface profiles (Run 13)

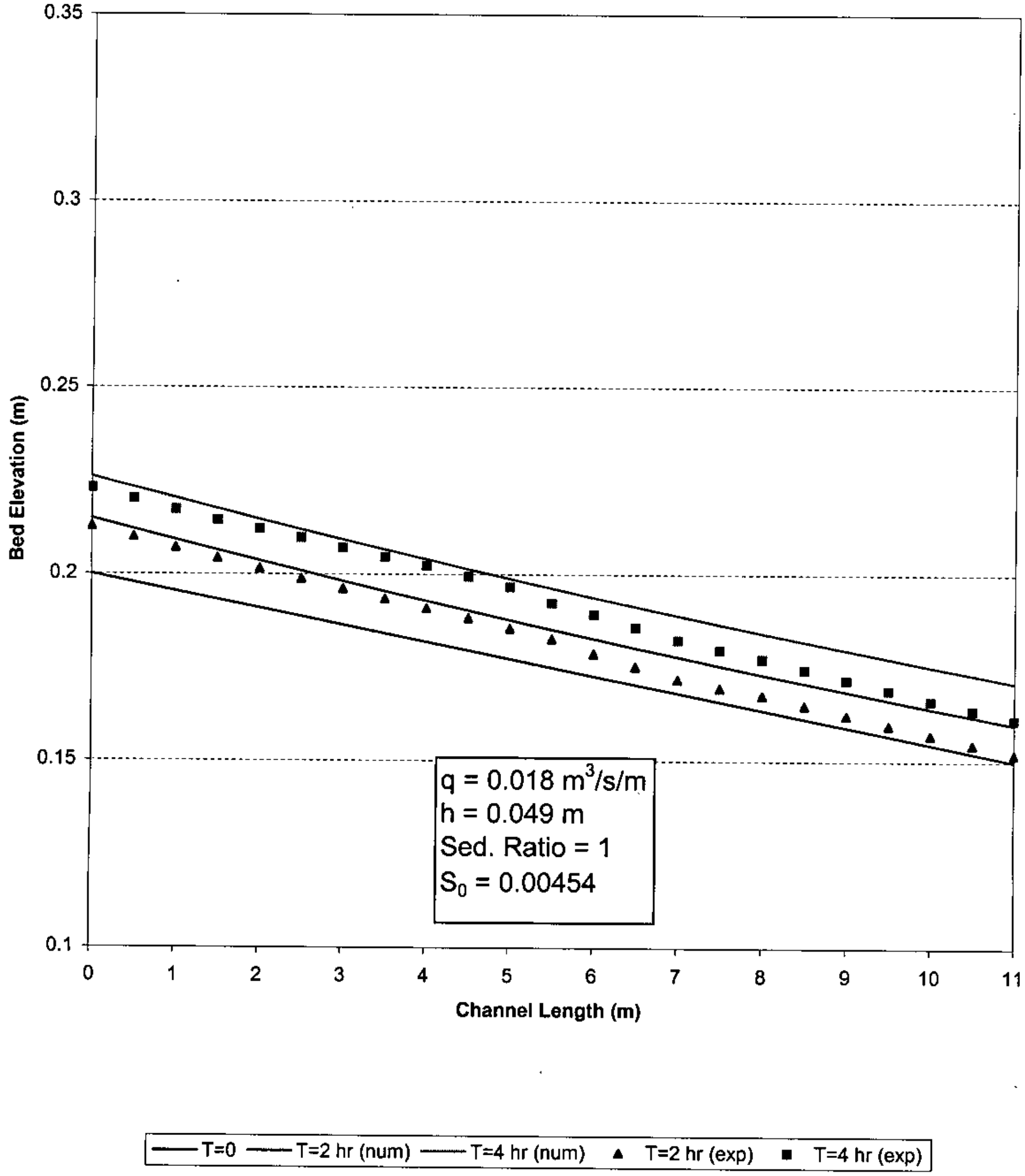

Fig. 6.14 Bed surface profiles (Run 14)

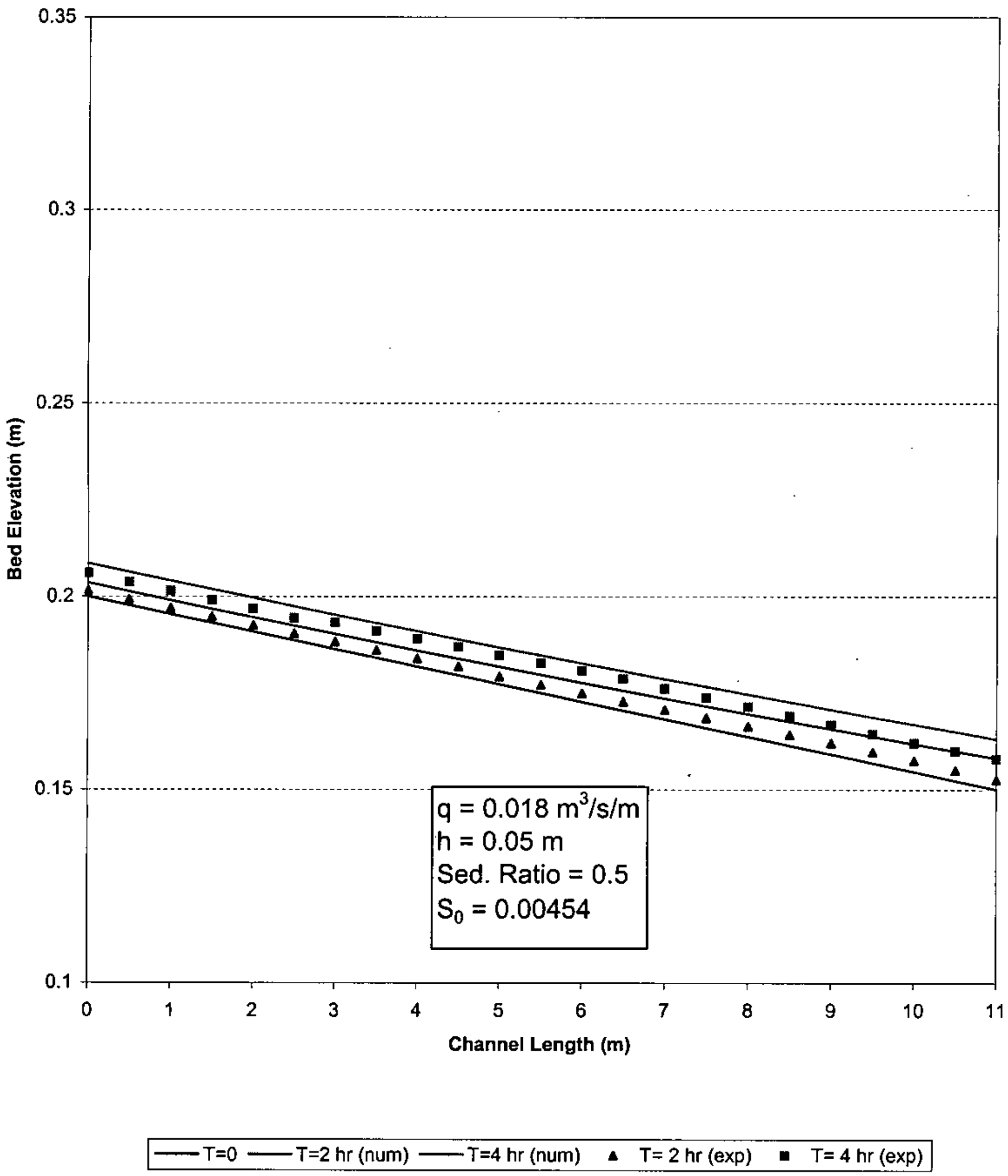

Fig. 6.15 Bed surface profiles (Run 15)

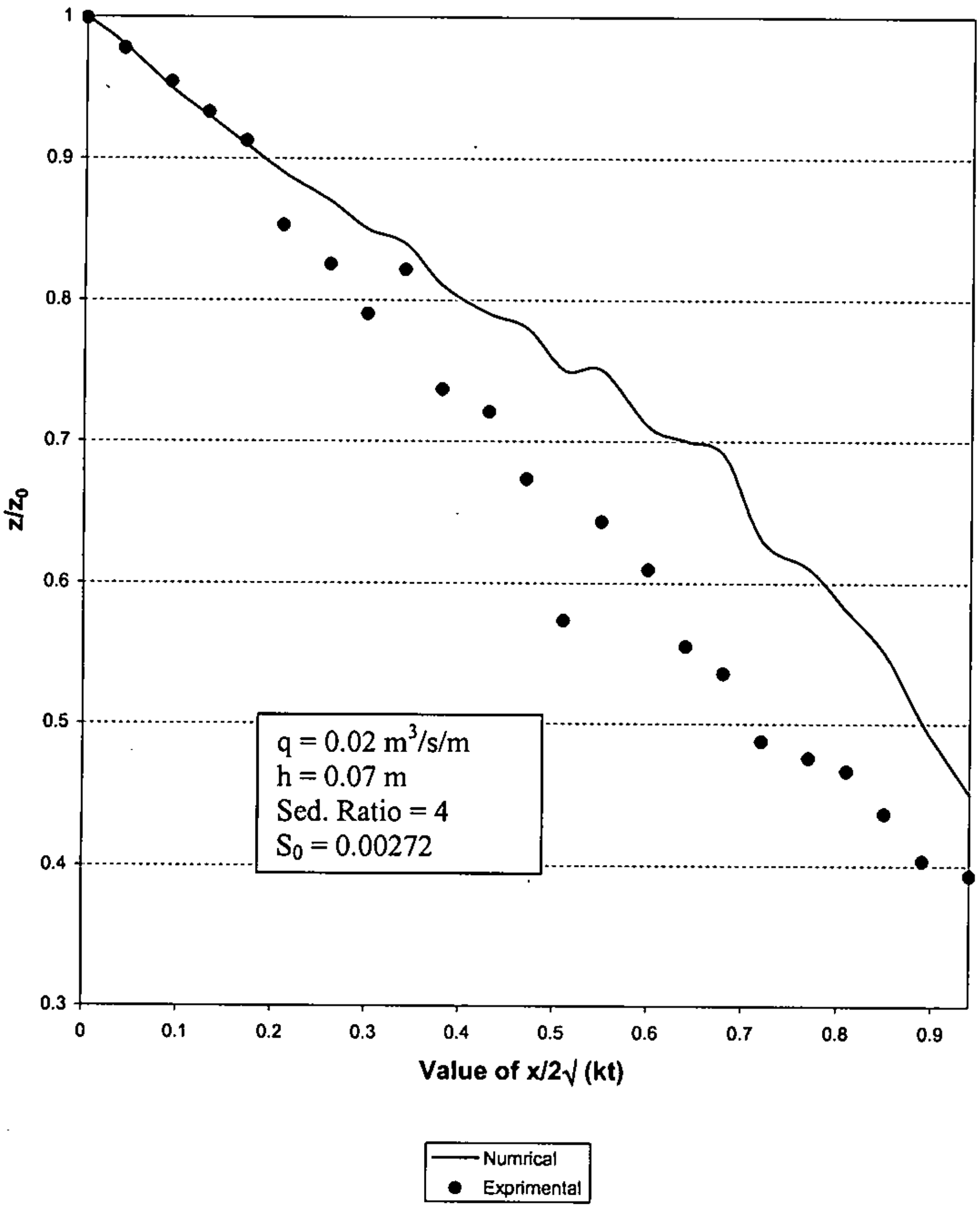

Fig. 6.16 Comparison of relative aggradation (Run 1)

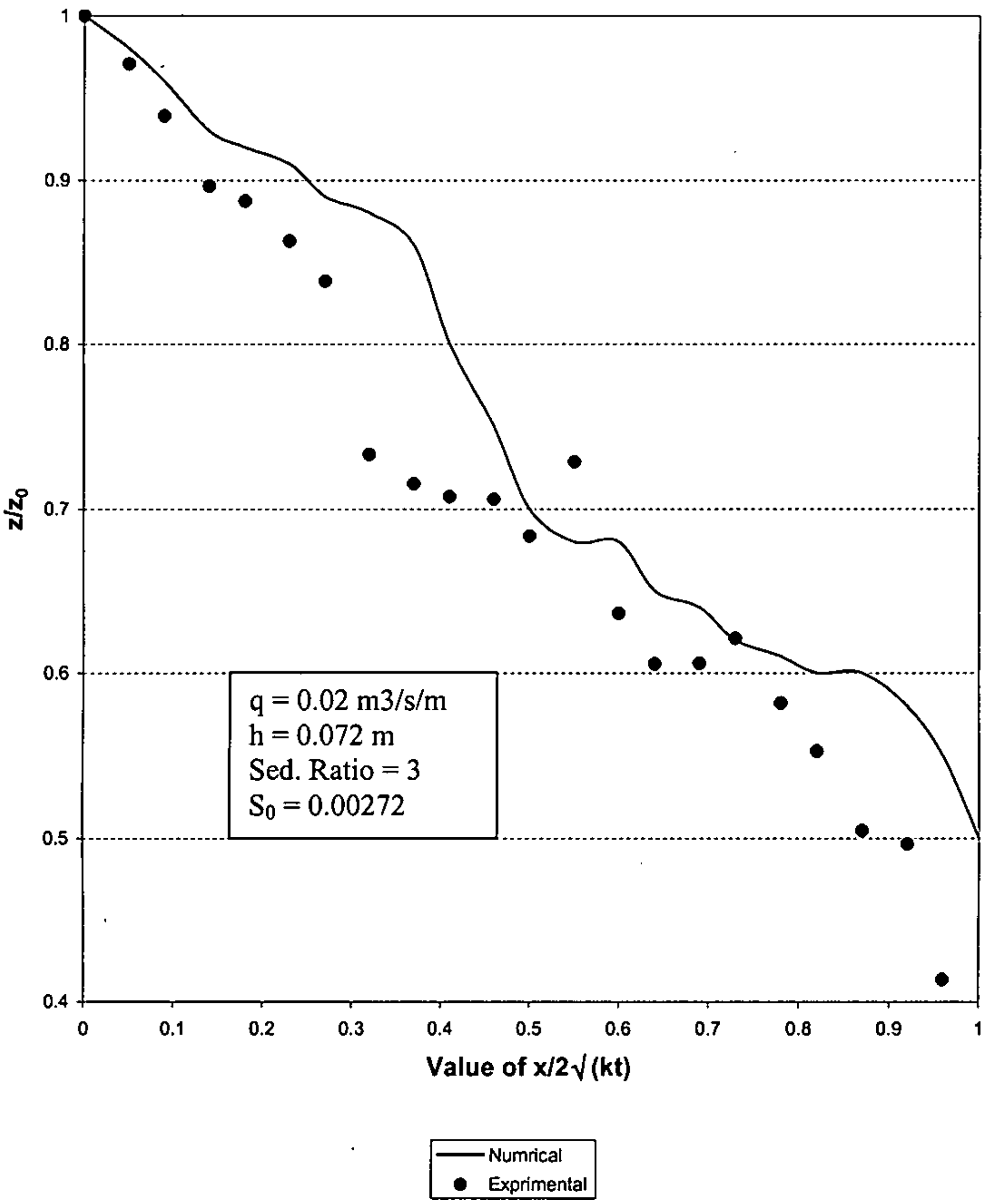

Fig. 6.17 Comparison of relative aggradation (Run 2)

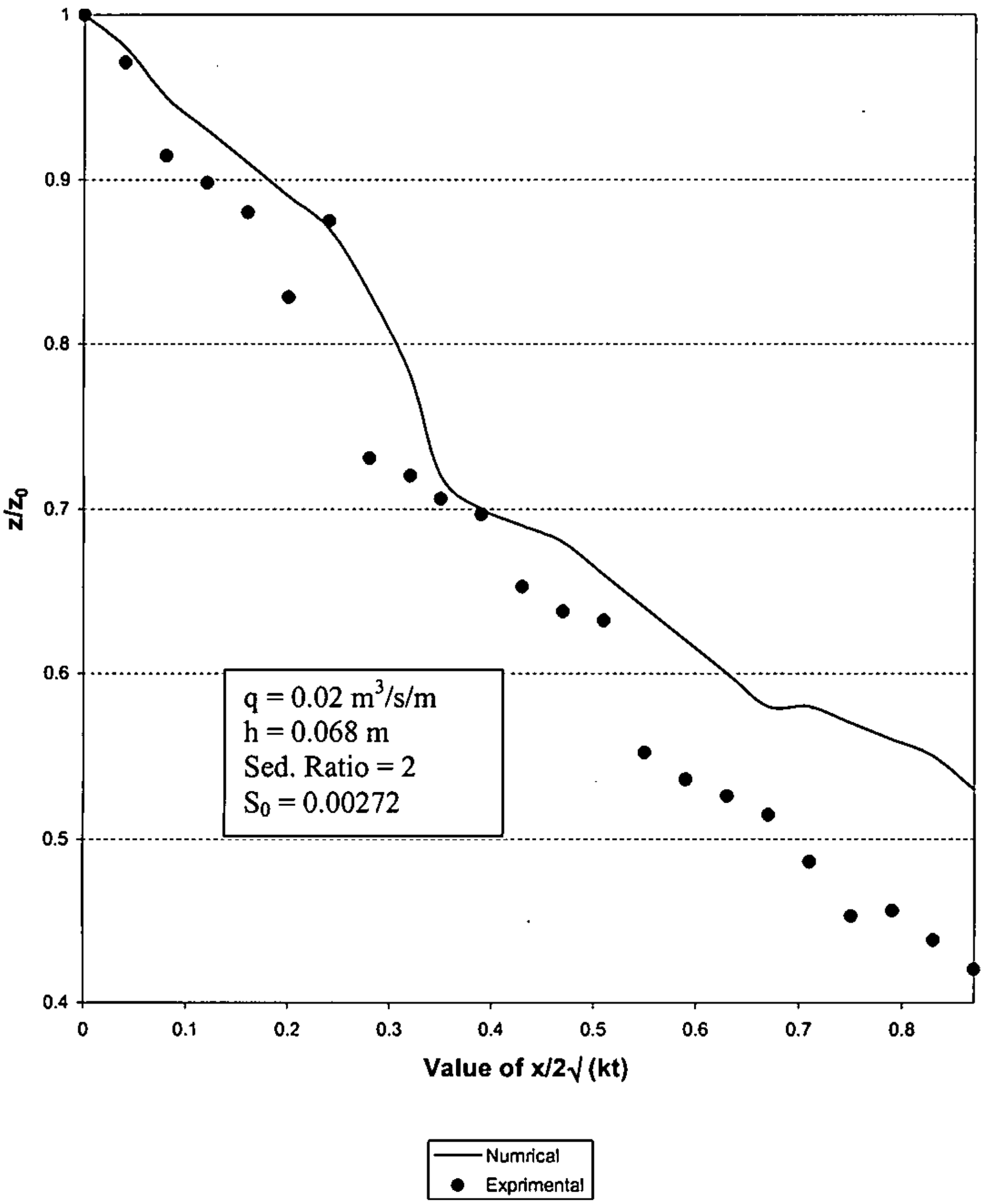

Fig. 6.18 Comparison of relative aggradation (Run 3)

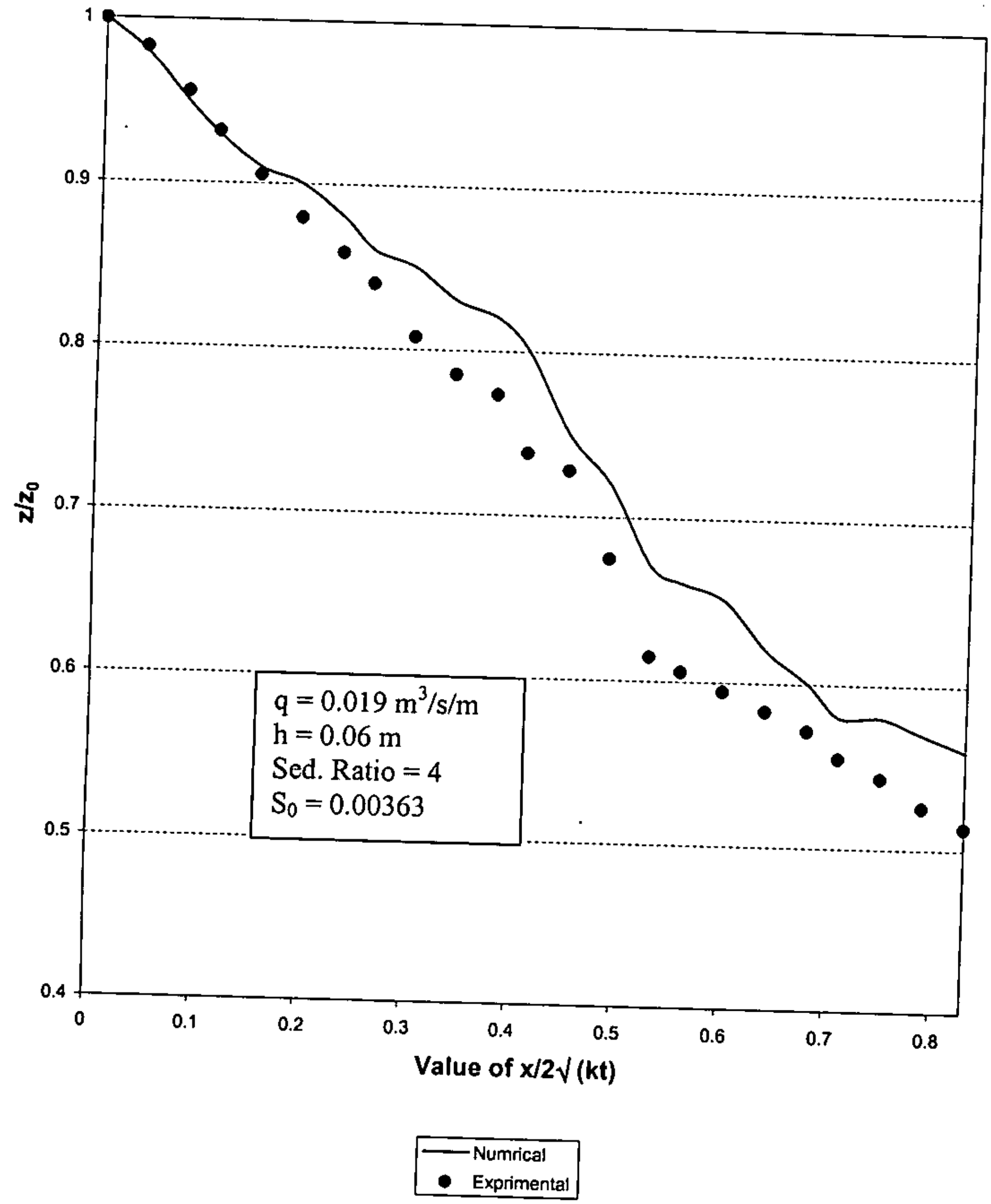

Fig. 6.19 Comparison of relative aggradation (Run 6)

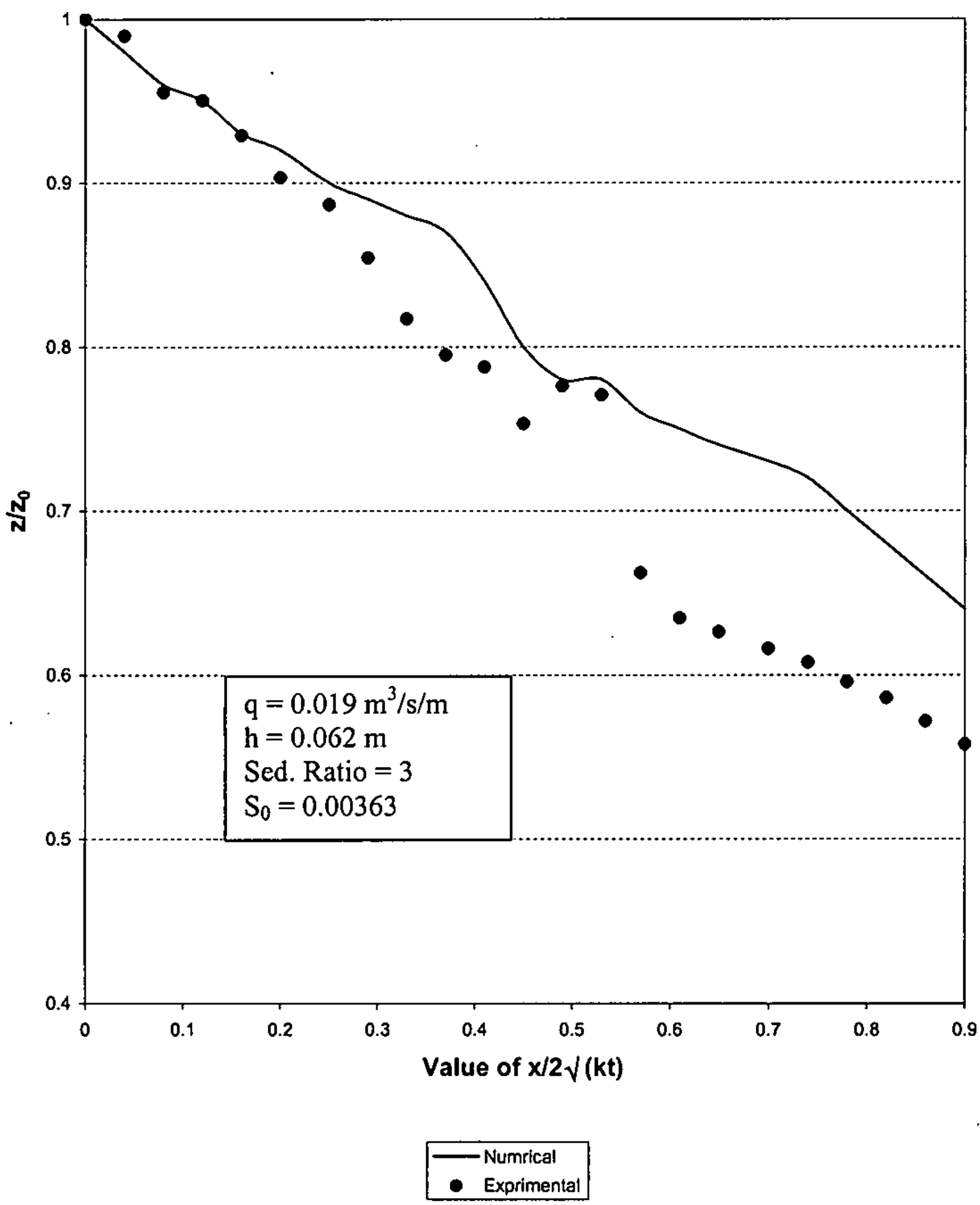

Fig. 6.20 Comparison of relative aggradation (Run 7)

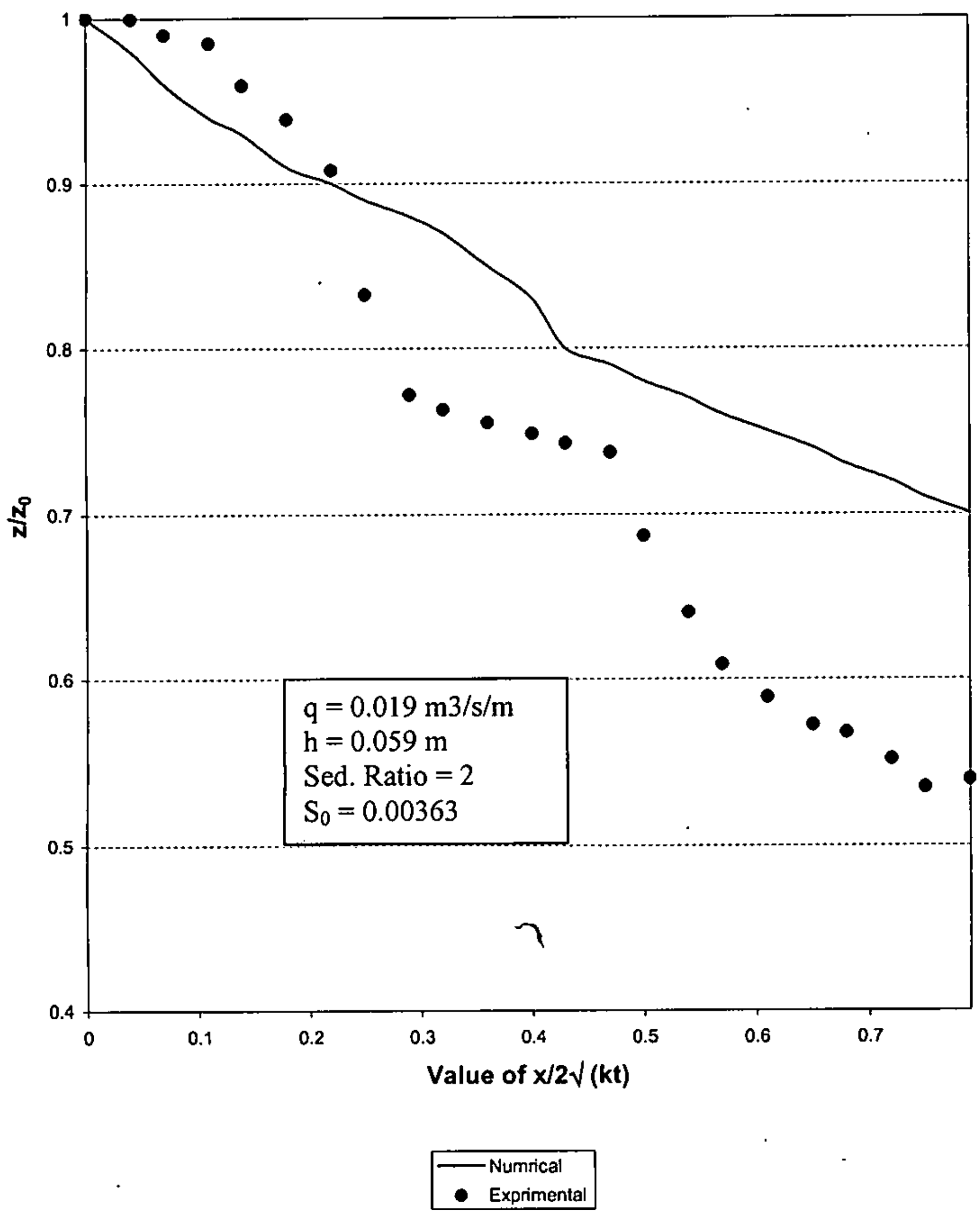

Fig. 6.21 Comparison of relative aggradation (Run 8)

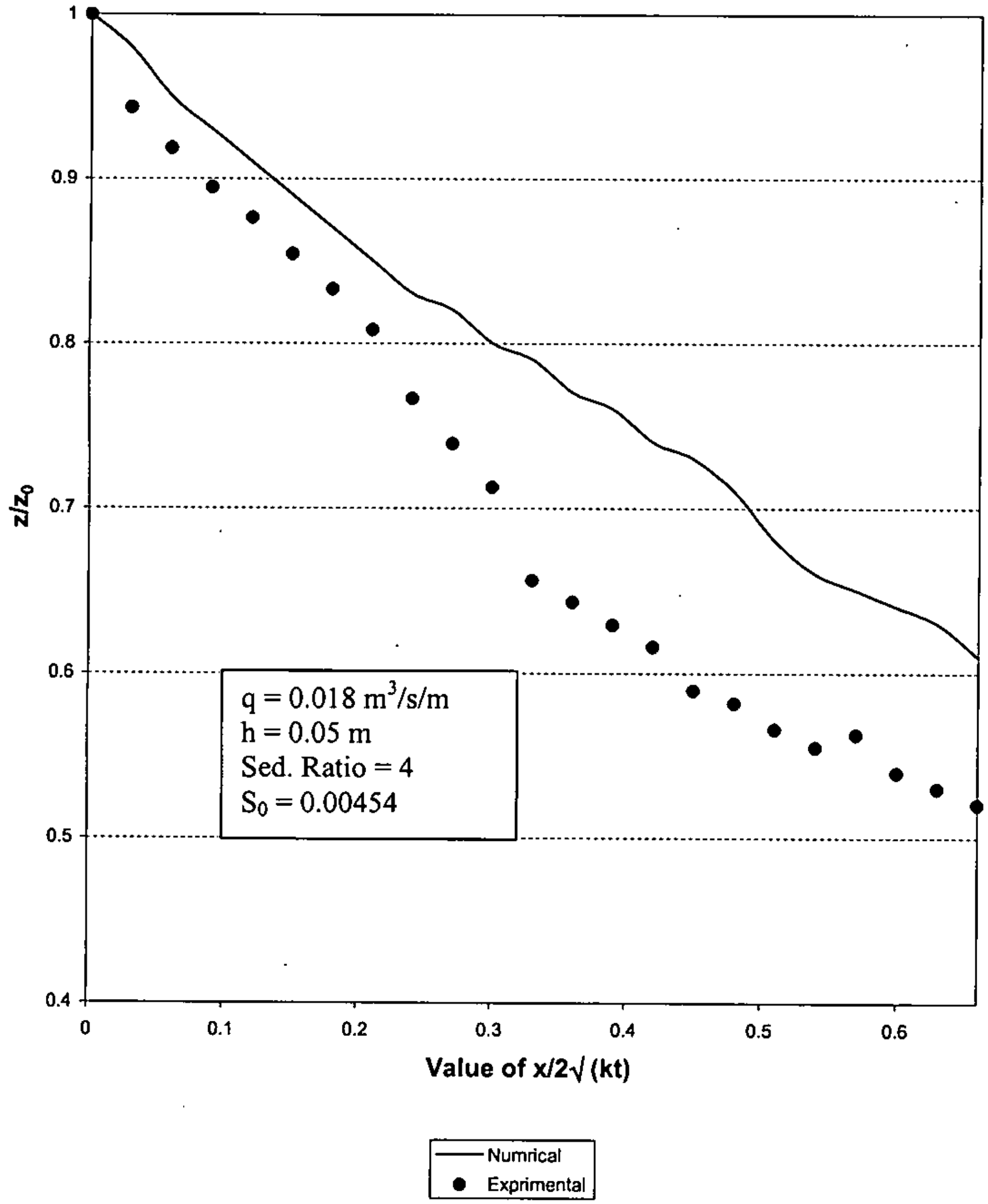

Fig. 6.22 Comparison of relative aggradation (Run 11)

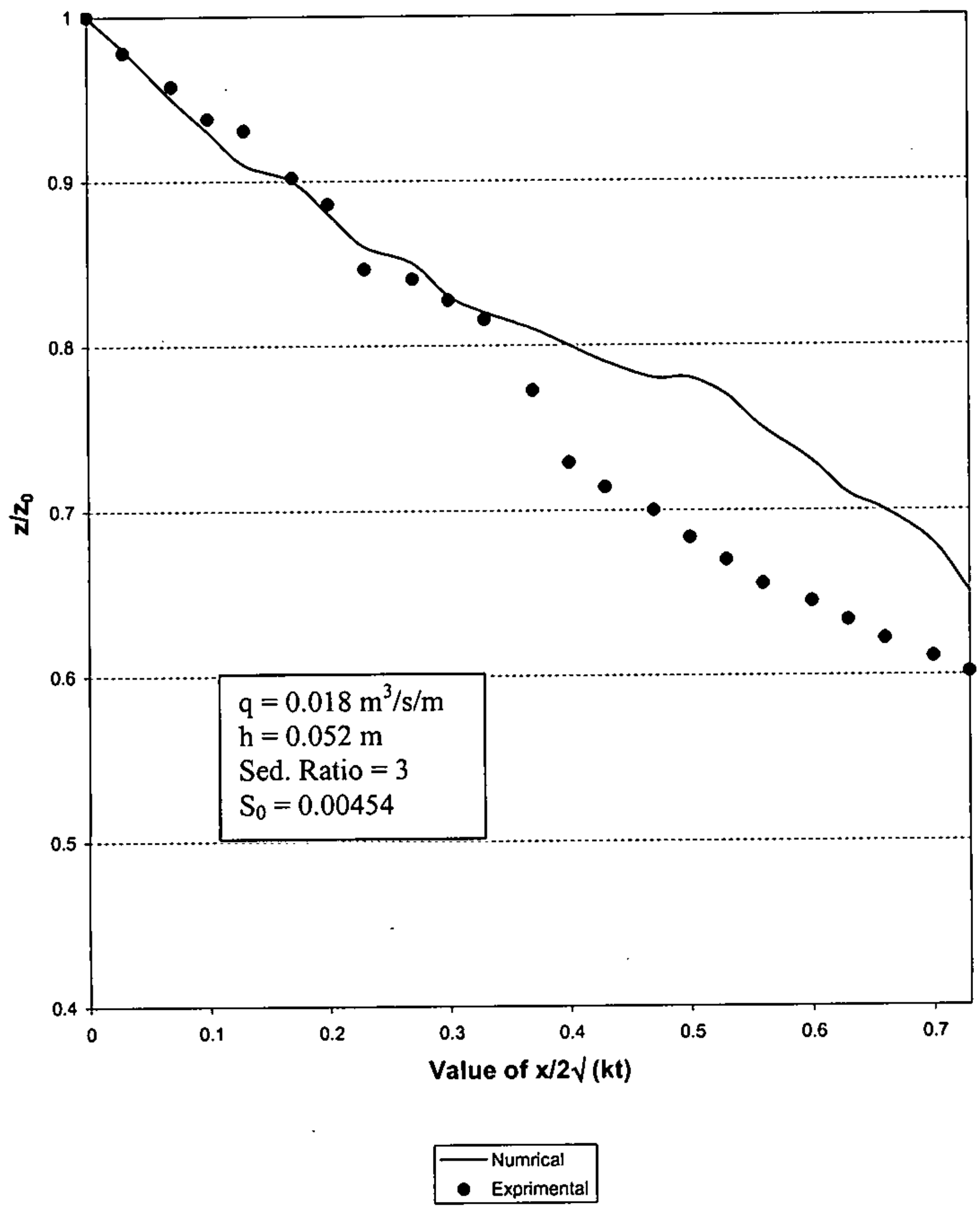

Fig. 6.23 Comparison of relative aggradation (Run 12)

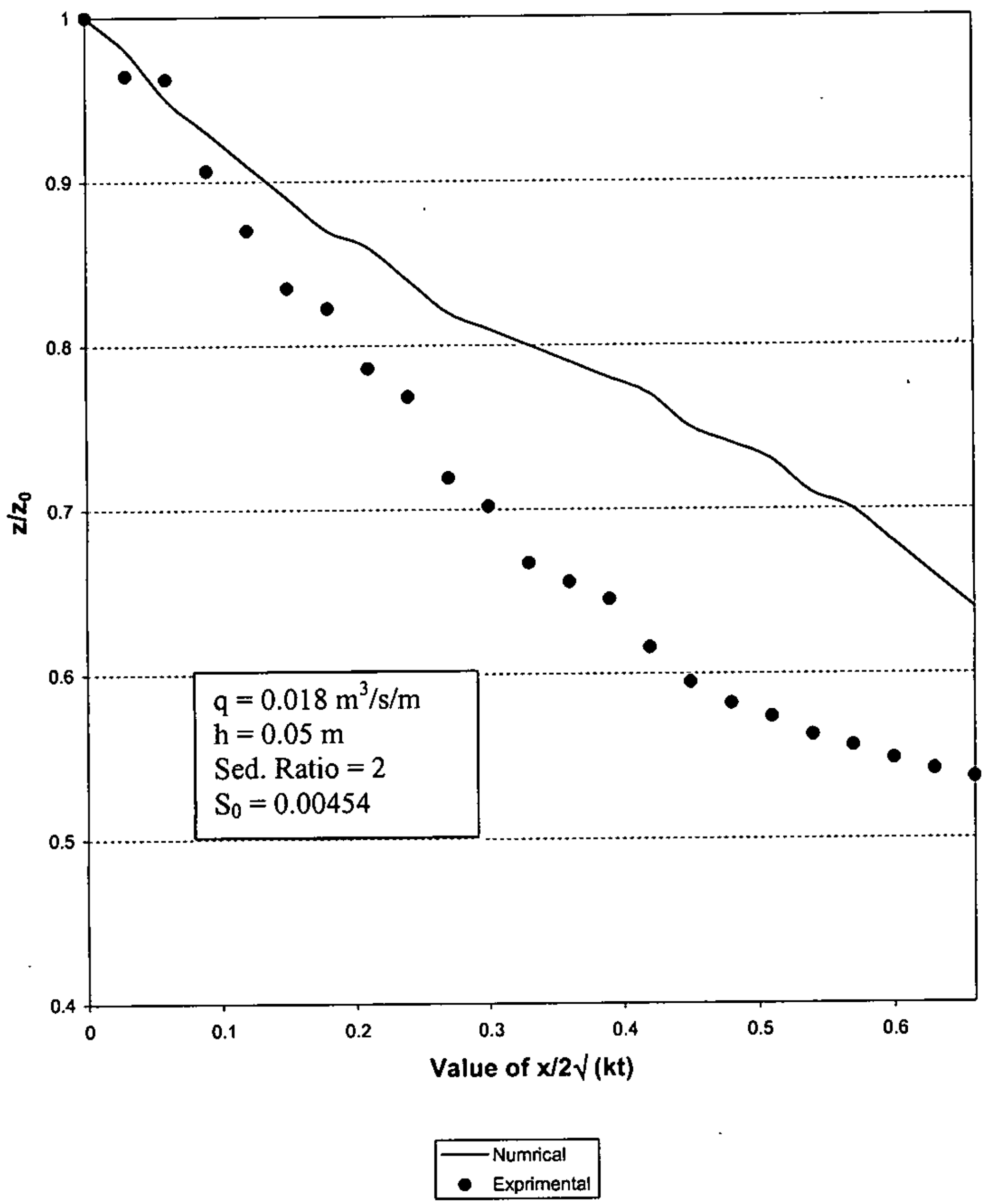

Fig. 6.24 Comparison of relative aggradation (Run 13)

PLATES

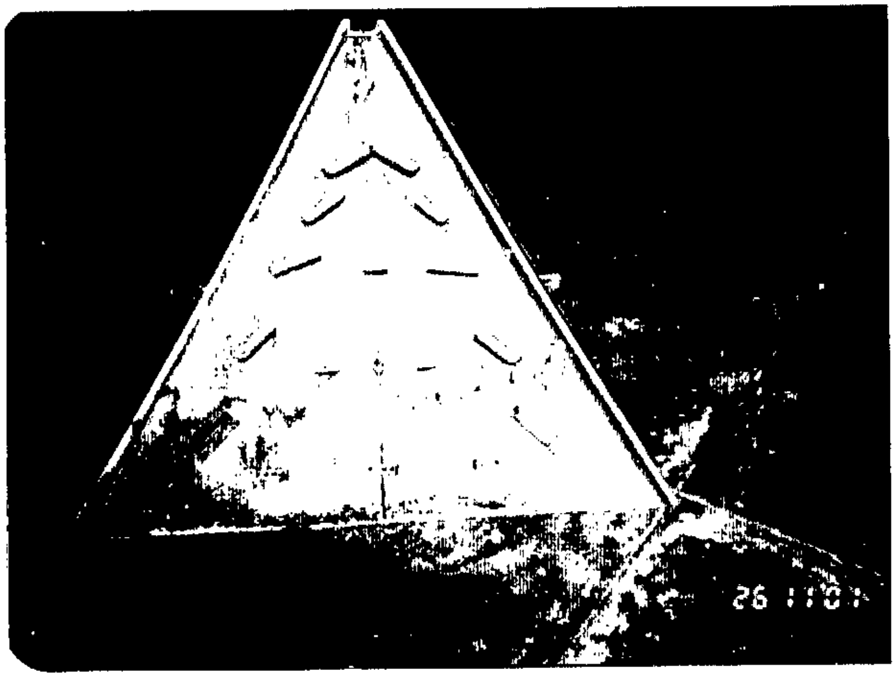

Plate 4.1: Wooden structure

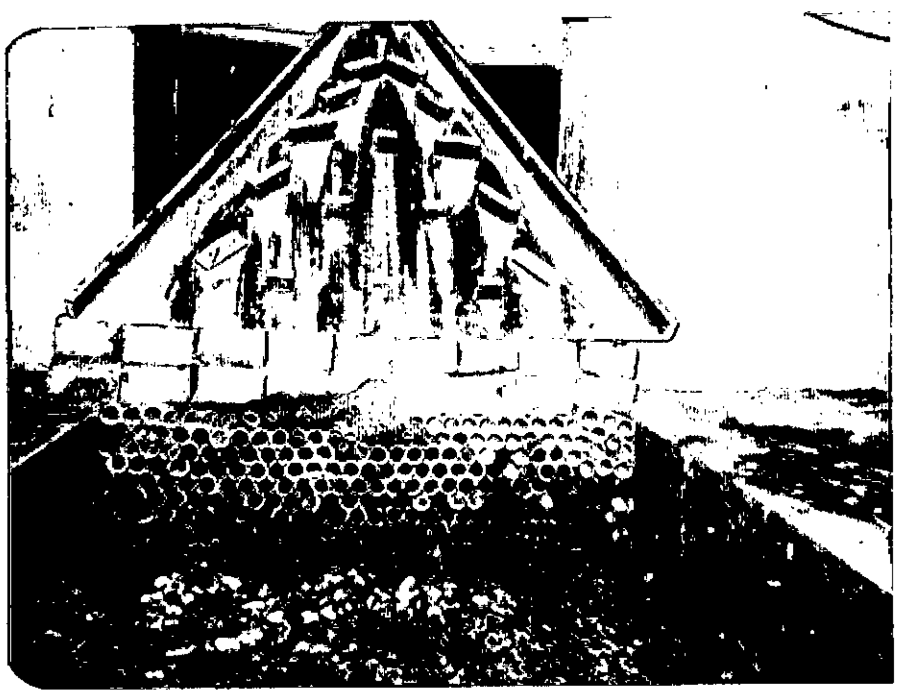

Plate 4.2: Wooden structure which distributes sediment uniformly over the channel width

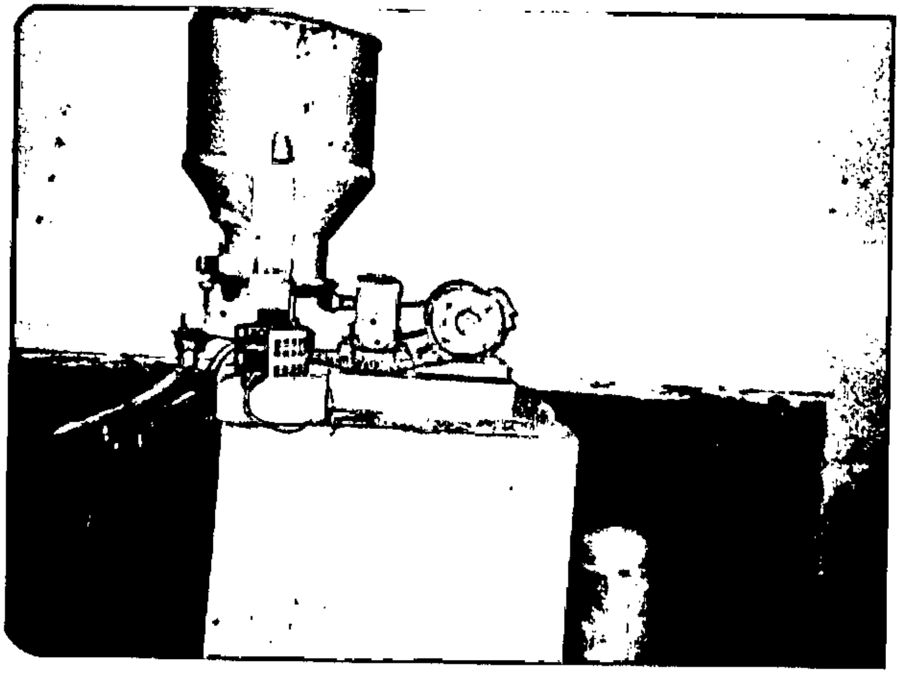

Plate 4.3: Sand Feeder - 1

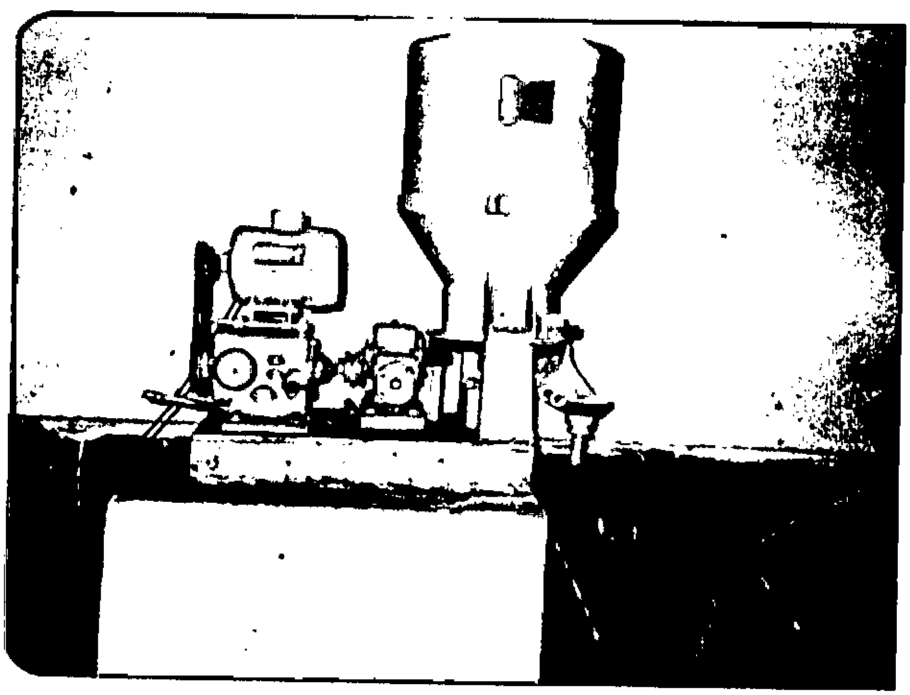

Plate 4.4: Sand Feeder - 2

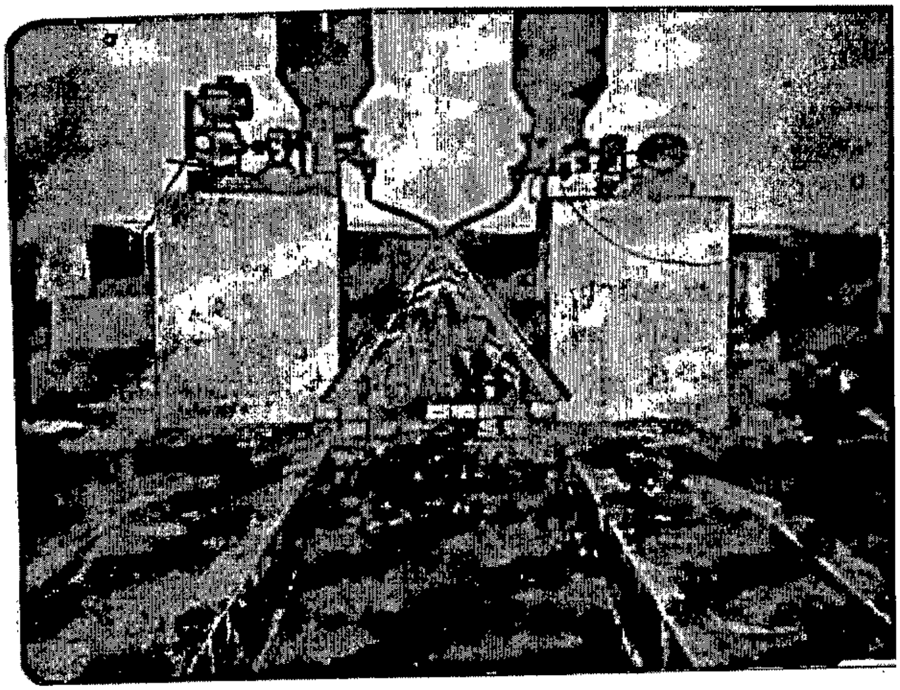

Plate 4.5: Sediment is being added in the channel flow

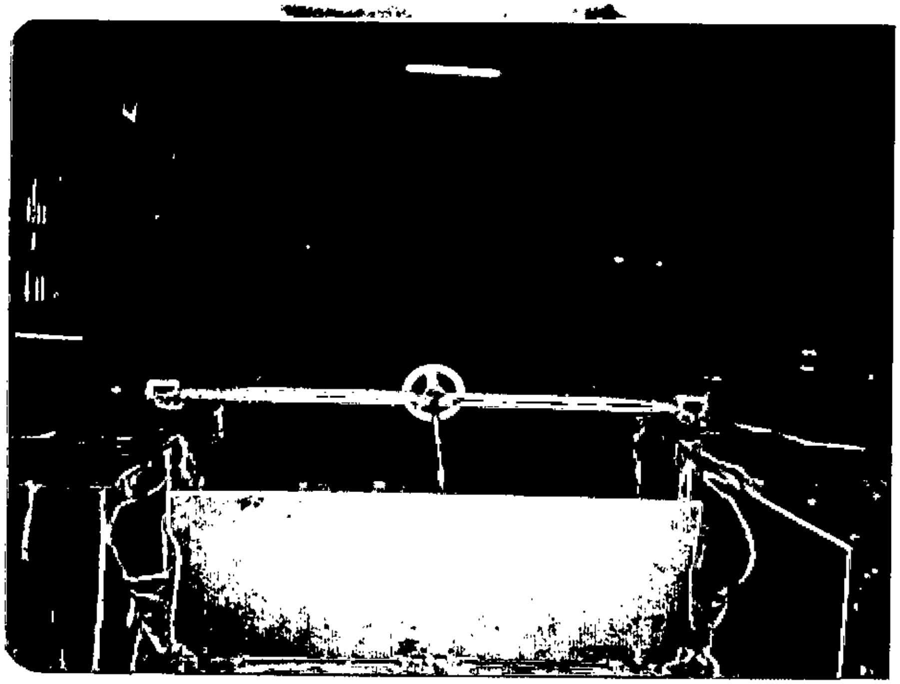

Plate 4.6: View of the Main Channel

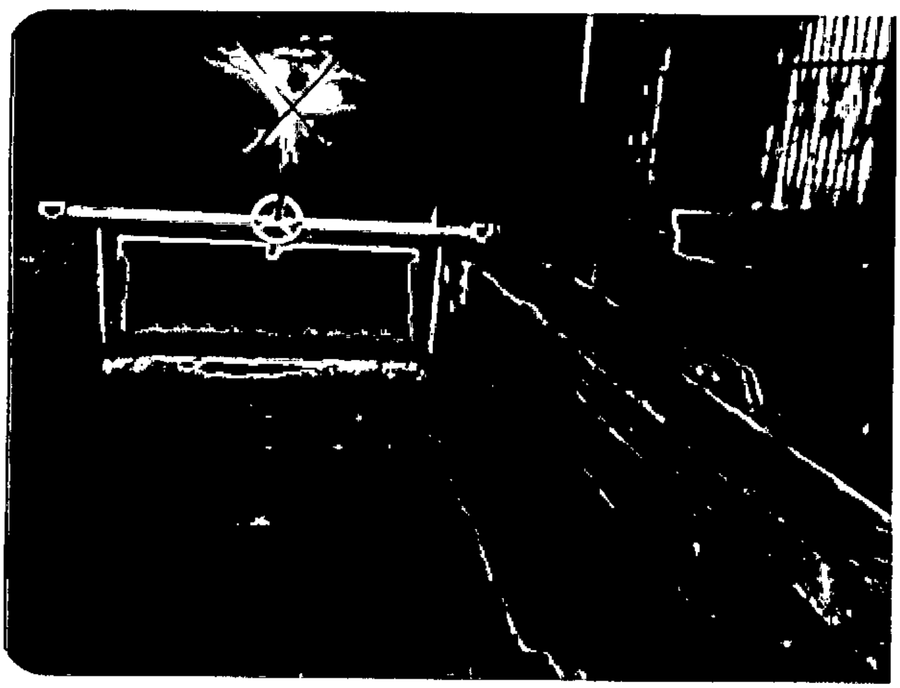

Plate 4.7: View of Sand Trap

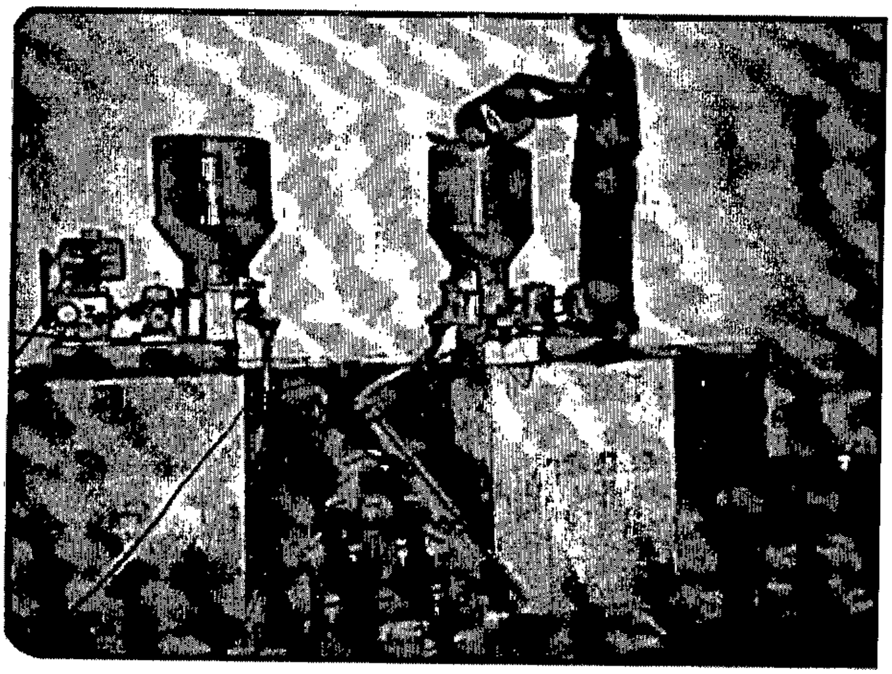

Plate 4.8: Sediment feeding in the sand feeder

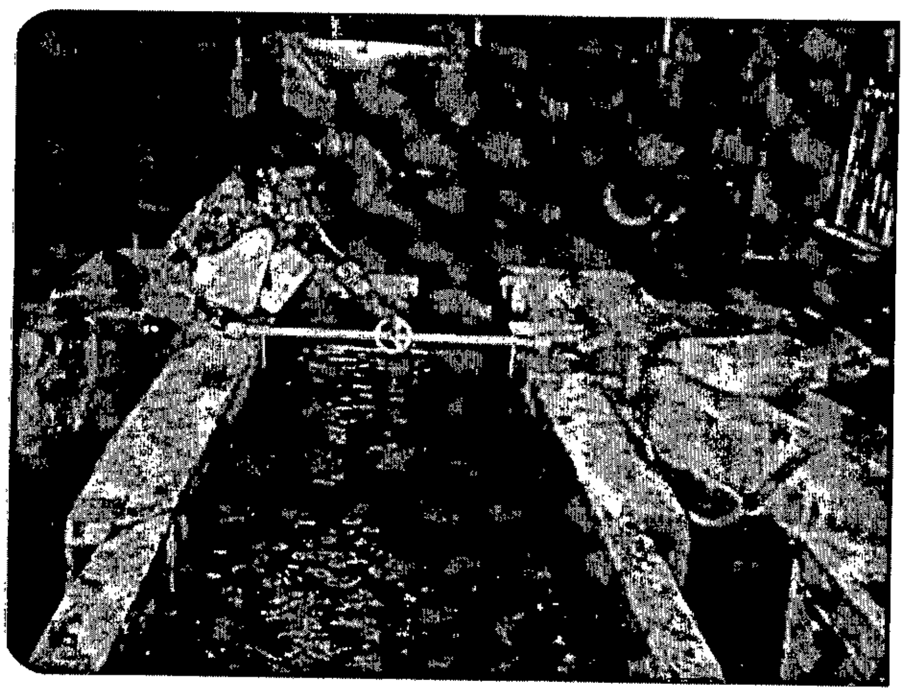

Plate 4.9: Tail gate is being operated

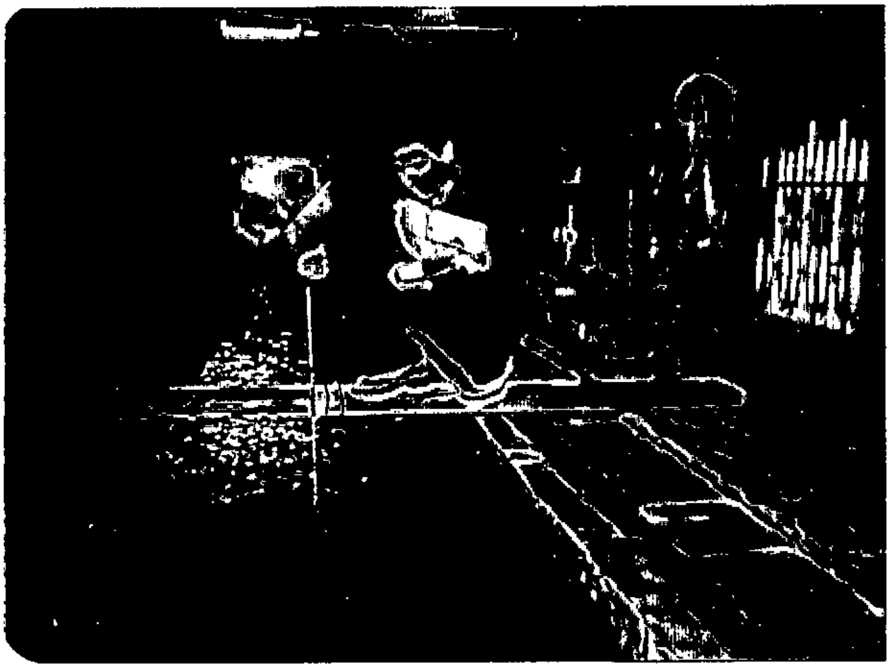

Plate 4.10: Measurement of flow velocity by current meter

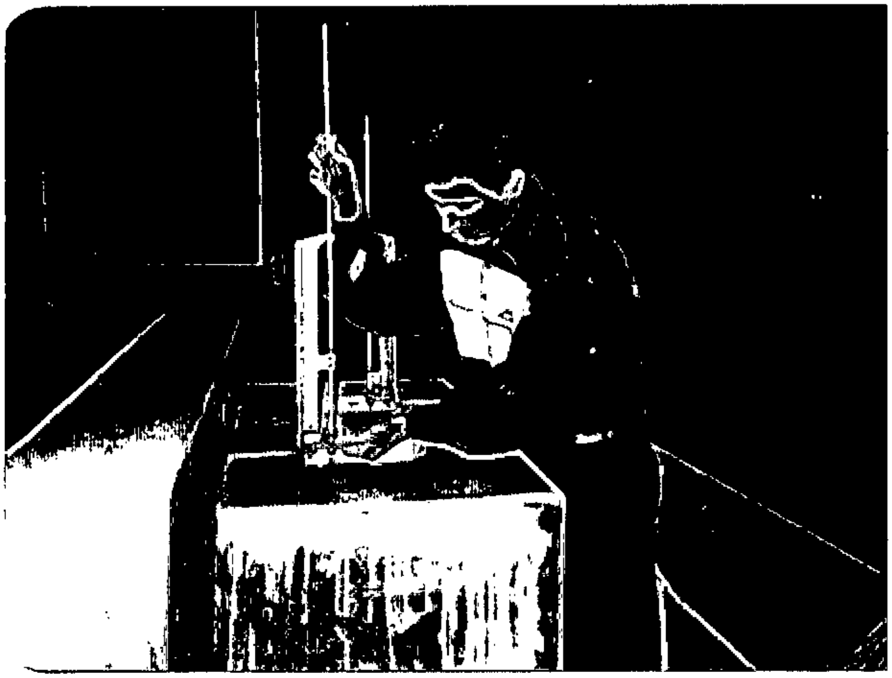

Plate 4.11: Measurement of discharge

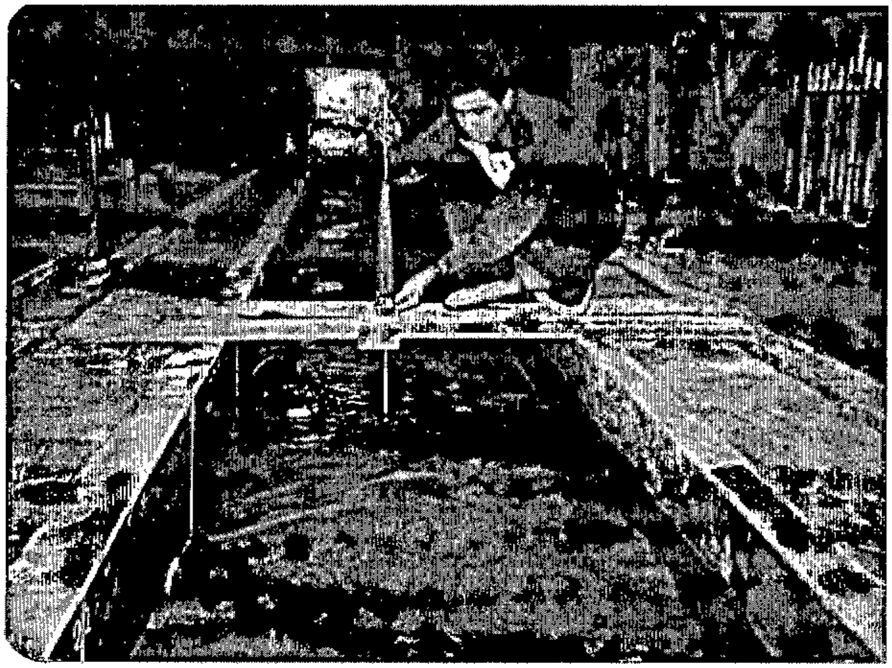

Plate 4.12: Taking bed elevation reading using point gauge after an experimental run

APPENDICES

APPENDIX- A

DETAIL OF THE REHBOCK WEIR

The discharge is measured by the use of Rehbock weir. The discharge equation of a Rehbock weir is (ISO, 1975):

$$Q_R = C_e \frac{2}{3}\sqrt{2g}\,b h_c^{\frac{3}{2}}$$

with

$h_c = h + k_h = h + 0.0012$

$C_e = 0.602 + 0.083h/p$

where

Q_R = is the discharge measured over the Rehbock weir;

C_e = is the coefficient of discharge;

b = is the measured width of the weir;

h_c = is the effective piezometric head with respect to the level of the crest;

h = is the measured head;

k_h = is an experimentally determined quantity which compensates for the influence of surface tension and viscosity;

p = is the apex height in meters.

The Width And The Apex Height Of The Rehbock Weir are Given Below:

p=0.1719m
b = 0.4969 m

Calibration chart of the Rehbock Weir was made with this equation from which directly the discharge was derived dependent on the measured head h.

APPENDIX - B

ACCURACY OF THE REHBOCK WEIR

The accuracy of the Rehbock weir was determined with the help of well-known statistical methods.

B.1 Discharge Equation Of A Rehbock Weir Is (Iso, 1975):

$$Q_R = C_e \frac{2}{3}\sqrt{2g}\,b h_c^{\frac{3}{2}} \tag{B.1}$$

with $h_c = h + k_h = h + 0.0012$

$C_e = 0.602 + 0.083h/p$

where

Q_R = is the discharge measured over the Rehbock weir;

C_e = is the coefficient of discharge;

b = is the measured width of the weir;

h_c = is the effective piezometric head with respect to the *level* of the crest;

h = is the measured head;

k_h = is an experimentally determined quantity which compensates for the influence of surface tension and viscosity;

p = is the apex height in meters.

B.2 Sources Of Possible Error

The sources of possible error can be identified by examining Eq. (B.1); these sources are:

1. The discharge coefficient Cc;
2. The dimensional measurement of b;
3. The measured head h;
4. The corrective term k_h..

The total error results from a contribution of all these errors. According to the quadratic error propagation method the relative error on the rate of flow is calculated with:

$$X_{Q_R} = \pm\sqrt{X_{C_{ce}^2} + X_h^2 + \left(\frac{3}{2}X_{h_e}\right)^2} \qquad \text{(B.2)}$$

where

X_{QR} = is the relative error in Q_R;

X_{Ce} = is the relative error in C_e;

X_b = is the relative error in b;

X_{he} = is the relative error in h_c;

B.3 Estimate Of The Total Error

As can be seen in Eq. (B.2) the total relative error can be calculated once the individual relative errors are found.

Error in Cc:

In ISO (1975) it can be found that the relative error in the coefficient of discharge can be expected to be $X_{Ce} = + 1.0$ %

Error in b:

In Eq. (B.2) X_b is defined as:

$$X_b = \frac{\varepsilon_b}{b} \qquad \text{(B.3)}$$

where ε_b is the error in the measurement of width b.

The width b was measured with a ruler divided into 1 mm intervals; therefore $\varepsilon_b = + 0.5$ mm.

From Eq. (B.3) it can now be found that $X_b = +(0.5/500) = +0.1\%$.

Given this small value, the contribution of X_b to the total error (see Eq.B.2) is considered to be negligible.

Error in h_e:

In Eq. (B.2) the relative error in h_c is used:

$$X_{h_e} = \frac{\sqrt{\varepsilon_{h_1}^2 + \varepsilon_{h_2}^2 + \ldots + \varepsilon_{k_h}^2 + 4\delta_m^2}}{h_c} \qquad \text{(B.4)}$$

Where

$\varepsilon_{h1}, \varepsilon_{h2}, \cdots$ = are the errors in the measurement of head h,

ε_{kh} = is the error in the k_h term;

$2\delta_m$ = is the error in the mean of the readings of the head measurement.

According to ISO (1975): ε_{kh}=0.3 mm.

The head-measuring device was divided into 0.1 mm intervals.

The head h was therefore read to $\varepsilon_{h1} = +\ 0.05$ mm; the zero *was* set to within $\varepsilon_{h2} = +\ 0.05$ mm.

The standard deviation in the mean of ten head measurements proved to be $d_m = 0.03$ mm.

It should be realized that X_{he}, and therefore also X_{QR}, is not single-valued for a weir: it will vary with the discharge. A worst-case value can however be given: ISO (1975) sets a minimum value for h: h>0.03 m. As a result:

$h_e \geq 0.03+0.0012 = 0.0312$ m

$X_{he} \leq +\ 1\ ;0\ \%$.

Total error:

With the results of the various contributions, the total relative error made for the rate of flow (in the worst-case) can now be calculated using Eq. (B.2).

$$X_{Q_R} = \pm\sqrt{1.0^2 + \left(\frac{3}{2}1.0\right)^2} = \pm 1.8\% \qquad \text{(B.5)}$$

APPENDIX -C

MATHEMATICAL MODEL

```
***************************************************************************
***************************************************************************

C       COMPUTATION OF AGGRADATION PROFILE DUE TO SEDIMENT OVERLOADING
C       CONT. FLOW DEPTH AND WATER DISCHARGE ALONG THE CHANNEL IS USED
C       AS INITIAL CONDITION
C       CONSTANT WATER DISCHARGE AT UPSTREAM BOUNDARY AND CONSTANT FLOW
C       DEPTH AT DOWNSTREAM BOUNDARY
C       TRANSIENT CONDITIONS ARE PRODUCED BY SUPPLYING EXTRA SEDIMENT
C       LOAD AT UPSTREAM SECTION
C
C     ******************     NOTATION      ************************
C
C       CHL= CHANNEL LENGTH
C       Cmn= MANNING'S COEFFIENT
C       g = ACCELERATION DUE TO GRAVITY
C       NSEC= NUMBER OF CHANNEL SEGMENTS
C       q = WATER DISCHARGE
C       qs = SEDIMENT DISCHARGE
C       So = CHANNEL BOTTOM SLOPE
C       TLAST = TIME FOR TRANSIENT FLOW COMPUTATION
C       y = FLOW DEPTH AT DIFFERENT SECTIONS
C       p = CHANNEL BED SOIL POROSITY
C       ****************************************************
C
      DIMENSION y(60),q(60),qs(60),z(60),yp(60),qp(60),qsp(60),zp(60),
     +ynew(60), qnew(60), znew(60), qsnew(60), zi(60)
      DOUBLE PRECISION y,yp,yc,ynew,q,qp,qc,qnew,DT,
     +DTNEW,qs,qsp,qsc,qsnew,DTDX,exp
C
      OPEN(5,FILE='D:\B\INPUT.TXT')
      OPEN(6,FILE='D:\B\OUTPUT.TXT')
C
      READ(5,*)g,NSEC,TLAST
      READ(5,*)CHL,Cmn,So,qo,yo,zo,p,a,b,Cn,sedratio
      READ(5,*)S1
C
      qso=a*(qo/yo)**b
      delqs=sedratio*qso
      exp=10.0/3.0
      T=0.0001
C
C     STEADY-STATE CONDITIONS
C
      DX=CHL/FLOAT(NSEC)
      DT=Cn*DX/(qo/yo+SQRT(g*yo))
      DTDX=DT/DX
      I=1
```

```
      zi(I)=zo
      NP=NSEC+1
      DO WHILE(I.LE.NP)
      q(I)=qo
      y(I)=yo
      qs(I)=qso
      I=I+1
      zi(I)=zi(I-1)-So*DX
      END DO
      WRITE(6,15)CHL,p,sedratio,So,Cmn,qo,yo,NSEC,TLAST,Cn
C
C     COMPUTE TRANSIENT CONDITIONS
C
      I=1
      DO WHILE(I.LE.NP)
      z(I)=zi(I)+0.00000001
      I=I+1
      END DO
      k=0
      DO WHILE(T.LE.TLAST)
C     PRINT*, T,'******** PROGRAM RUNNING*******'
      IF((k.EQ.0).OR. (k.EQ.900).OR. (k.EQ.1800).OR. (k.EQ.2400).OR.
     +(k.EQ.3600).OR. (k.EQ.5400).OR. (k.EQ.7200).OR. (k.EQ.9000).OR.
     +(k.EQ.10800).OR. (k.EQ.14400).OR. (k.EQ.18000).OR.
     +(k.EQ.21600).OR. (k.EQ.28800).OR. (k.EQ.36000).OR.(k.EQ.43200).OR.
     +(k.EQ.50400).OR.(k.EQ.57600).OR.(k.EQ.64800).OR. (k.EQ.72000).OR.
     +(k.EQ.180000).OR.(k.EQ.360000).OR.(k.EQ.720000).OR. (k.EQ.1080000)
     +)THEN
C     PRINT*,  T
      dc=b*qso/(3*So*(1-p))
      dcl=dc*(0.885/Sl)**2
C     IF(k.EQ.9000)zog=delqs*T/(1.13*(1-p)*SQRT(dc*T))
      WRITE(6,30) T
      WRITE(6,60)
      I=1
      x=0.0
      DO WHILE(I.LE.NP)
      IF((k.EQ.0).OR.(k.EQ.900).OR.(k.EQ.1800).OR. (k.EQ.2400).OR.
     +(k.EQ.3600).OR. (k.EQ.5400).OR. (k.EQ.7200).OR. (k.EQ.9000).OR.
     +(k.EQ.10800).OR. (k.EQ.14400).OR. (k.EQ.18000).OR.
     +(k.EQ.21600).OR. (k.EQ.28800).OR. (k.EQ.36000).OR.(k.EQ.43200).OR.
     +(k.EQ.50400).OR.(k.EQ.57600).OR.(k.EQ.64800).OR. (k.EQ.72000).OR.
     +(k.EQ.180000).OR.(k.EQ.360000).OR.(k.EQ.720000).OR. (k.EQ.1080000)
     +)THEN
C     PRINT*,  zog,dc
      eta= x/(2*SQRT(dc*T))
      etal= x/(2*SQRT(dcl*T))
      delz=z(I)-zi(I)
      zog=z(1)-zi(1)
      coeff1= delz/zog
c     coeff1= z(I)/zo
      wl=y(I)+z(I)
      WRITE(6,40) x,y(I),q(I),qs(I),z(I),wl,eta,coeff1,etal
c     ELSE
c     wl=y(I)+z(I)
c     WRITE(6,50) x,y(I),q(I),qs(I),z(I),wl
      ENDIF
```

```
              I=I+1
              x=x+DX
        END DO
        ELSE
        ENDIF
        T=T+DT
C
C       INTERIOR NODES
C
C       PREDICTOR STEP
C
        I=1
        DO WHILE(I.LE.NSEC)
        yp(I)=y(I)-DTDX*(q(I+1)-q(I))
        qp(I)=q(I)-DTDX*(q(I+1)*ABS(q(I+1))/y(I+1)-
     +q(I)*ABS(q(I))/y(I)+g/2*(y(I+1)**2-y(I)**2))-
     +g*y(I)*DTDX*(z(I+1)-z(I))-
     +g*y(I)*DT*(q(I)*ABS(q(I)))*Cmn**2/(y(I)**exp)
        qsp(I)=a*(qp(I)/yp(I))**b
        zp(I)=z(I)+1.0/(1-p)*(qs(I)*y(I)/q(I)-qsp(I)*yp(I)/qp(I))
     +-DTDX/(1-p)*(qs(I+1)-qs(I))
        I=I+1
        END DO
C
C       CORRECTOR STEP
C
        I=2
        DO WHILE(I.LE.NSEC)
        yc=yp(I)-DTDX*(qp(I)-qp(I-1))
        qc=qp(I)-DTDX*(qp(I)*ABS(qp(I))/yp(I)-
     +qp(I-1)*ABS(qp(I-1))/yp(I-1)+g/2*(yp(I)**2-yp(I-1)**2))
     +-g*yp(I)*DTDX*(zp(I)-zp(I-1))-
     +g*yp(I)*DT*(qp(I)*ABS(qp(I)))*Cmn**2/(yp(I)**exp)
        qsc=a*(qc/yc)**b
        zc=zp(I)+1.0/(1-p)*(qsp(I)*yp(I)/qp(I)-qsc*yc/qc)-
     +DTDX/(1-p)*(qsp(I)-qsp(I-1))
        ynew(I)=(y(I)+yc)*0.5
        qnew(I)=(q(I)+qc)*0.5
        znew(I)=(z(I)+zc)*0.5
        qsnew(I)=a*(qnew(I)/ynew(I))**b
        I=I+1
        END DO
C
C         UPSTREAM END
C
        qnew(1)=qo
        ynew(1)=2*ynew(2)-ynew(3)
        qsnew(1)=a*(qnew(1)/ynew(1))**b
        znew(1)=z(1)+1.0/(1-p)*((qs(1)*y(1)/q(1)-qsnew(1)*ynew(1)/
     +qnew(1))+DTDX*(qso+delqs-qs(1)))
C
C       DOWNSTREAM END
C
        ynew(NP)=yo
        qnew(NP)=2*qnew(NSEC)-qnew(NSEC-1)
        znew(NP)=2*znew(NSEC)-znew(NSEC-1)
        qsnew(NP)=a*(qnew(NP)/ynew(NP))**b
```

```
C
C     CHECK FOR STABILITY
C
      J=1
      DO WHILE(J.LE.NP)
      DTNEW=Cn*DX/(qnew(J)/ynew(J)+SQRT(g*ynew(J)))
      IF(DTNEW.LE.DT) DT=DTNEW
      J=J+1
      END DO
      DTDX=DT/DX
C
C       REDUCE DT FOR STABILITY AND RECALCULATE
C
      I=1
      DO WHILE(I.LE.NP)
      q(I)=qnew(I)
      Y(I)=ynew(I)
      z(I)=znew(I)
      qs(I)=qsnew(I)
      I=I+1
      END DO
      kk=T
      IF(kk.EQ.k) THEN
             k=kk+1
      ELSE
             k=kk
      ENDIF
      END DO
15    FORMAT(5X,'CHANNEL LENGTH(m)=',F10.2,/5X,'SOIL POROSITY=',F10.2,
     +/5X,'SEDIMENT RATIO=',F10.2,/5X,'BED SLOPE=',F10.6,/5X,
     +'MANNING"S n='F10.5,/5X,'qo=',F10.3,/5X,'yo=',F10.3,/5X,'NSEC=',
     +I10,/5X,'TLAST=',F10.2,/5X,'Cn=',F10.2)
30    FORMAT(/1X,'T=',F14.2,'     Seconds')
c40   FORMAT(F6.2,F6.4,F6.4,F10.8,F10.7,F10.7,F10.3,F10.3,F10.3)
40    FORMAT(3F10.4,3F10.8,3F10.2)
c50   FORMAT(F9.2,3F12.2,F8.3)
60    FORMAT(7x,'x',9x,'y',9x ,'q',7x,'qs',8x,'z',9x,'wl',9x,
     +'eta',7x,'z/zo',5x,'etal')
      CLOSE(5)
      CLOSE(6)
      STOP
      END
```